Innate immunity, developmental speed and their trade-offs in two hexapod models

Cheng, S.

Chapter 4

A novel allele of large effect that alters developmental time and mediates trade-offs

Shixiong Cheng, Elisa A. Mogollón Pérez, Daipeng Chen, Joep van de Sanden, Amke Hackmann, Roeland M. H. Merks, Joost van den Heuvel, Maurijn van der Zee

Abstract

During current climate change, insect developmental time can adapt quickly to match shifted host plant or prey availability. However, the genetic basis of such adaptation in developmental timing is hardly studied. Here, we show that ecdysone signaling starts dorsal closure and is the main target of long-term artificial selection for fast embryonic development in replicate, outbred populations of the beetle *Tribolium castaneum*. Pooled whole genome resequencing (Pool-seq), RNAseq, qPCR, and a small RNAi screen pinpoint a 222 bp deletion upstream of the ecdysone degrading enzyme *Cyp18a1*. This allele contains Tramtrack and Broad binding sites which are responsible for chromatin architectural alterations, and may act as an enhancer regulating expression of *Cyp18a1*. Using CRISPR-Cas9 technology, we recreated this deletion in the homogeneous genetic background of the Georgia lab strain, and demonstrate that this single allele advances the ecdysone peak inducing dorsal closure, accelerates larval development and causes a trade-off with fecundity. Our study demonstrates the relevance of ecdysone during embryonic development, and reveals the presence of large-effect life-history alleles in natural populations.

Introduction

When global warming affects species differently, ecological mismatches in seasonal timing occur (Kharouba et al., 2018; Samplonius et al., 2021; Thackeray et al., 2016). Mismatches with host plant or prey availability exert strong selection on developmental time in insects (Singer and Parmesan, 2010; Visser and Gienapp, 2019). Eggs of the winter moth *Operopthera brumata*, for instance, decreased their temperature sensitivity to synchronize larval hatching with the budburst of their primary food source, the oak *Quercus robur* (Brinkman, 2017). Failure to adapt to changes in seasonal timing can lead to population extinction (McLaughlin et al., 2002; Singer and Parmesan, 2010). It is thus of great importance to understand to what extent insects can respond to such selective pressures on developmental time (Franks and Hoffmann, 2012; Renner and Zohner, 2018).

New phenotypes are thought to generally arise from selection on standing genetic variation, but the ultimate source of new alleles is mutation. These mutations eventually affect protein networks, and manifest themselves through development and physiology as phenotypic variation (Gissis et al., 2011; Shapiro, 2011). Such alleles can increase in frequency by natural selection, but fluctuating environments, trade-offs, balancing selection and drift in small populations can make natural selection complicated (Brakefield, 2003). Such problems are avoided in artificial selection experiments (Brakefield, 2003).

Artificial selection has long been practiced by humans to produce animals and crops with desirable phenotypic traits in their offspring. This strong selection has led to innovations in both animals and plants and has affected human evolution and the biosphere as a whole (Larson and Fuller, 2014; Xiang

et al., 2018). Artificial selection is a useful tool for evolutionary geneticists too. The underlying genetics of rapidly changed phenotypic traits can be investigated (Brakefield, 2003; Franks et al., 2018). Most importantly, constant environments and large populations can facilitate the study of evolution compared to natural selection in field populations. Finally, using replicate populations increases statistical power of artificial selection experiments (Brakefield, 2003).

Insects provide excellent models for experimental evolution, as they can be kept in large numbers and are the most diverse animal group (Grimaldi and Engel, 2005). Most artificial selection studies have been performed in *D. melanogaster*, such as on egg-to-adult developmental time (Chippindale et al., 1997; Nunney, 1996; Prasad et al., 2000; Sharma et al., 2020; Yadav and Sharma, 2013; Zwaan et al., 1995), fitness components (Rose, 1984), mating speed (Manning, 1961), or a courtship signal (Ritchie and Kyriacou, 1996). Finding the genetic targets of selection is a current challenge for biology.

Evolve-and-resequence (E&R) studies combine experimental evolution with next-generation sequencing of pools of individuals (Pool-seq). E&R can thus examine SNP frequency differences to identify causative alleles or genes (Schlötterer et al., 2014) and the loci underlying complex traits (Vlachos and Kofler, 2019). E&R studies have not only been successfully applied in bacteria and yeast, but also in *Drosophila* (Long et al., 2015). These experiments in *Drosophila* have focused on genome-wide responses to selection for generation time or time of reproduction (Burke et al., 2010; Graves et al., 2017; Teotonio et al., 2009). Also in the silkworm *Bombyx mori*, targets of artificial selection during domestication have been revealed (Yukuhiro et al., 2012; Zhu et al., 2019), for instance by resequencing genomes of 29 domesticated and 11 wild *B. mori* lines (Xia et al., 2009).

The red flour beetle *Tribolium castaneum* has become the second most important emerging model insect species after *Drosophila*, and is a ubiquitous Coleopteran pest of stored grain, flour, and other cereal products (Campbell et al., 2022; Klingler and Bucher, 2022; Pointer et al., 2021). Its embryos exhibit many ancestral features shared with most insects, such as short-germ development, embryonic leg development and an extensive extraembryonic serosa (Klingler, 2004; Panfilio, 2008; Schröder et al., 2008). This serosa protects the egg against desiccation and can mount a full-range immune response (Jacobs et al., 2013; Jacobs et al., 2014; Jacobs and van der Zee, 2013; Rafiqi et al., 2008). Since the genome of *T. castaneum* was published, plenty of available resources and technologies had been further developed for *Tribolium* researchers, such as CRISPR-Cas9 and systematic RNA interference (RNAi) (Bucher et al., 2002; Gilles et al., 2015). Knockdown phenotypes can be induced at all life stages and functionally transferred to the offspring through parental RNAi (pRNAi) (Consortium, 2008; Dönitz et al., 2015; Linz et al., 2014). In addition, long-term live imaging data of *T. castaneum* embryos can display the complete, continuous embryogenesis and did expand our knowledge of morphogenetic concepts beyond the *Drosophila* paradigm (Strobl and Stelzer, 2014).

Here, we have performed an E&R study on *T. castaneum*, artificially selecting for fast and slow embryonic development. During current climate change, it is important to understand to what extent insects can respond to selection on developmental time (Franks and Hoffmann, 2012; Renner and Zohner, 2018), as ecological mismatches in seasonal timing occur when global warming affects species differently (Kharouba et al., 2018; Samplonius et al., 2021; Thackeray et al., 2016). A striking example is the selective pressure on developmental time of the winter moth *O. brumata* to match shifted oak tree leaf-out (Van Asch et al., 2013). Until now, selection experiments have mainly been restricted to egg-to-adult developmental time in *Drosophila* (Chippindale et al., 1997; Nunney, 1996; Prasad et al., 2000; Sharma et al., 2020; Yadav and Sharma, 2013; Zwaan et al., 1995) and a few other insects (Fischer et al., 2007; Seslija and Tucic, 2003). Selection experiments on embryonic developmental time in have been scarce or reported as unsuccessful (Marinkovic, 1986; Neyfakh and Hartl, 1993). In chapter 3, I have reported the response to this selection in our six selection lines: fast A (Fa), fast B (Fb), non-selected A (Na), non-selected B (Nb), slow A (Sa) and slow B (Sb).

Here, we performed pooled resequencing on these lines in order to unravel the genetics underlying embryonic developmental time. We identify the cytochrome P450 Cyp18a1 as a main target of selection. This enzyme catabolizes active ecdysone (E20) by 26-hydroxylation (Guittard et al., 2011; Rewitz et al., 2010). The steroid hormone 20E is crucial in controlling developmental timing such as molting and metamorphosis, and is synthesized by other cytochrome P450 enzymes collectively called the Halloween genes. In this chapter, we also study the function of the Halloween genes and other cytochromes in larval, pupal and embryonic development. We report an ecdysone peak during embryonic development that initiates dorsal closure, one of the last stages of embryonic development during which the lateral ectodermal sides of the embryo dorsally meet to include the yolk (Panfilio, 2008). We find an allele, a 222 base pairs (bp) deletion upstream of *Cyp18a1*, that increased in frequency in the fast lines over the course of the selection. We demonstrate with CRISPR-Cas9 technology that this single deletion advances the embryonic ecdysone peak, advances dorsal closure, accelerates embryonic development, and trades off with fecundity, by regulating expression of *Cyp18a1* and accumulation of ecdysone.

Materials and methods

Selection lines of *Tribolium castaneum* beetles

The fast A (Fa), fast B (Fb), non-selected A (Na), non-selected B (Nb), slow A (Sa) and slow B (Sb) selection lines of T. castaneum are described in Chapter 3 (see materials and methods section, outbred populations of *Tribolium castaneum* beetles). After selection, they were kept as in (van der Zee et al., 2005).

Pooling genomic resequencing

Around 100 eggs of every selection line were dechrionated in commercial bleach (5% NaClO) and washed well with tap water. DNA was extracted using a standard phenol-chloroform extraction (phenol:chloroform:isoamyl-alcohol 25:24:1). The pooled DNA was sequenced on an Illumina Hiseq4000 machine with a paired-end 150 basepair layout. Reads have been deposited as NCBIs BioProject PRJNA942224.

SNP analysis

The raw reads were trimmed using TRIMMOMATIC (v 0.27, LEADING:3, TRAILING:3, SLIDINGWINDOW:4:15, MINLENGTH:70) (Bolger et al., 2014). The trimmed reads were aligned on the Tcas 5.2 (GCF_000002335.3) genome using bwa mem (v 0-7-15, default parameters, http://arxiv.org/abs/1303.3997). After mapping reads were filtered for quality (20) and sorted using samtools (v 0.1.19) (Li et al., 2009). We then removed duplicate using picard tools (v.2.8.2, http://picard.sourceforge.net) and performed realignment around indels with GATK (v .3.7-0) (McKenna et al., 2010).

The resulting BAM files were combined in mpileup format (samtools, mpileup, default parameters, v 0.1.19) (Li et al., 2009), after which SNPs and indels were separately called using varscan (v 2.3.9, using mpileup2snps and mpileup2indel resp., --output-vcf 1, --min-var-freq 0.05) (Koboldt et al., 2009) for which we only kept those variants that differed between the samples. The resulting raw vcf files was then annotated with snpEff (v 4.3)(Cingolani et al., 2012) using the Tcas 5.2 GCF_000002335.3 annotation file (GFF) (Herndon et al., 2020) as input. The resulting vcf files were further filtered using vcfR (v 1.8.0) (Knaus and Grunwald, 2017).

For the contrast between the fast and non-selected, as well as the slow and non-selected a similar approach was used. Only biallelic SNPs were analyzed that had a minimum coverage between the 0.05 and 0.98 quantiles (using quantile() function) of total depth for all samples. Furthermore, SNPs were

removed if they lay near indels (<10 bp) and if they were not present on the major chromosome scaffolds. A generalized linear model (GLM) was fitted with binomial error structure testing for treatments against non-selected, which was previously shown to be a powerful test for a evolve and re-sequence experiment (Hoedjes et al., 2019).

To create a H_0 permutated p value distribution, the two other possible sample configurations were used, and a GLM was run as well. For instance, for fast against non-selected, we tested FastA and FastB against NSA and NSB as the observed GLM. Then FastA and NSA were tested against FastB and NSB as the first permutation and FastA and NSB were tested against FastB and NSA as a second permutation. These two permutated distributions were then used to calculate the permutated p value distribution (empPvals(observed,c(H0_1,H0_2),pool=TRUE) and the resulting permutated p values were transformed into qvalues using the qvalue function (qvalue package). Loci were called significant when this qvalue was below 0.01.

Embryo fixation and DAPI staining

Fifty embryos of the selection lines were collected every 8 h at 25°C until more than 50% of all eggs hatched. Eggs were fixed in a 1:1 mix of 3.7% formaldehyde in PBS (PBS, pH 7.4) and heptane for 20 min , and devitellinized using a methanol shock. They were brought back to PBST (PBS with 0.2% Tween 20) , and, stained with 4′-6-diamidino-2-phenylindole (DAPI) for 15 min, and finally mounted on microscope slides to take pictures. Embryos were photographed under a Zeiss Axioplan 2 imaging microscope (Zeiss, Mannheim, Germany) equipped with a DAPI filter (XF–06, excitation 330–390 nm, emission 410–490 nm). Images were processed using Adobe Photoshop (version 23.5). The embryonic stage values were attributed to each embryo according to the staging scheme in Supplementary Figure 4-1). The average stage values are reported in Figure 4-2.

Sample collection for transcriptional analysis

Embryonic development of the selection lines for transcriptional analysis was decided according to fluorescent microscopic analysis. For RT-qPCR and RNAseq, total RNA of approximately 200-300 eggs was isolated by Trizol extraction (Invitrogen) after which the RNA was purified and DNA digested on column with the RNeasy kit (Qiagen). The quality of isolated RNA was measured spectro-photometrically and on a 1.0% agarose gel. We collected three biological samples for the fast (Fa and Fb) and the non-selected lines (Na and Nb) at 76 h post-oviposition according to *T. castaneum* embryos live imaging results (Figure 4-2), giving a total of 12 biological samples. For RNAseq, cDNA library synthesis and sequencing was performed by ZF-screens (Leiden, the Netherlands) sequencing company on an Illumina HiSeq2500 sequencer. For qPCR analysis, we collected four biological samples for the fast (2 samples of Fa and 2 of Fb) and the non-selected lines (2 samples of Na and 2 of Nb),at 76, 92 and 108 h post-oviposition.

RNA sequencing analysis

The raw reads were checked for quality using FastQC version 0.11.9 (https://www.bioinformatics.babraham.ac.uk/projects/fastqc/). Reads were trimmed by eliminating any ambiguous or low-grade reads and the adaptor sequences using Trimmomatic (v0.39; HEADCROP:10 MINLEN:50 TRAILING:20). The trimmed paired end reads were aligned and mapped to the Tribolium genome 5.2 using STAR (2.7.10a). Read counts per gene were quantified using htseq-count (Anders et al., 2015). Differential expression analysis were performed using DEseq2 version 1.34.0 (Love et al., 2014). The significant difference is represented in gene expression by more than 1.25-fold upregulation and 0.8-repression both with a threshold adjusted $P < 0.05$. The false discovery rate (FDR) was performed as described as in (Jacobs et al., 2014).

cDNA synthesis and qPCR

The experimental RNA was collected as described under 'Sample collection for transcriptional analysis'. One microgram of total RNA was performed for cDNA synthesis (Promega Reverse Transcription system). 2 µL of 1:10 diluted original cDNA was used in every RT-qPCR reaction. qPCR reactions were done using the SsoAdvanced Universal SYBR Green Supermix (Bio-rad) on a CFX96 thermocycler (Bio-rad). Thermal conditions were as follow: an initial step at 95 °C for 30s; 40 cycles of 95°C for 15 s, 60°C for 30 s, 72°C for 30 s; this was followed by dissociation analysis of a ramp from 65°C to 95°C with a read every 0.5°C. RPL13a gene was used as internal control to calculate ΔCT values (Lord et al., 2010). Relative expression was calculated with regard to the average of the non-selected lines (Figure 4-5) or a defined time point (Figure 4-13, Figure 4-14, Figure 4-15) using the $2^{-\Delta\Delta C}$T method (Livak and Schmittgen, 2001), or presented as fraction of RPL13a expression (Figure 4-33). Total RNA for each treatment was isolated two times (biological replication) and each sample was measured by RT-qPCR twice (technical replication). All candidate genes and their acronyms are listed in Supplementary Table 4-1. All of primers used for qPCR were in Supplementary Table 4-2. Significance of fold change differences was estimated by a student's t-test, shown in Figure 4-5.

Molecular cloning and RNAi

The *Tribolium* stock used for RNAi was the other common wild-type strain of *Tribolium*, Georgia-1 (GA-1). RNAi for all of candidate genes were performed as described in (van der Zee et al., 2005; Zee et al., 2006). All target genes were searched from GenBank and showed in Supplementary Table 4-3 and Supplementary Table 4-4. Gene fragments were cloned into the pCR™II-TOPO™ TA vector (Invitrogen), and inserts were confirmed by Sanger sequencing. The plasmids were linearized with an appropriate restriction enzyme to generate DNA templates for in vitro transcription with SP6 and T7 polymerases, and resulting dsRNA was purified using the Ambion MEGAscript RNAi kit. The control dsRNA was synthesized as a 500 bp the pCR™II-TOPO™ TA vector sequence (Invitrogen) (Jacobs et al., 2013; Jacobs et al., 2014).

For parental RNAi (pRNAi), a mixture of 0.4 µL of 0.5-1.0 µg/µL dsRNA was also performed according to (Bucher et al., 2002; Zee et al., 2006). 2h egg lays were put in on the selection machine (see in Chapter 3) to measure developmental time next to a control RNAi with dsRNA from the 500 bp bacterial vector sequence without target in the *Tribolium* genome (Jacobs et al., 2013; Jacobs et al., 2014). Measurements were performed in triplicate and significance of the difference with control developmental time was determined by a student's t-test.

For larvae RNAi, a mixture of 0.4 µL of 0.5-1.0 µg/µL dsRNA was injected into the dorsal segments of the penultimate-instar or last-instar larvae. For pupae RNAi, a mixture of 0.2 µL of 0.5-1.0 µg/µL dsRNA was injected into the abdomen of both female and male pupae (Linz et al., 2014). For embryonic RNAi, 4-6 h old eggs of LifeAct-nGFP line (van Drongelen et al., 2018) were injected as much as possible but avoiding leaking much yolk (Berghammer et al., 2009).

Ecdysone detection

At the desired timepoint after a 2h egg lay, 50 eggs were dechorionated in 0.5% bleach for 2 min, homogenized in 300 µl of methanol, and centrifuged for 10 min at 12,000rcf. The supernatant was collected into a new 1.5 mL tube, dried completely in a vacuum centrifuge, and the precipitate was redissolved in 120 µl EIA buffer provided by a competitive enzyme immune assay (EIA) kit for 20-hydroxyecdysone (20E, Bertin Pharma). After 2h incubation at room temperature, the samples were diluted 4 times in EIA buffer and applied to the detection plate according to the manufacturers protocol. The plate was developed with 200 µl of Ellman's reagent and incubated with an orbital shaker at in the dark at RT. After 90 min, the plate was measured at a wavelength of 410 nm on a

Tecan Spark microplate reader. The concentrations were determined by a four parameter logistic fitting.

In situ hybridization

An 1124 bp fragment of *Cyp18a*1 and a 837 bp fragment of *Spo* were cloned into the pCR™II-TOPO™ TA vector (Invitrogen). The fragments of *Cyp18a1* and *spook* (*Spo*) used here was same with that used for RNAi (Supplementary Table 4-3 and Supplementary Table 4-4). Templates were generated using M13 primers. DIG-labeled antisense probes were synthesized using SP6 polymerase for Cyp18a1 and T7 polymerase for Spo (Ambion) with Roche RNA labeling mix (Roche). Sense probes were synthesized as control. *In situ* hybridizations on whole mount fixed eggs (see embryo fixation and dapi staining) were essentially performed as described in (Tautz and Pfeifle, 1989), but without the ProteinaseK step. To manually dissect eggs containing the serosa from the vitelline membrane, we used Tc-CHS1 RNAi eggs, as the serosa tightly associates with the vitelline membrane (Jacobs et al., 2014).

PCR genotyping

DNA from individual beetles was extracted using the phenol-chloroform extraction (phenol:chloroform:isoamyl-alcohol 25:24:1), after 1.5 µg/µl proteinaseK incubation overnight at 55°C. PCRs with Bio SeqAMP polymerase (Takara) using the primers 5′-AAGGGGCCCTCTCAAACATC-3′ and 5′-CAGGCACCTCTGCGTTATCC-3′ generated a 942 bp band for homozygotes containing both repeats, a 720 bp band for homozygotes for the deletion, and both bands plus a hybrid band running slower because of the formed loop for the heterozygotes.

Population genetic modeling

Using the genotyping data from generations 0, 3, 7, and 21, we fitted a model with and without fitness differences for the three genotypes. For each generation, the initial allele frequency for F was fitted. For each of the parameter settings, the model was calculated forward and the multinomial probability of finding the actual genotype counts was calculated and denoted as the likelihood of the model. The two models, with or without selection were then tested for significant difference using the likelihood ratio test, which was tested against the χ^2 distribution using

$$\chi 2 = -2(L_{WFF==WFS==WSS} - L_{WFF!=WFS!=WSS}) \qquad (1)$$

where L is the log likelihood. The models were fitted starting from the estimated initial frequency for F, using the count data at generation 0 and equal fitness values for the genotypes FF, FS and SS. Then the likelihood of the model was calculated, and the parameters updated using a change randomly drawn from a normal distribution (mean 0, std of 0.01). The new parameters for allele frequency were limited such that they would not be smaller than 0 or larger than 1. For fitness, the changes were not allowed to become lower than 0. At each iteration, the maximum fitness was set to 1. When the likelihood of the model was higher than the previous best fit, the parameters were updated using the new best fit parameters.

CRISPR/Cas9 constructions and *Tribolium* injection

The oligonucleotides 5′-AGTGAAATATAGGGTGTTCCATT-3′ and 5′-AAACAATGGAACACCCTATATTT-3′ were ligated into the BsaI-digested p(U6a-BsaI-gRNA) vector (Addgene) (Gilles et al., 2015) for in vivo expression of the desired gRNA. This construct and the TrueCut Cas9 Protein v2 (Invitrogen) were co-injected each at a concentration of 500 ng/µl into 2h old embryos of the Georgia laboratory strain according to (Berghammer et al., 2009). A brief process diagram of Crispr/Cas experiment for a repeated region is shown in Figure 4-1. Single crosses of virgin G0 animals were set up, and their G1 offspring was collected. A PCR (as described above for

genotyping) on the mosaic G0 parents was performed to get an impression of excision efficiency. Offspring from G0 parents that still showed the repeat containing 942 bp band was rejected, leaving G1 offspring from 6 G0 pairs. Among the remaining G1 offspring, 22 single virgin crosses were set-up, and their G2 offspring was collected. G1 parents were genotyped by PCR in order to choose a pair to set up the stock. PCR products were cloned to determine the sequence of all 4 alleles present in the stock (Figure 4-30).

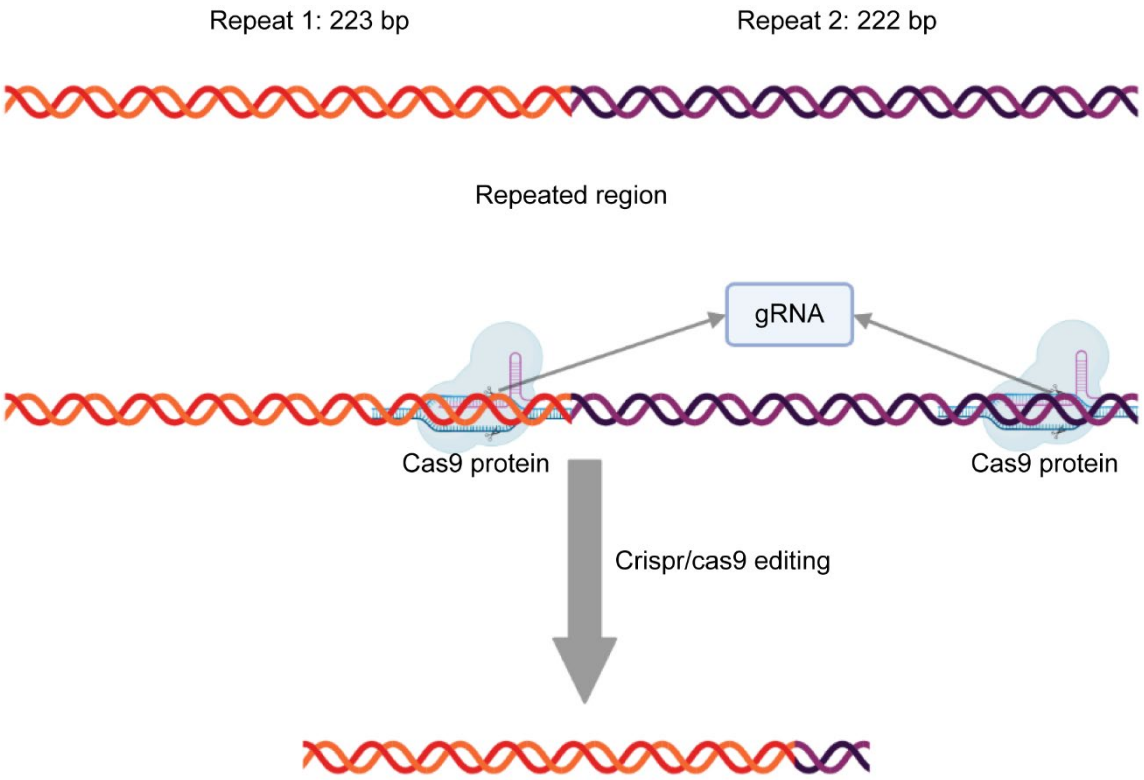

Figure 4-1. A brief process diagram of Crispr/Cas experiment to obtain the CRISPR-induced deletion strain of *Tribolium castaneum*.

Live imaging

200 females of the nGFP line (Sarrazin et al., 2012) were selected at the pupal stage, and 100 of these females were crossed with 100 males of GA-1, and the other 100 females were crossed with 100 males of the CRISPR line (see above). These two groups of 200 parents were allowed to lay eggs for 20 minutes, and 10-15 of their eggs were imaged under a Nikon AX confocal laser scanning microscope (Nikon Europe B.V., Amsterdam, Netherlands) taking full scans every 26 minutes.

Binding site analysis

Binding matrices for Br (var.4), Ttk, and EcR::usp, we downloaded from JASAPAR (Castro-Mondragon et al., 2022), and used to search motifs in the whole intergenic region upstream of Cyp18a1 (chromosome 9: NC_007424.3[1611573..1619999]) with FIMO (Grant et al., 2011).

Results

Variation under artificial selection is in the timing at start of dorsal closure

To investigate whether the different embryonic developmental times (see in Chapter 3) were caused by overall acceleration or deceleration, or whether specific developmental processes sped up or slowed down, we defined a numerical staging table (Supplementary Figure 4-1). We fixed and DAPI stained around 50 eggs of selection lines every 8 h until hatching. By fluorescent microscopic analysis, we found that embryonic development among selection lines do not show any difference before germband extension, of which the judgement value is defined as 8. After 72 h post-oviposition, the eggs of the fast lines directly start to develop into next stage which is called "start of dorsal closure" and is characterized by formation of the dorsal organ, the retracting serosa (Supplementary Figure 4-1j). However, embryonic development of both non-selected and slow lines continued in the retracted germband stage for another 8 and 16 h, respectively, while eggs of fast lines are already in the hatching stage after these 16h. Thus, the average stage values demonstrate that the start of dorsal closure differs among the lines, and that the start of dorsal closure occurs earlier in the fast lines (Figure 4-2).

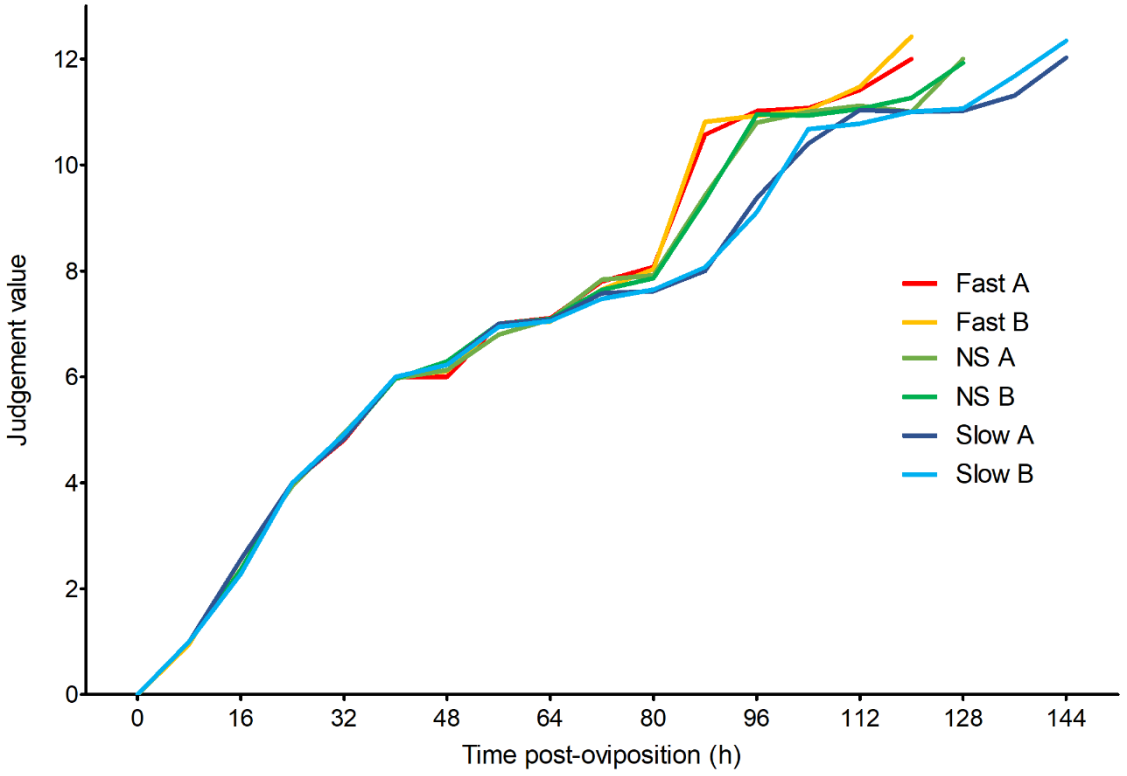

Figure 4-2. Developmental stage during embryonic developmental time (hours after egg lay) of the selection lines (stage values defined in Supplementary Figure 4-1). Start of dorsal closure is the first stage at which a difference in timing can be detected among the selection lines. Judgement values given to fourteen embryonic stages are used to score embryonic development of the selection lines. 0=no nuclei at surface; 1=undifferentiated blastoderm; 2=differentiated blastoderm; 3=gastrulation; 4=extending germband; 5=extended germband; 6=limbs growing and extending; 7=retracting germband; 8=completely retracted germband; 9=start of dorsal closure (dorsal organ formation); 10=dorsal closure in progress; 11=dorsal closure completed; 12=hatching; and 13=hatched. See more details in Supplementary Figure 4-1. Fast A, fast B, non-selected A (NS A), non-selected B (NS B), slow A and slow B are shown with red, orange, green, light green, dark blue, and light blue lines.

Pooled whole-genome resequencing reveals 45 candidate genes under selection

Manhattan plots show that SNP frequency differences between the slow lines and the non-selected lines are hardly ever below q=0.01 (i.e. -log(p) is above 33.0538; red line in Supplementary Figure 4-2). Only 1258 SNPs differed significantly in frequency between the slow and non-selected lines (Supplementary Figure 4-2). However, 8469 SNPs differed significantly in frequency between the fast and non-selected lines (Figure 4-3A). Two areas, on chromosome 3 and on chromosome 9, contain a high number of these very significant SNPs and appear to have been under strong selection in the fast lines (Figure 4-3A). We focus on these two genomic regions in the remainder of this study.

In these regions (position 13.8-15.8 MB on chromosome 3 and position 0.5-4 MB on chromosome 9), we identified 48 principal SNPs based on significance of allele frequency differences Supplementary Table 4-1)). In detail (Supplementary Table 4-1), principal SNPs have an allele frequency difference >0.6 and do not have a higher SNP within 10kb. On chromosome 3, principal SNPs have a -logp value > 58.5. On chromosome 9, principal SNPs have a -logp > 60. All principal SNPs are indicated in red (Figure 4-3B, C). In addition, we also selected 9 very significant SNPs (-logp value > 40, Supplementary Table 4-1) neighboring these principal SNPs. We defined these principal and significant SNPs together as our lead SNPs in this study. We associated these 57 lead SNPs with 45 candidate genes in total (numbered in Figure 4-3B, C). See all lead SNPs, genes and their annotations in Supplementary Table 4-1. For instance, a gene called Cytochrome P450 18A1 was identified by the most significant SNP on chromosome 9 at position 1,613,665 (Cyp18a1, gene 32, Figure 4-3C, Supplementary Table 4-1). Melted was identified by the principal SNP 6 that has the highest frequency difference of all these lead SNPs (at position 14,086,409, gene 5, Figure 4-3B, Supplementary Table 4-1).

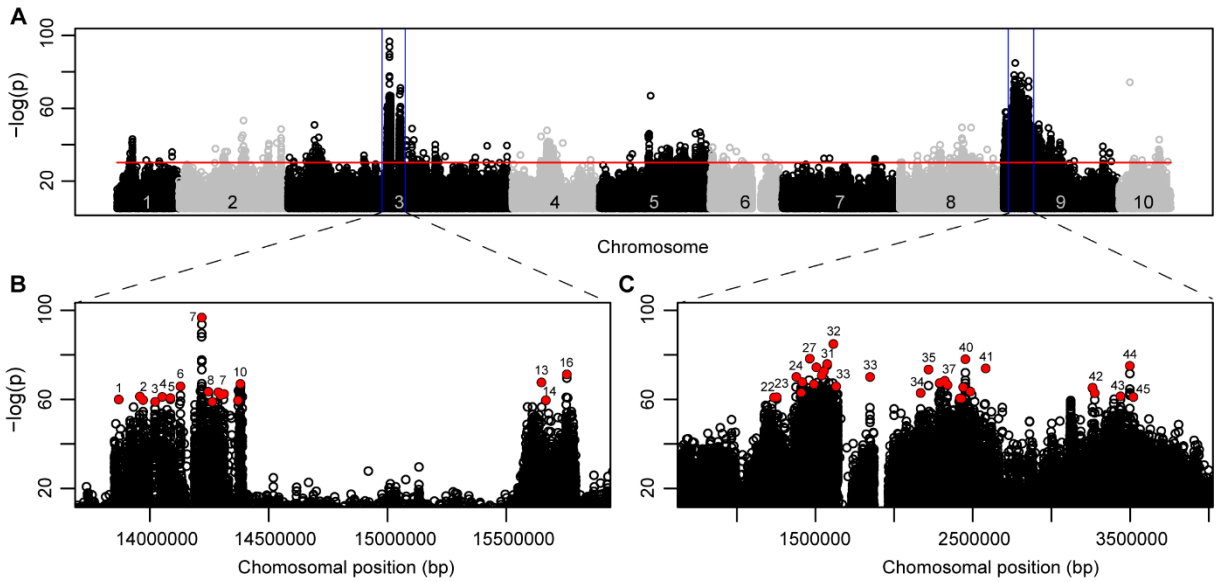

Figure 4-3. SNP analysis on whole genome of *Tribolium castaneum* between the fast lines and the non-selected lines (A). of which, red line represents q = 0.01 or -log(p) > 30.2275. The significance of allele frequency differences zoomed in on chromosome 3 (B) and 9 (C), respectively. Principal SNPs are indicated in red. Numbers refer to the associated genes with 48 principal SNPs. See all SNPs and their associated genes in Supplementary Table 4-1.

Expression analysis restricts the number of candidate genes to 15

As none of our 57 lead SNPs leads to alternative proteins, we first investigated differential gene expression between the fast and the non-selected lines using RNAseq. We isolated RNA at 76h, just

before the differences among the selection lines become apparent during embryonic development (Figure 4-3).

A total of 739 genes were upregulated (FC > 1.25 and padj < 0.05) and 258 genes were downregulated (FC < 0.8 and padj < 0.05) in the embryos of the fast lines compared to the samples of the non-selected lines (all dots in Figure 4-4). However, only 7 of these overlapped with the 45 genes that were identified as targets of selection in the SNP analysis. These are *mGluR*, *Cyp18a1*, *Lac2*, *LOC657682*, *Lipase*, *Cyp306a1* and *Sec61α* that were significantly upregulated in the fast lines. And *Deadpan* and *LOC103314169* that were significantly down-regulated in the fast embryos compared to the non-selected samples. If the more stringent fold-change cut-off of >2 and <0.5 was applied, the number of differentially expressed genes was restricted to 122 (red and green dots Figure 4-4), and reduced the candidate genes to *mGluR* and *Cyp18a1*.

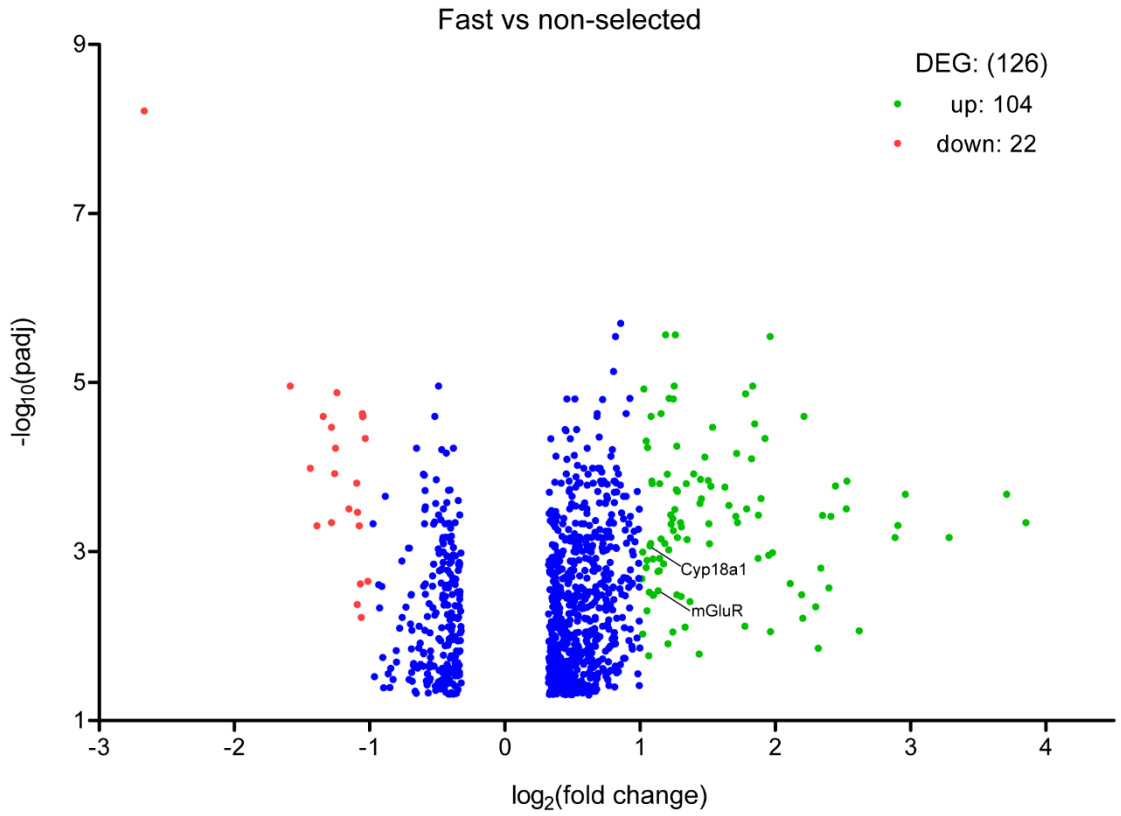

Figure 4-4. Volcano plot of differentially expressed genes in the fast and non-selected lines, with *Cyp18a1* labeled. Differentially expressed genes were selected by |log2 (fold change)| > 1 and padj < 0.05. X-axis, the fold change in gene expression between fast and non-selected lines; y-axis, statistical significance of the differences. Dots represent different genes. Green dots represent significantly up-regulated genes >2 fold. Red dots represent significantly down-regulated genes <0.5 fold. Blue dots stand for genes with padj < 0.05 but 1.25 < FC < 2, or 0.5< FC < 0.8.

To get more precise insight in the differential expression over time of the 45 candidate genes identified in the Pool-seq SNP analysis, we performed qPCR on all of these 45 genes before (76 h post-oviposition), during (92 h) and after (108 h) dorsal closure. Of two polycystin-related genes (genes 22 and 23), we could not detect any expression, but of the remaining 43 genes, 27 showed significant differential expression at one of the three timepoints at least (Figure 4-5).

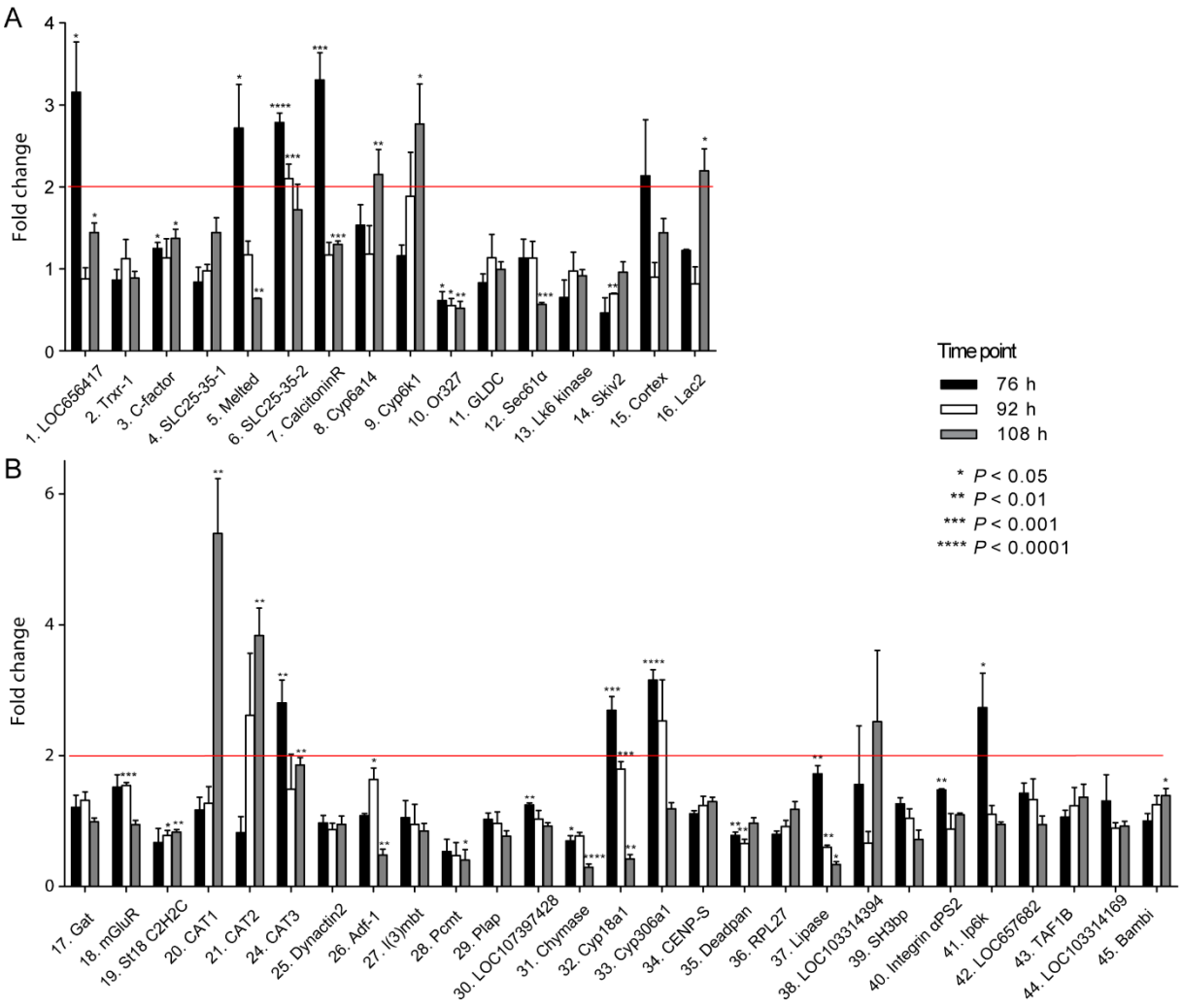

Figure 4-5. Fold change (FC) in the expression of candidate genes. A, FC on chromosome 3, and B, FC on chromosome 9 when we compared between fast and non-selected lines at 76, 92 and 108 hours post-oviposition. Each vertical bar represents the mean fold change plus standard error based on four biological replicates (each replicate is the mean of two technical replicates), of which 2 biological replicates from A line, and 2 from B line. The student t-test was performed to compare the control and treatments. Asterisks, significant difference between fast and non-selected lines. P-values are shown in the figure and indicated with *, $P < 0.05$; **, $P < 0.01$; ***, $P < 0.001$; ****, $P < 0.0001$.

In particular, before dorsal closure, fast developing embryos showed significantly higher expression of 12 genes (P <0.05), of which 5 genes were located on chromosome 3, and 7 genes on chromosome 9. We also observed significantly lower expression (P <0.05) of 1 gene on chromosome 3, and 2 on chromosome 9. During dorsal closure, 3 genes on chromosome 3 and 6 on chromosome 9 were differentially expressed (P <0.05). After dorsal closure, 10 genes were significantly upregulated (P <0.05), including 6 on chromosome 3, and 4 on chromosome 9. At this last timepoint, 9 genes were significantly downregulated (P <0.05); comprising 3 genes on chromosome 3, and 6 on chromosome 9 (Figure 4-5).

We then applied a more stringent rule: fold change of a gene is greater than 2 or less than 0.4 times. This resulted in 15 selected genes shown in Table 4-1, including *Cyp18a1*, *Lac2*, *lipase* and *Cyp306a1* that were also found in the RNAseq analysis, but not *mGluR*, *Sec61a* and *deadpan*.

Table 4-1. All genes on chromosome 3 and 9 that show a higher than 2 or smaller than 0.4 fold change in qPCRs at 76, 92 or 108 h post-oviposition.

Time point	Chromosome	Genes acronym	Mean of fold change
76 h	3	1. *LOC656417*	3.16
		5. *Melted*	2.72
		6. *SLC25-35-2*	2.78
		7. *CalcitoninR*	3.30
	9	24. *CAT3*	2.81
		32. *Cyp18a1*	2.69
		33. *Cyp306a1*	3.15
		41. *Ipk1*	2.73
92 h	3	6. *SLC25-35-2*	2.10
108 h	3	8. *Cyp6a14*	2.15
		9. *Cyp6k1*	2.77
		16. *Lac2*	2.20
	9	20. *CAT1*	5.39
		21. *CAT2*	3.83
		31. *Chymase*	0.29
		37. *Lipase*	0.34

A pRNAi screen identifies four genes under selection that are involved in developmental timing

We performed parental RNAi (pRNAi) screening on these 15 identified candidate genes from Table 4-1 to identify those genes functionally involved in the timing of embryonic development. The primers to generate templates for dsRNA synthesis are shown in Supplementary Table 4-3.

The results showed that the embryos from the mothers injected with *Cyp18a1* dsRNA developed significantly slower (167 h) than those from the mothers injected with the control dsRNA (152 h), as confirmed by a student's t-test ($P< 0.0001$). While two thirds of the eggs hatched to larvae in the control pRNAi, only one third of the Cyp18a1 RNAi eggs hatched to larvae. Of these larvae, a quarter displayed normal hatching times, whereas three quarters hatched with a strong delay compared to control pRNAi larvae (Figure 4-6). Furthermore, there was no difference in embryonic development between the control pRNAi and blank control (Supplementary Figure 4-3), where we did not inject any mothers but collected the eggs from the same number of females.

We also found slower developmental time upon *Melted* (160 h) and *SLC25-35-2* (161 h) pRNAi, and slightly delayed development upon *CAT1* dsRNA injections (155 h) into *Tribolium* mothers. pRNAi against other candidate genes did not show a significant effect on the time of embryonic development compared to the control (Figure 4-6).

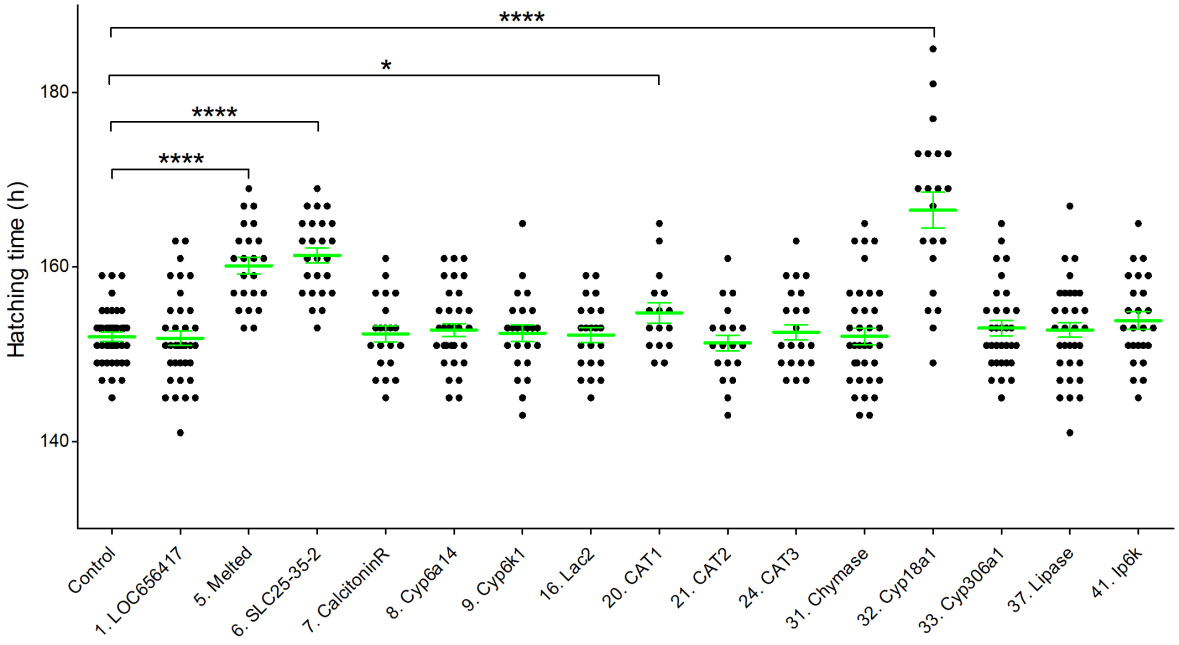

Figure 4-6. The embryonic developmental time of offspring embryos upon a pRNAi screen. It was significantly delayed upon *Melted*, *SLC25-35-2*, *CAT1* and *Cyp18a1* dsRNA injections into 50 *Tribolium* mothers, compared to injections of non-targeting control dsRNA. Key: Green lines, mean of embryonic developmental time plus standard error. Black dot, the time of every hatched embryo. The student t-test was performed to compare the control and treatments. Asterisks, significant difference in hatching time (*, $P < 0.05$; ****, $P < 0.0001$).

Hatching rate upon *Melted*, *SLC25-35-2* and *Cyp18a1* pRNAi is 56, 63 and 33%, respectively, compared to a 67% hatching rate upon control RNAi. These hatching rates are also reflected in the number of adults observed. When we collected all eggs laid within 2 days from 50 injected mothers, 132, 120, 128 and 11 adults were found upon control, *Melted*, *SLC25-35-2* and *Cyp18a1* pRNAi, respectively (Figure 4-6).

In conclusion, the pRNAi screen has identified four interesting target genes involved in developmental timing: *Melted*, *SLC25-35-2*, *CAT1* and *Cyp18a1*, of which knockdown of *Cyp18a1* caused the largest developmental delay.

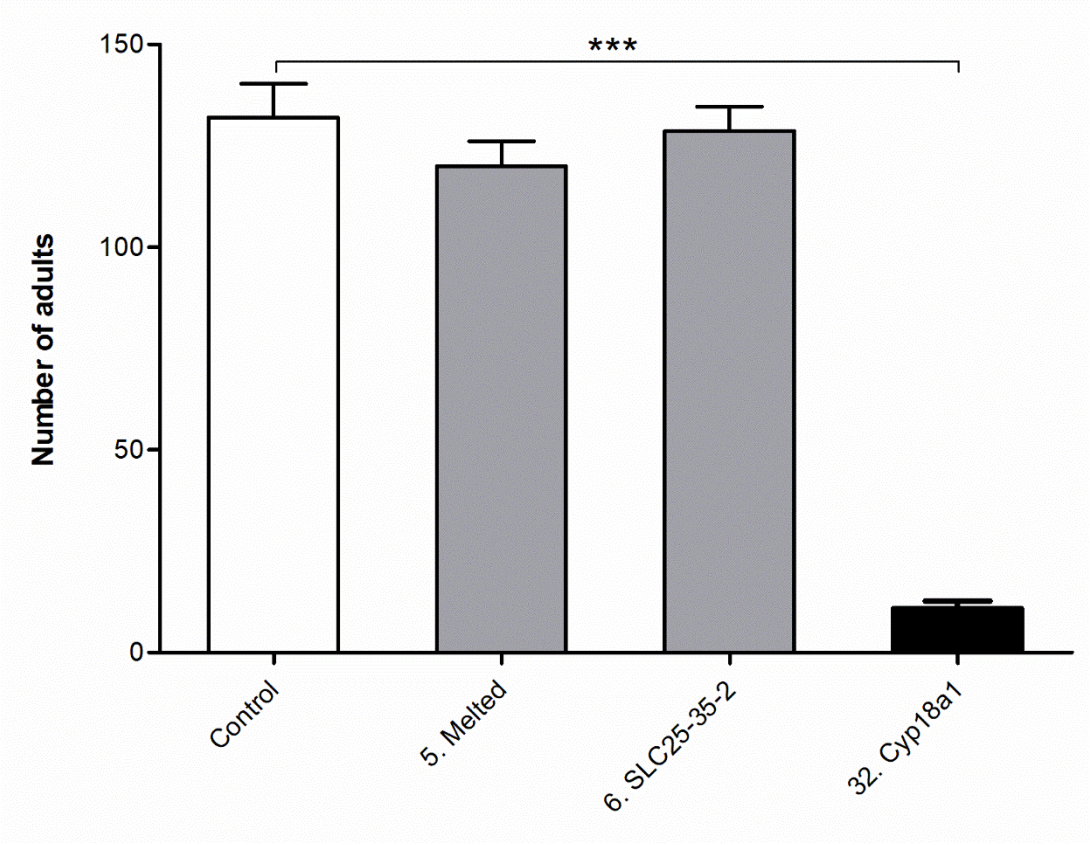

Figure 4-7. Number of adults upon pRNAi, when we collected eggs within 2 days upon control, *Melted*, *SLC25-35-2* and *Cyp18a1* pRNAi, respectively. Measurements were performed in triplicate. Each vertical bar represents the mean fold change plus standard error. The student t-test was performed to compare the control and treatments. Asterisks, significant difference in number of adults (***, $P < 0.001$).

Cyp18a1 is required for pupation and eclosion

Cyp18a1 is a Cytochrome P450 enzyme that catabolizes active ecdysone (20E) by 26-hydroxylation (Guittard et al., 2011; Rewitz et al., 2010). The steroid hormone 20E is crucial in regulating developmental timing events such as larval moulting, pupation and eclosion (Nijhout et al., 2014). 20E is synthesized by other Cytochrome P450 enzymes, such as Phantom (Cyp306a1), Spook (CYP307A1), Shadow (CYP315A1) and Shade (Cyp314A1), collectively called the Halloween genes (Niwa and Niwa, 2016). Besides *Cyp18a1*, three other Cytochrome P450 enzymes are differentially expressed among our selection lines, including one known Halloween gene (*Phantom*, *Cyp306a1*), and two others: *Cyp6a14* and *Cyp6k1*.

As ecdysone regulates tractable developmental events such as pupation and eclosion, we first analyzed the role of these four cytochromes (*Cyp6a14*, *Cyp6k1*, *Cyp18a1*, and *Cyp306a1*) in these timing events. We did this by RNA with a high concentration of dsRNA (0.8 mg/ml), alongside a combined RNAi against the ecdysone receptors *EcR* and *Ultraspiracle* (*Usp*) in similar concentration as positive control. The results showed that *Cyp18a1* RNAi had caused the highest mortality in both larvae (97%, n = 30) and pupae (100%, n=30) (Figure 4-8). All the pupae injected with 0.2 µL of the highly concentrated (0.8 µg/µL) Cyp18a1 dsRNA arrested their development within 3 d post-injection and then died owing to the melanization reaction (Figure 4-9). The second higher mortality was found in the positive control group in larvae (87%) and pupae (40%) (Figure 4-8). At the same time, no obvious increase in mortality was observed upon *Cyp6a14*, *Cyp6k1* and *Cyp306a1* RNAi in larvae and pupae

compared to non-targeting control dsRNA injections (Figure 4-8). All of primers of the Halloween genes to clone templates for RNAi are listed in Supplementary Table 4-5.

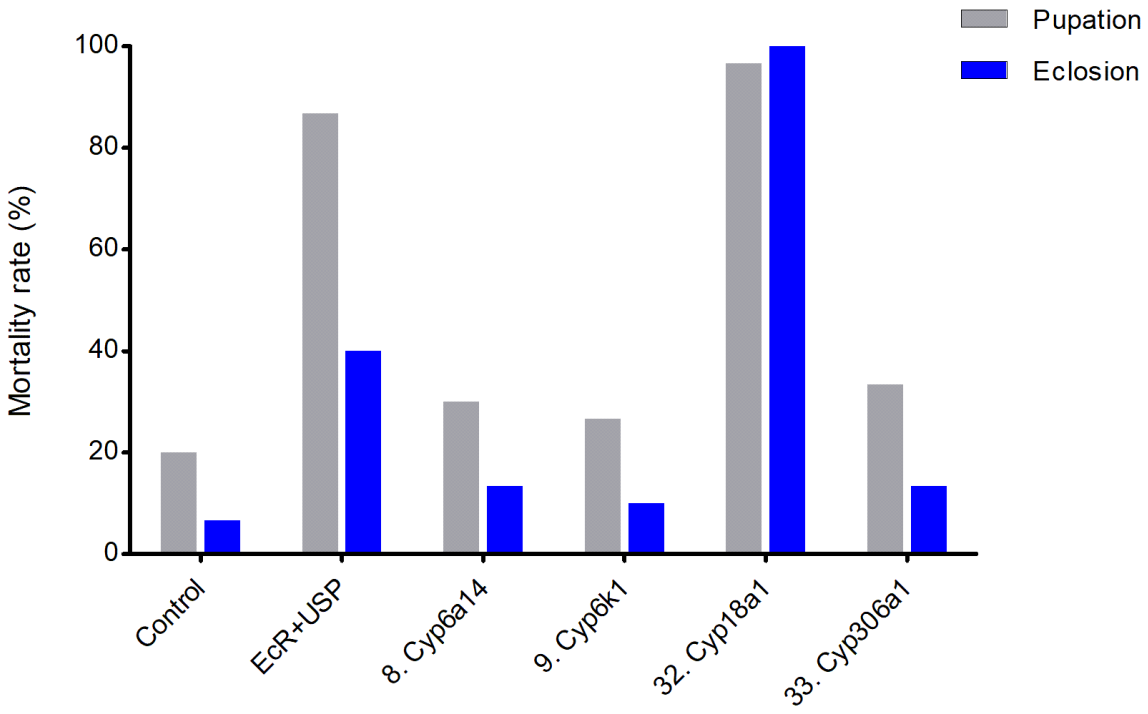

Figure 4-8. Mortality of *Tribolium* larvae and pupae after injections of non-targeting control, the positive control (*Ecr* and *USP*), or the four cytochrome P450s (*Cyp18a1*, *Cyp306a1*, *Cyp6k1* & *Cyp6a14*) dsRNA during pupation (grey columns) and eclosion (blue columns), respectively. n = 30 per treatment.

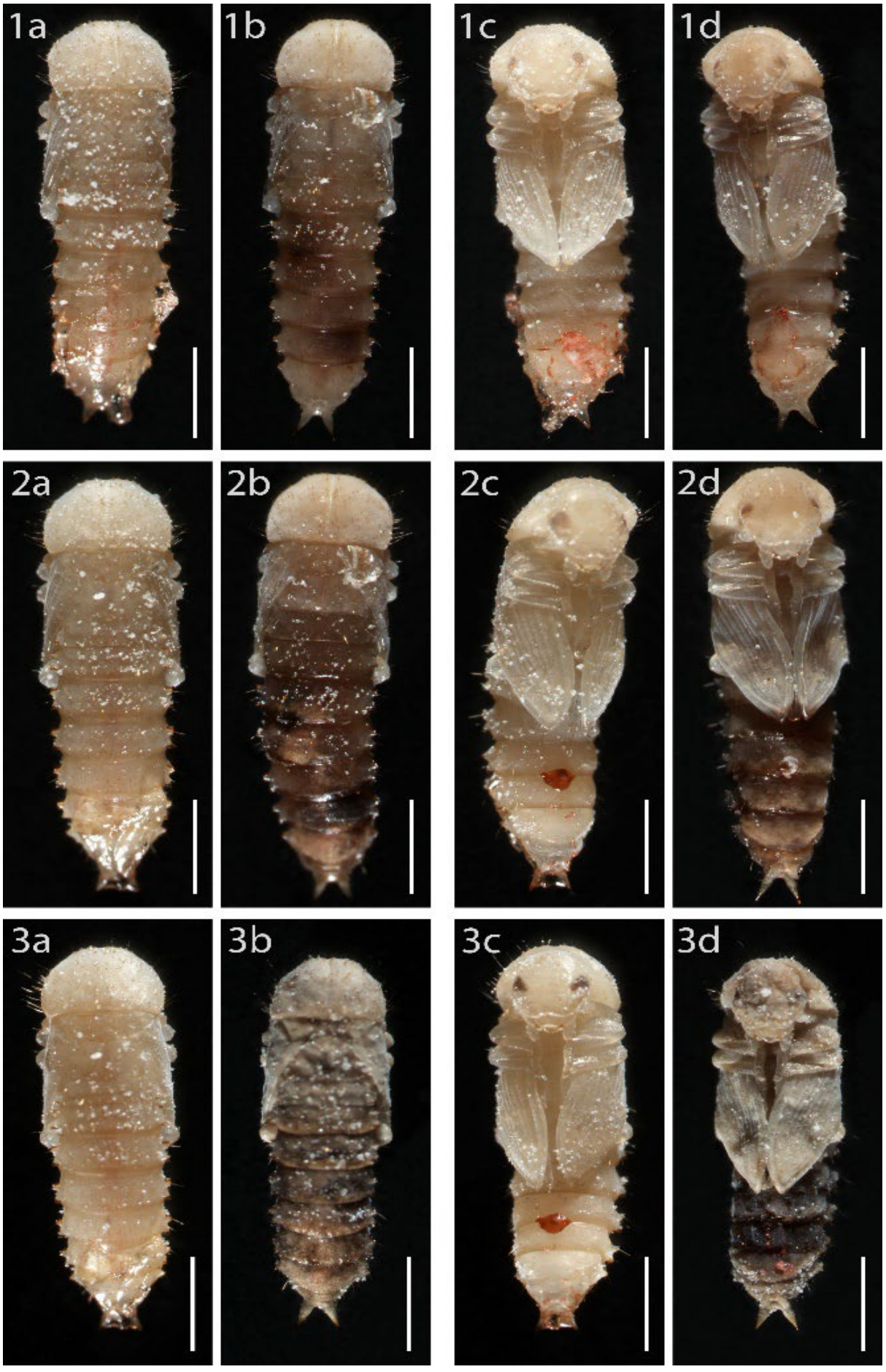
1a
1b
1c
1d
2a
2b
2c
2d
3a
3b
3c
3d

Figure 4-9. *Cyp18a1* RNAi phenotypes in pupae. All the pupae injected with *Cyp18a1* dsRNA arrested their development within 3 days post-injection. Letters "a" and "c" represent the dorsal and ventral side of pupae upon the control gene RNAi, respectively. While "b" and "d" are from the *Cyp18a1* RNAi. "1", "2" and "3" indicate 1 day, 2 days and 3 days post-injection, respectively. Scale bar: 1 mm.

Of the surviving RNAi larvae, the *EcR/USP* RNAi and *Cyp6a14* RNAi (0.8 ug/ul) delayed development to some extent, but the strongest delay was observed upon the strong *Cyp18a1* RNAi (0.8 ug/ul) (Figure 4-10). Surprisingly, no effect on developmental timing was observed upon RNAi against the known Halloween gene *Cyp306a1*.Taken together, *Cyp18a1* RNAi arrested development (Figure 4-9) or led to strong developmental delay (Figure 4-10), whereas no strong indication for involvement of *Cyp6a14*, *Cyp6k1* or *Cyp306a1* was found.

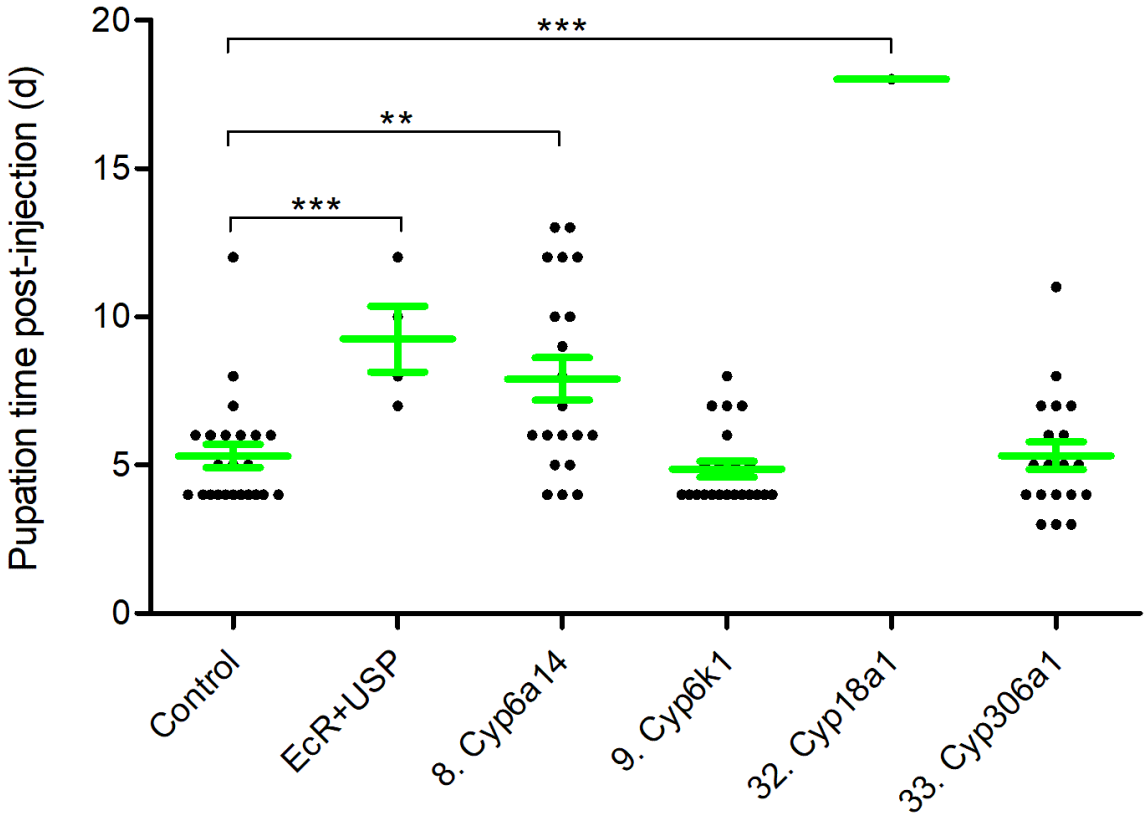

Figure 4-10. Pupation time post-injection with non-targeting control, the positive control or the four cytochrome P450s (*Cyp18a1*, *Cyp306a1*, *Cyp6k1* & *Cyp6a14*) dsRNAs in 15 day old larvae. Key: Green lines, mean of developmental pupation time plus standard error. Black dot, the pupation time of every surviving beetle. The student t-test was performed to compare the control and treatments. Asterisks, significant difference in pupation time post-injection (**, $P < 0.01$; ***, $P < 0.001$).

To reduce the high mortality upon *Cyp18a1* RNAi (Figure 4-8), and in order to study a developmental phenotype in more detail, we reduced volume and concentration of the dsRNA injections by half (to a 0.1 ul injection of 0.4 ug/ul dsRNA). All the quiescent larvae (prepupae) (n=22) never pupated upon the injections of *Cyp18a1* dsRNA and showed abnormal body color and melanization (Figure 4-11). While 55% (12/22) quiescent larvae can hatch to pupae upon non-targeting control RNAi. This shows that that *Cyp18a1* is required for pupation.

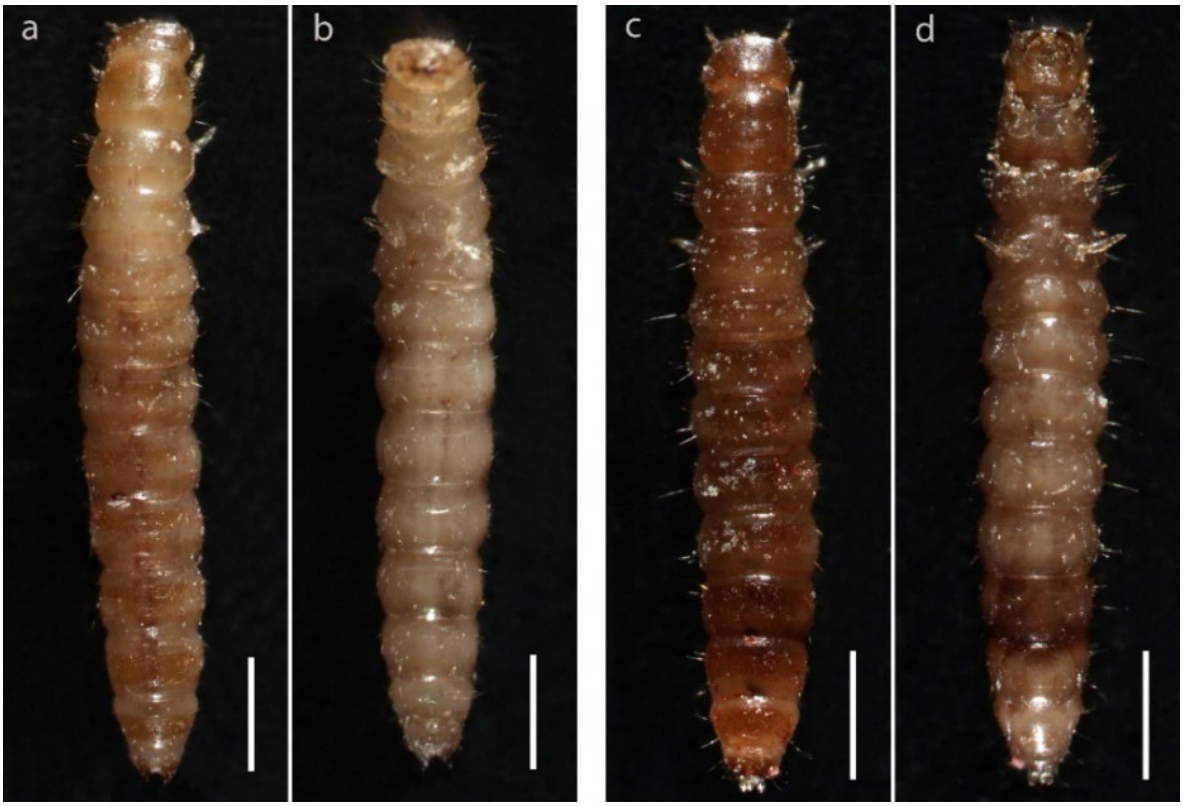

Figure 4-11. *Cyp18a1* RNAi phenotypes in prepupae at 30 hours post-injection. Letters "a" and "b" represent the dorsal and ventral sides, respectively, of prepupae after injections of the control dsRNA; "c" and "d" are results upon *Cyp18a1* RNAi. Scale bar: 1 mm.

For pupae injections, a mixture of 0.1 µl of 0.4 µg/µl dsRNA was injected into the abdomen of 0-day pupae. All of the control injected pupae (n = 20) eclosed as adults (Figure 4-12a-c). However, 85% of the *Cyp18a1* dsRNA injected pupae (n =17/20) never eclosed (Figure 4-12dg,eh,fi). These pupae sclerotized, but did never develop typical adult features, such as the folding of wings and elytra over the abdomen (Figure 4-12dg,eh,fi). In conclusion, *Cyp18a1* is also required for eclosion.

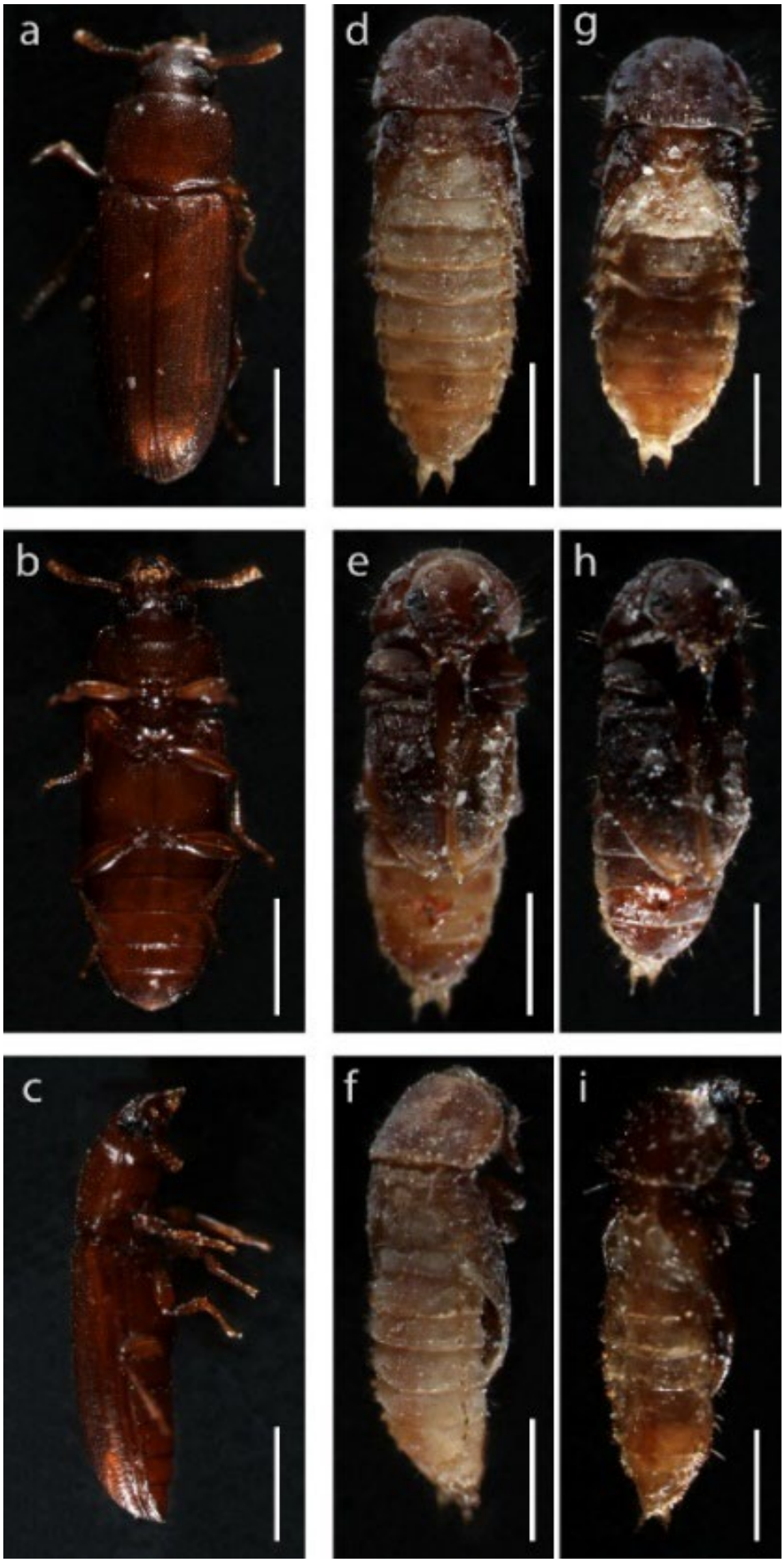
a
d
g
b
e
h
c
f
i

Figure 4-12. Low concentration (0.4 µg/ul) of *Cyp18a1* dsRNA injected beetles resulted in abnormal phenotypes in the folding of wings and elytra over the abdomen. The abnormal wing could not cover the dorsal side of the pupae and these pupae subsequently died due to dehydration (d, g, f, i). Sclerotization of the abdomen was incomplete (d, g, e, h, f, j). Letters "a", "b" and "c" represent the dorsal, ventral and lateral side of adult, respectively upon injections of the control dsRNA; "d", "e" and "f" are from pupae that failed to eclose after *Cyp18a1* dsRNA injections; "g", "h" and "i" are from older pupae which failed to eclose and died of dehydration after the *Cyp18a1* dsRNA injections. Scale bar: 1 mm.

Taken together, our RNAi data demonstrate that *Cyp18a1* is required for pupation and eclosion. We wondered whether *Cyp18a1* expression peaks during these developmental events. Therefore, we measured *Cyp18a1* expression in the lab-strain Georgia line using qPCR. Indeed, *Cyp18a1* expression increases in prepupae towards pupation (Figure 4-13), and increases in pupae towards eclosion (Figure 4-13B).

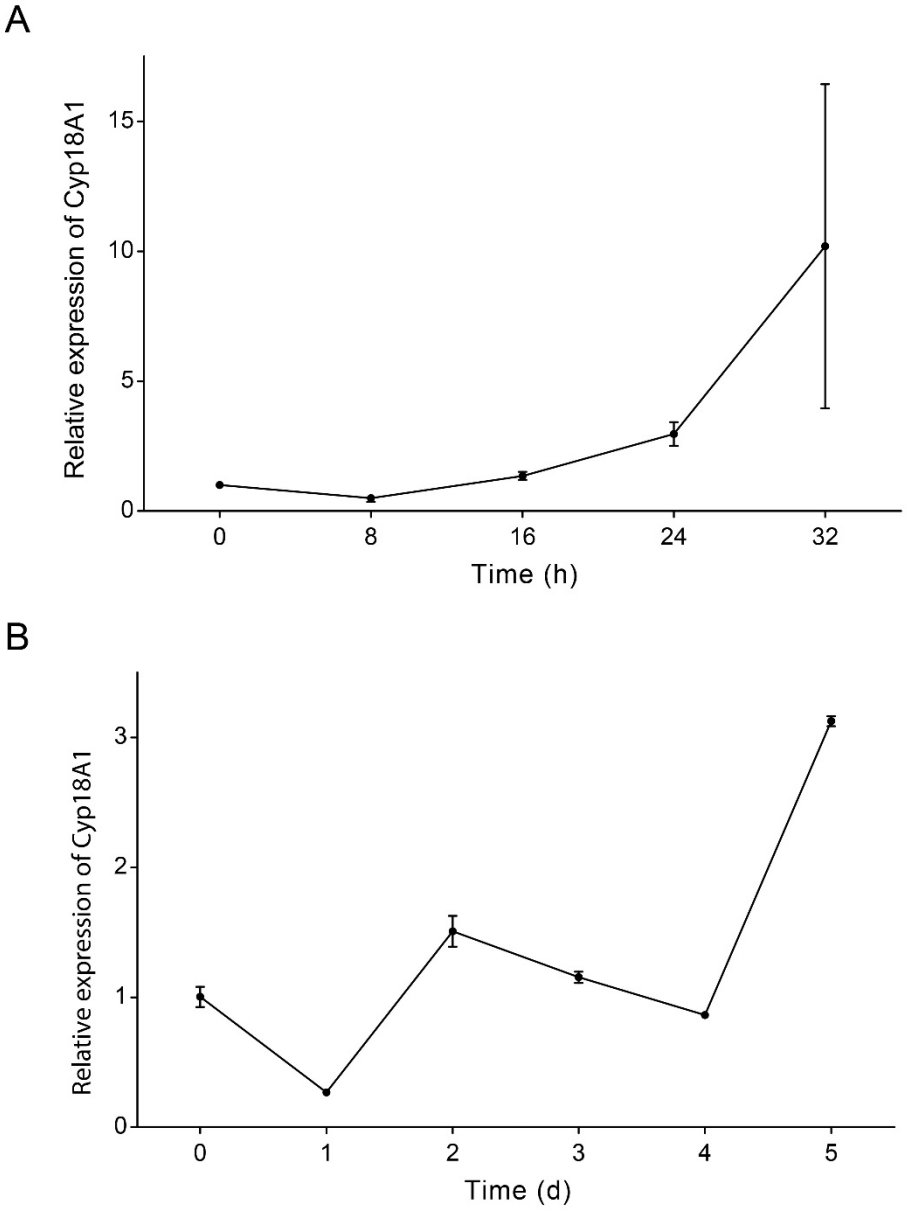

Figure 4-13. Relative expression of *Cyp18a1* in prepupa (A) and pupa (B) during their development. Each point represents the mean *Cyp18a1* expression based on two biological replicates (each replicate is the mean of two technical replicates).

Ecdysone titers and *Cyp18a1* expression levels rise during dorsal closure

Although Ecdysone is well known to regulate events such as molting or metamorphosis, an ecdysone peak has also been detected during embryogenesis in *Drosophila* (Kozlova and Thummel, 2003; Maróy et al., 1988). This peak has recently been shown to regulate dorsal closure (Yoo et al., 2021). We first investigated ecdysone levels, *Cyp18a1* expression, expression of the Halloween gene *Spook* (*Cyp307a1*) and of the ecdysone target gene *Broad* (Niwa and Niwa, 2016).

We found two peaks of 20E titers during GA-1 embryonic development: a weak peak (248.40 pg/mL) at 40 h and a strong peak (3711.34 pg/mL) at 120 h post-oviposition (Figure 4-14). Titers of 20E kept a relatively lower level between 40 h and 96 h post-oviposition. However, it started to gradually increase at 96 h and reached the peak level at 120 h post-oviposition. The following 20E levels dropped dramatically and then stayed at a relatively lower level until hatching. The peak at 120 h post-oviposition is preceded by high gene expression of the early Halloween gene *spook* (*Cyp307a1*, *Spo*) involved in the ecdysone biosynthesis (blue, Figure 4-14). The ecdysone-inactivating enzyme *Cyp18a1* starts to increase at 112-120 h, and remains high until hatching. The early ecdysone response gene *broad* (*Br*) follows the ecdysone peak with some delay (Figure 4-14). All of primers of the Halloween genes and *Br* for qPCR are listed in Supplementary Table 4-5.

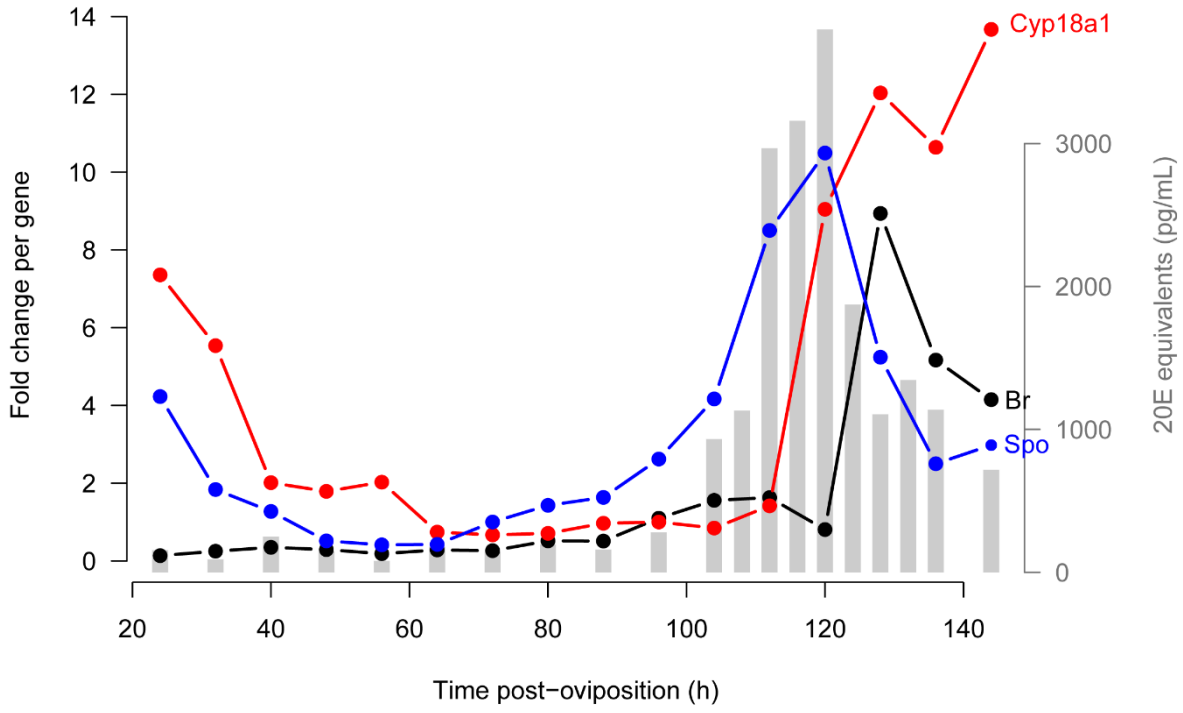

Figure 4-14. Ecdysone titers (grey columns) and the related gene expression (lines) during embryonic development of the wild-type Georgia strain of *Tribolium castaneum*. Black line stands for relative expression of *broad* (*Br*) over time, red line is *Cyp18a1*, and blue line is *spook* (*Cyp307A1*, *Spo*). The transcript level of *Br*, *Cyp18a1* and *Spo* was taken as 1 at 96 h, 96 h and 72 h post-egg laying, respectively. Each column stands for the mean of ecdysone level based on two technical replicates. Each point represents the mean fold change plus standard error based on two biological replicates (each replicate is the mean of two technical replicates according to the protocol of the kit).

In addition, we also quantified other Halloween genes involved in the ecdysone biosynthesis during embryonic development of *T. castaneum*, including *phantom* (*Cyp306A1*, *Phm*), *disembodied*

(*Cyp302A1*, *Dib*), *shadow* (*Cyp315A1*, *Sad*) and *shade* (*Cyp314A1*, *Shd*). *Phm* shows the highest expression level at 128 h post-egg laying. *Dib* is highly expressed at 32 h and shows the same expression pattern with *Phm* between 96 h and 136 h. *Sad* is highly expressed at both 24 h and 48 h. *Shd* shows two dramatic expression peaks at 48 h and 96 h, respectively (Figure 4-15).

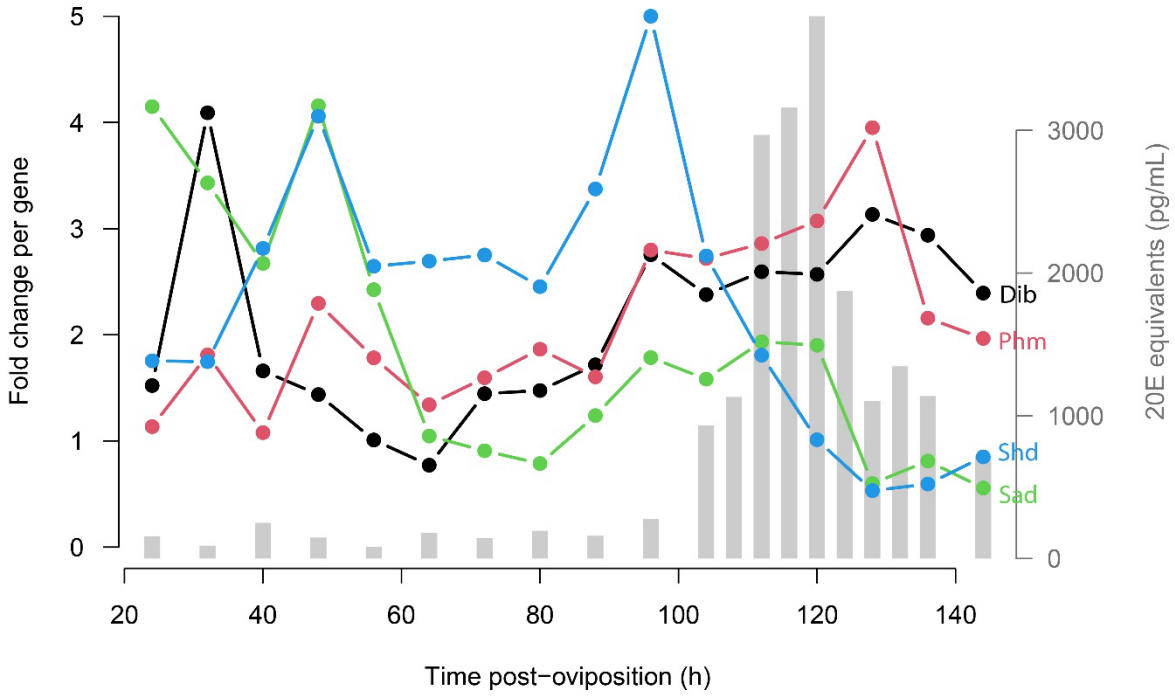

Figure 4-15. Ecdysone titers (grey columns) and some Halloween gene expression (lines) during embryonic development of the wild-type Georgia strain of *Tribolium castaneum*. Black line stands for relative expression of *disembodied* (*Cyp302A1*, *Dib*) over time, red line is *phantom* (*Cyp306A1*, *Phm*), blue line is *shade* (*Cyp314A1*, *Shd*), and green line is *shadow* (*Cyp315A1*, *Sad*). The transcript level of *Phm*, *Dib*, *Sad* and *Shd* was taken as 1 at 40 h, 56 h, 64 h and 120 h post-egg laying, respectively. Each column stands for the mean of ecdysone level based on two technical replicates. Each point represents the mean fold change plus standard error based on two biological replicates (each replicate is the mean of two technical replicates according to the protocol of the kit).

At the same time, around 50 GA-1 eggs were fixed and stained (DAPI) to assess the specific embryonic developmental stage at each time point of testing 20E titers. Judgement values were described under 'Variation under artificial selection is in the timing after germband extension, before dorsal closure' (Supplementary Figure 4-21). According to fluorescent microscopic results for GA-1 eggs, 40 h is at the stage of extended limbs, and 120 h post-oviposition is at the complete dorsal closure. Interestingly, 96 h is around the stage of start of dorsal closure (Figure 4-16).

In summary, a high ecdysone peak, and increasing *Cyp18a1* levels are found during dorsal closure, suggesting a role for ecdysone during dorsal closure.

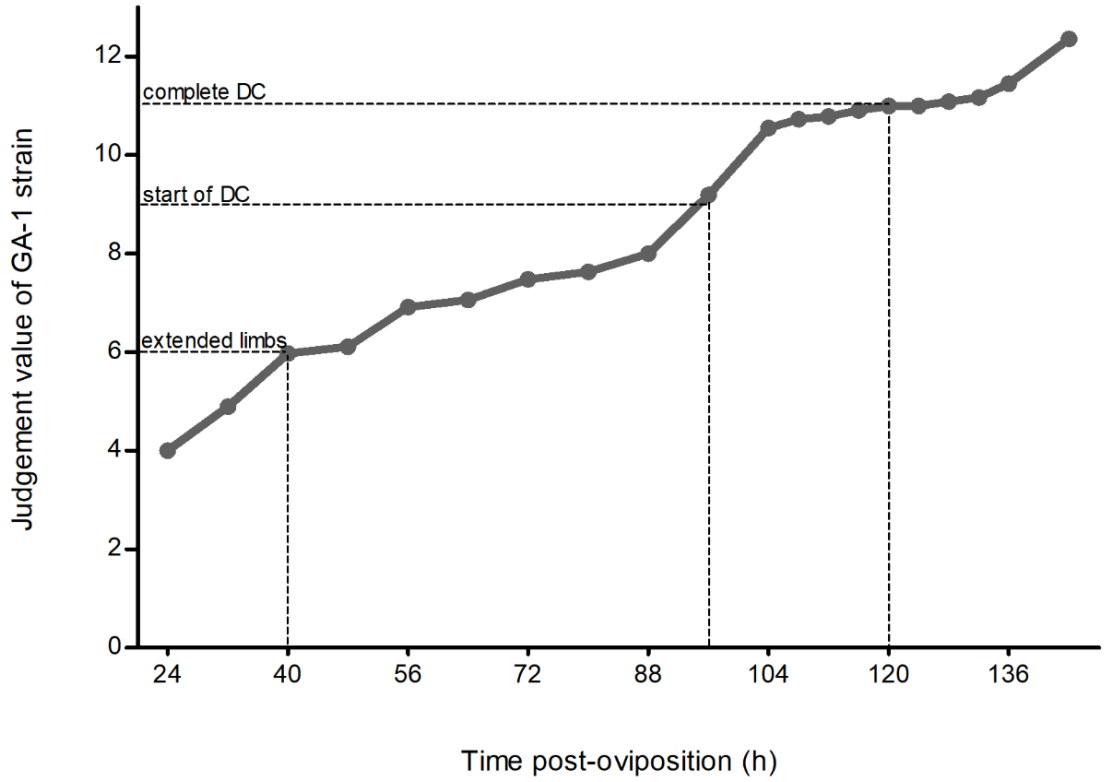

Figure 4-16. Judgement values given to fourteen embryonic stages are used to score embryonic development of wild-type Georgia strain. 0=no nuclei at surface; 1=undifferentiated blastoderm; 2=differentiated blastoderm; 3=gastrulation; 4=extending germband; 5=extended germband; 6=limbs growing and extending; 7=retracting germband; 8=completely retracted germband; 9=start of dorsal closure (dorsal organ formation); 10=dorsal closure in progress; 11=dorsal closure completed; 12=hatching; and 13=hatched. See more details in Supplementary Figure 4-1. Fast A, fast B, non-selected A (NS A), non-selected B (NS B), slow A and slow B are shown with red, orange, green, light green, dark blue, and light blue lines.

Cyp18a1 is expressed in the dorsal organ

To reveal what tissue is involved in ecdysone synthesis and degradation during dorsal closure, we performed *in situ* hybridization for *Spook* and *Cyp18a1*. We found that *Spo* is expressed in the dorsal ectoderm already before dorsal closure (Figure 4-17A), and continues this expression pattern during dorsal closure (Figure 4-17B). The dorsal closure process is shown schematically in Figure 1-6B (Chapter 1) and Supplementary Figure 4-4. In contrast, we could not detect expression of *Cyp18a1* during germband retraction (Figure 4-17C). At the beginning of dorsal closure, *Cyp18a1* starts to be expressed in the dorsal organ, the contracting serosa (Panfilio, 2008) (Figure 4-17D).

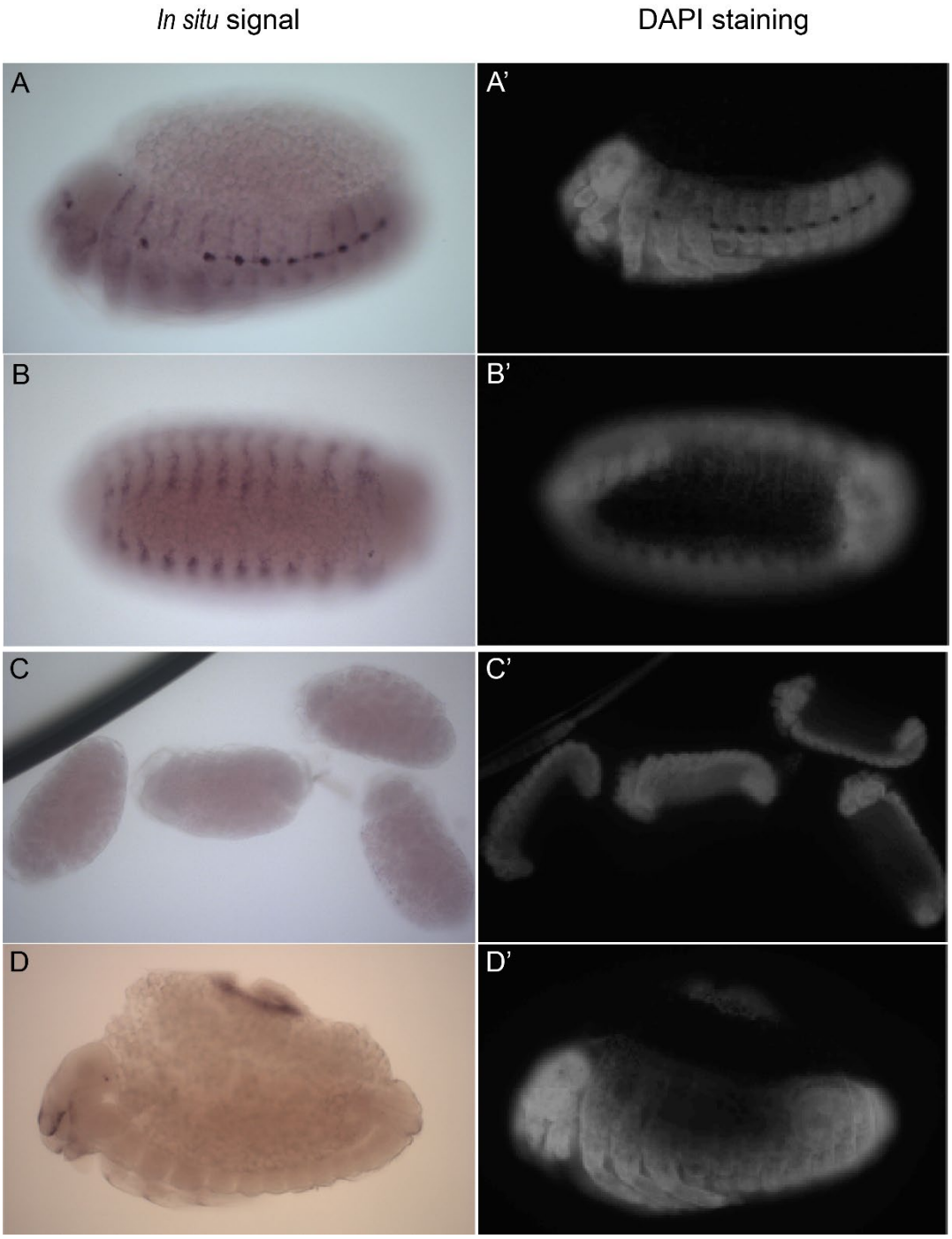

Figure 4-17. *In situ* hybridization for *spook* and *Cyp18a1*. A, *Spook in situ* hybridization at the retracted germband stage. B, *Spook in situ* hybridization during dorsal closure. C, *Cyp18a1 in situ* hybridization at the retracting or retracted germband stage. D. *Cyp18a1 in situ* hybridization at the stage of start of dorsal closure. A', B', C', and D', the corresponding embryos stained by DAPI, respectively.

Cyp18a1 degrades active ecdysone and is required for dorsal closure

To understand the role of Cyp18a1 during embryonic development, we injected 200 female beetles with *Cyp18a1* dsRNA. When they started to lay eggs, we fixed and stained (DAPI) these eggs every day before they hatch to larvae. When we observe the stage still after more than 24h, we define this as a developmental arrest. When we find a developmental stage later, but less than 24 h after this stage was observed in the control pRNAi, we categorize this as an developmental delay. For example, the formation of the blastoderm occurs in the 0-1 d old eggs. If we observed this stage in 1-2 d old eggs, we define this kind of eggs as a developmental delay. If we observed this stage at later stages (2-7 d old), we define this kind of eggs as a developmental arrest. As the stage of no nuclei at surface occurs at the very beginning of development, we define 1-7 d old eggs at this stage as "No start of development".

Fluorescent microscopic analysis showed that 20% of the *Cyp18a1* RNAi eggs (out of 147) showed no start of development, compared to only 8% in the control (out of 248 eggs). During blastoderm, germband extension and dorsal closure, a total of 43% eggs showed a developmental arrest upon *Cyp18a1* RNAi (Table 4-2). The eggs arrested during germband extension remained a short germband during further development (Figure 4-18A), suggesting a role for Cyp18a1 in segmentation or germ band extension. Most importantly, the embryos that were arrested during dorsal closure were left dorsally open (Figure 4-18B, Figure 4-19). This demonstrates that Cyp18a1 is required for dorsal closure.

Table 4-2. Summary of phenotypic percentage of the eggs upon the control and *Cyp18a1* pRNAi. No start of development stands for the stage of no nuclei at surface.

Development of the eggs		Control (%)	Cyp18a1 (%)
Normal development		88	33
No start of development		8	20
Developmental delay		4	4
	during blastoderm	0	5
Developmental arrest	during germband extension	0	13
	during dorsal closure	0	25

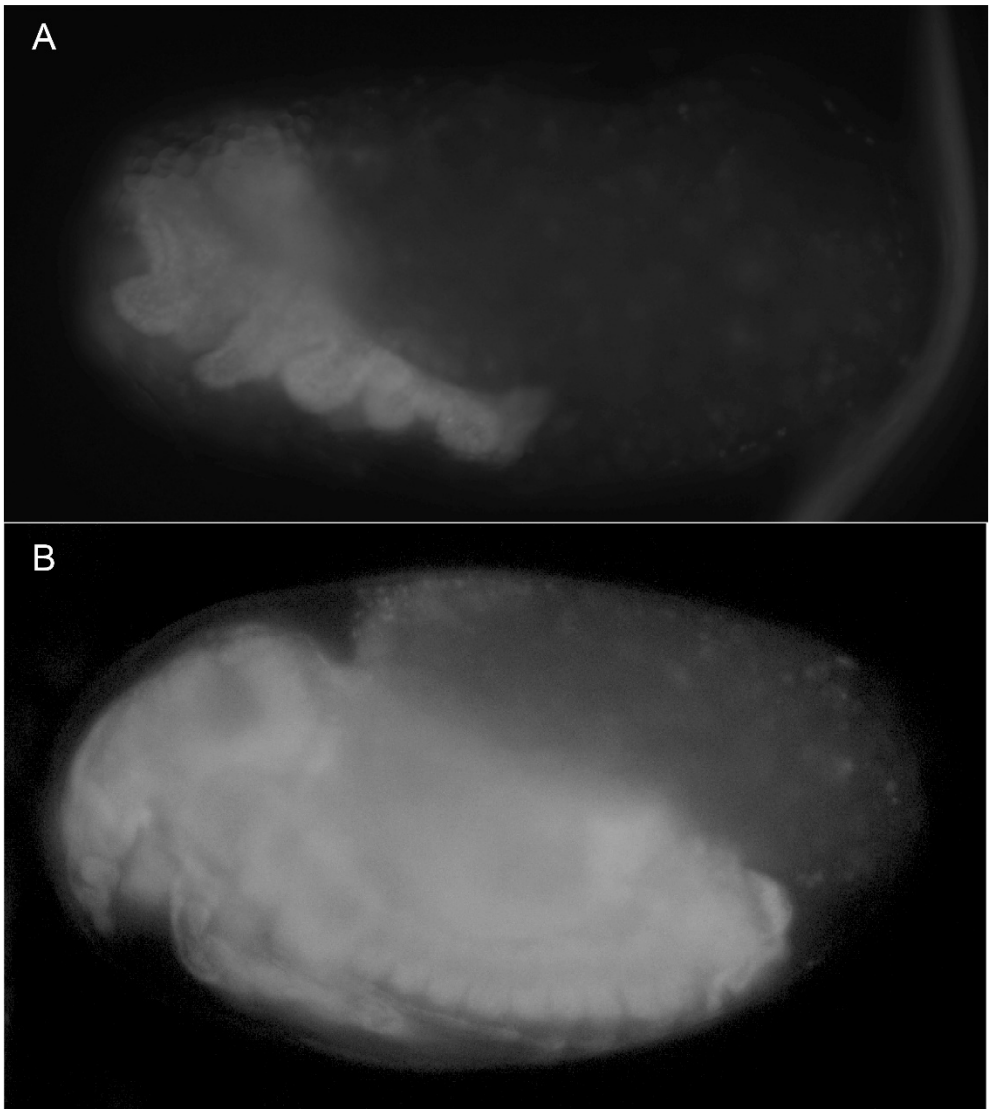

Figure 4-18. Phenotypes upon *Cyp18a1* pRNAi during germband extension, showing a short germband (A) and a dorsally open embryo at dorsal closure (B).

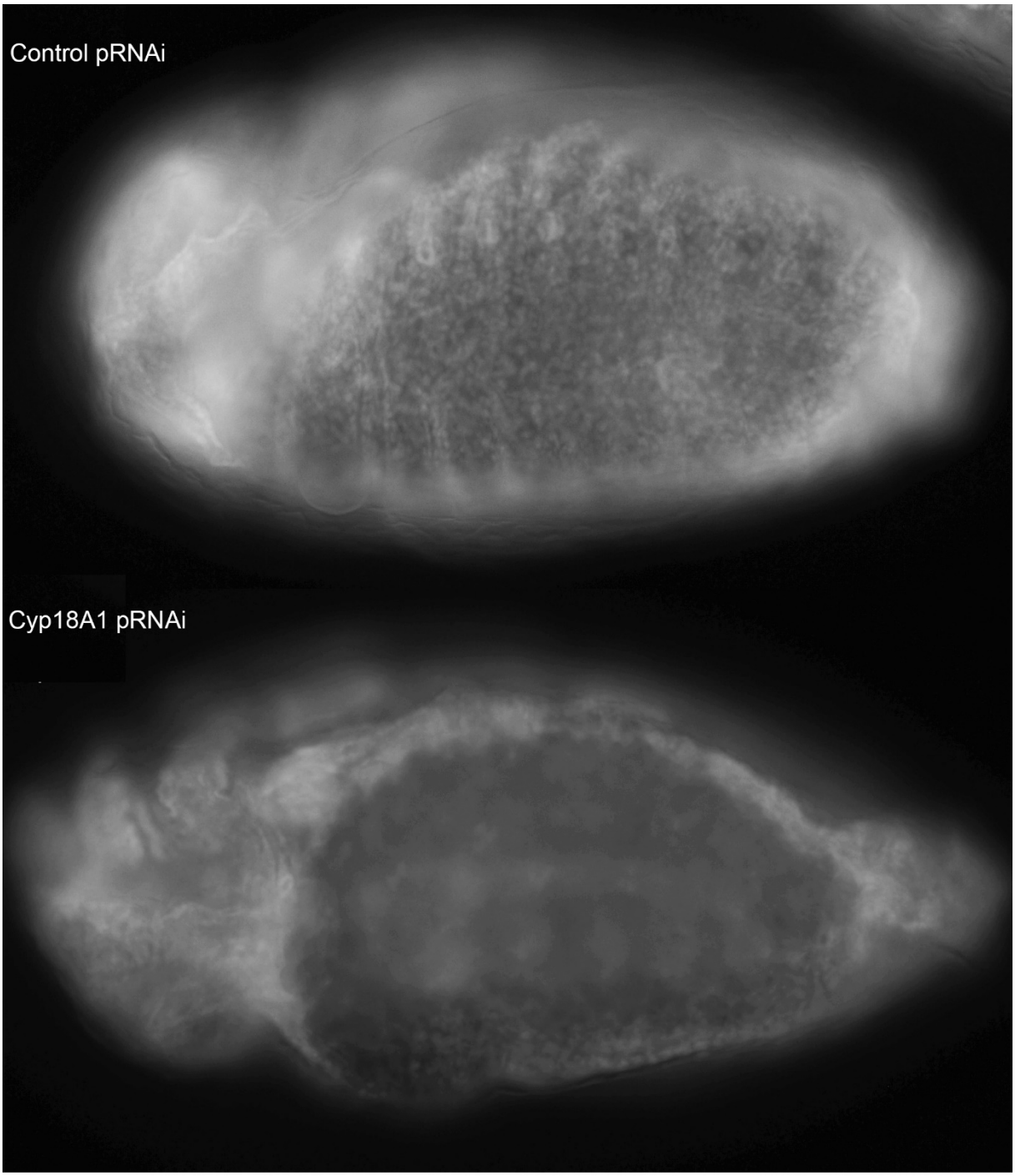

Figure 4-19. Phenotypes of the embryos upon control and *Cyp18a1* pRNAi, respectively. Upon control pRNAi, the dorsal side of the embryo is well-closed, while the dorsal side of the embryo is still open upon *Cyp18a1* pRNAi.

By combining *Cyp18a1* pRNAi results from the pRNAi screen (Figure 4-6) and fluorescent microscopic analysis (Table 4-2), we assessed embryonic development of the eggs upon *Cyp18a1* pRNAi (Figure 4-20). It is estimated that 20% eggs are not fertilized or do not start development (see first line in Figure 4-20). In addition, 5%, 13% and 25% eggs are arrested during blastoderm, germband extension and dorsal closure, respectively (Figure 4-20). Of the eggs that hatch, 8% eggs hatch with a normal developmental time, whereas 25% eggs delay their development, as we observed in Figure 4-6.

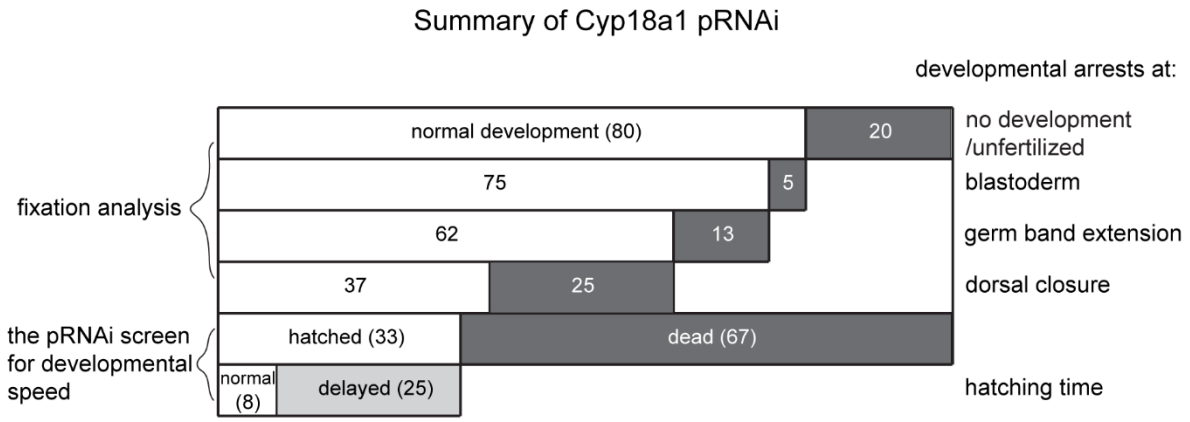

Figure 4-20. The assessment for embryonic development of the eggs upon *Cyp18a1* pRNAi. Normal development of the eggs is in white boxes. The death or failure of development are indicated with a certain percentage in dark grey boxes. Of one third hatched eggs, the developmental delay is indicated with a certain percentage in a light grey box.

As Cyp18a1 degrades active ecdysone (Guittard et al., 2011; Rewitz et al., 2010), the 20E levels of the eggs upon *Cyp18a1* pRNAi were measured focusing on the dorsal closure stage. For measuring 20E titer, we collected the precipitate from 20 eggs for each time point and did not dilute it with EIA buffer. We collected 96 to 160 h old eggs post-oviposition upon Cyp18a1 *pRNAi*. The results showed that 20E titers gradually reached the relatively higher level at 128 h and gave rise to the highest titer at 160 h post-oviposition (Figure 4-21). This confirms that, also in *Tribolium*, Cyp18a1 degrades active ecdysone. Together with the morphological analysis, it also shows that a pulse of ecdysone is required for dorsal closure and that mere high levels are not sufficient.

.

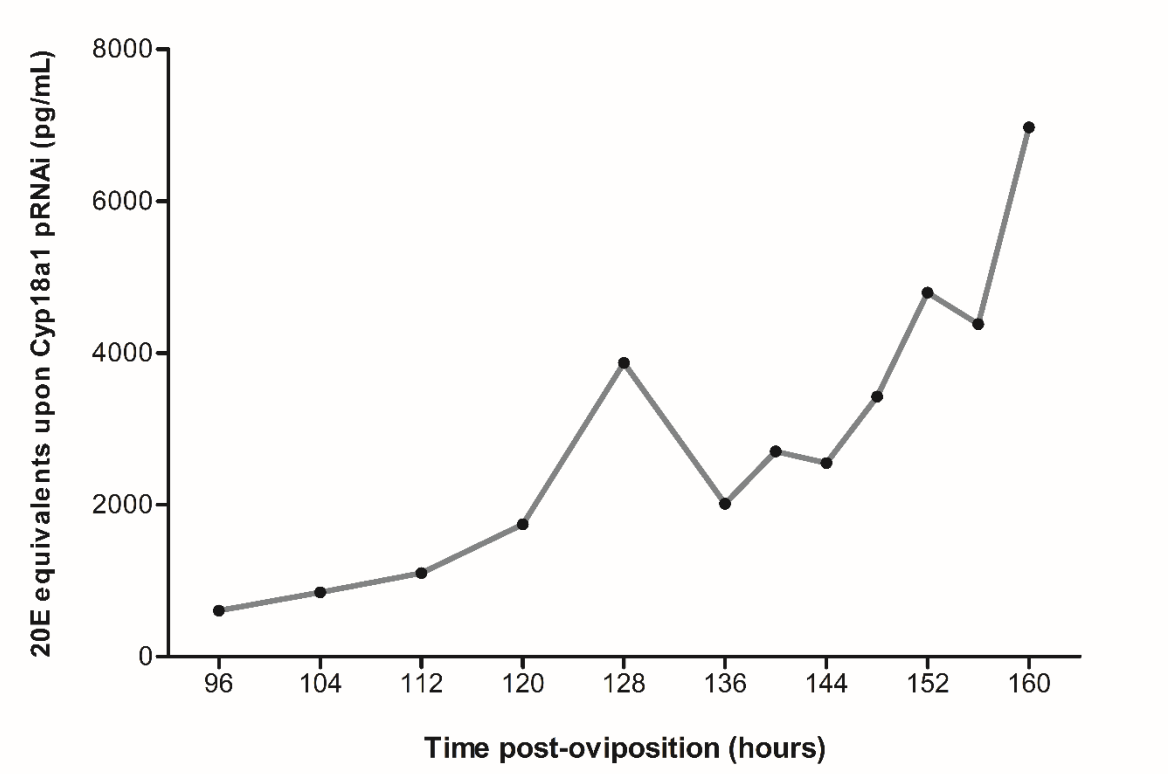

Figure 4-21. Ecdysone titers of the eggs upon *Cyp18a1* pRNAi. Black dots stand for ecdysone levels measured in duplicate according to the manufacture's instruction.

In summary, when *Cyp18a1* is knocked down, ecdysone levels continue to increase, and a significant fraction of the embryos remain dorsally open and do no complete dorsal closure.

Spook may be involved in segmentation or germband extension

We also attempted to investigate the role of the other Halloween genes during embryonic development. However, using parental RNAi, we found that no eggs were laid within a month post-injection against *Cyp307a1* (*spook*, *Spo*), *Cyp315a1* (*shadow*, *Sad*), *Cyp314a1* (*shade*, *Shd*), and the mix of *EcR* and *USP*. The beetles did lay eggs upon *Cyp306a1* (Figure 4-6) and *Cyp302a1* (*disembodied*, *Dib*) pRNAi. As reported before (Figure 4-6), pRNAi against *Cyp306a1* did not alter developmental time. In addition, we did not find significant difference of the embryonic developmental time upon *Cyp302a1* RNAi, compared to the control pRNAi (Figure 4-22).

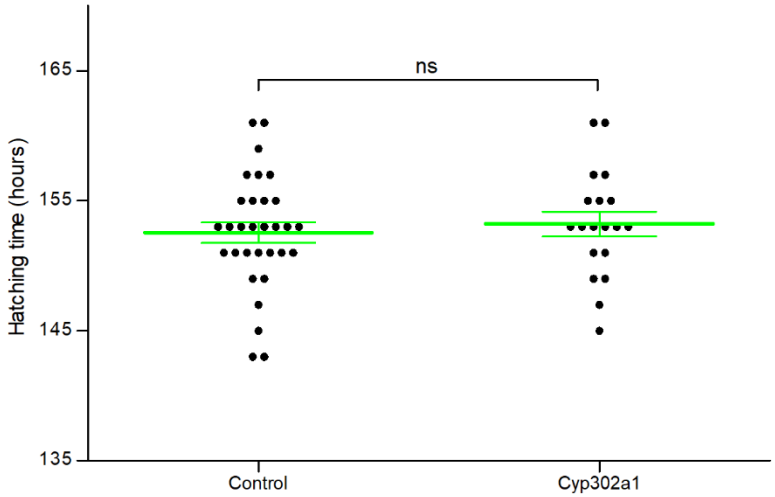

Figure 4-22. The embryonic developmental time of offspring embryos upon *Cyp302a1* dsRNA injections into 50 *Tribolium* mothers, compared to injections of non-targeting control dsRNA. Key: Green lines, mean of embryonic developmental time plus standard error. Black dot, the time of every hatched embryo. The student t-test was performed to compare the control and *Cyp302a1* pRNAi. Key: ns, no significant difference observed in hatching time.

To circumvent adult sterility upon pRNAi, we studied the role of Spo, Sad and Shd during embryonic development, using embryonic RNAi (eRNAi) on 4-6 h old eggs of the LifeAct-nGFP line (van Drongelen et al., 2018). In total, 140 eggs were injected per gene. Embryos were checked under a Zeiss Axioplan 2 microscope once a day post-injection. Fluorescent microscopic analysis showed that all eggs could hatch to larvae upon Sad and Shd RNAi. The percentage of hatched eggs were 15.7% and 21.4% upon *Sad* and *Shd* eRNAi, respectively, compared to 29.3 percent hatching upon the control RNAi. However, no eggs hatched upon injections of *Spo* dsRNA. The vast majority of *Spo* RNAi eggs died during germband extension, suggesting a role for Spo during germband extension or segmentation (Figure 4-23).

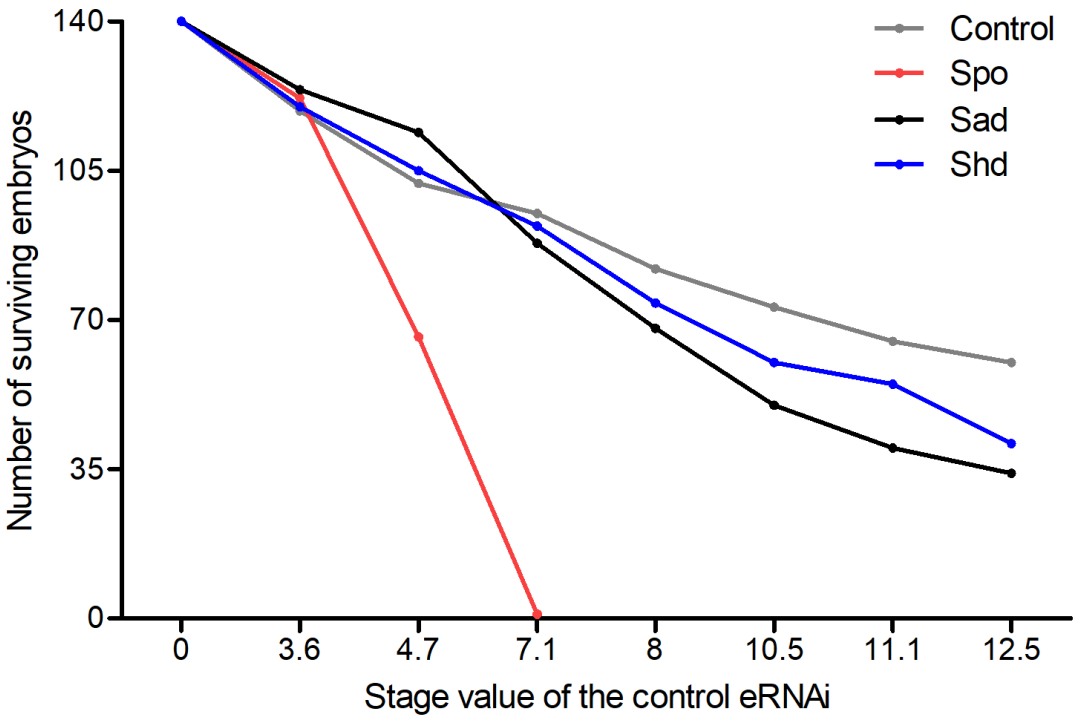

Figure 4-23. The number of surviving embryos upon the control (grey line), *Spo* (*Cyp307a1*, *spook*, red line), *Sad* (*Cyp315a1*, *shadow*, black line) and *Shd* (*Cyp314a1*, *shade*, blue line) eRNAi. 0=no nuclei at surface; 3=gastrulation; 4=extending germband; 5=extended germband; 6=limbs growing and extending; 7=retracting germband; 8=completely retracted germband; 10=dorsal closure in progress; 11=dorsal closure completed; 12=hatching; and 13=hatched. See more details in Supplementary Figure 4-1.

Embryonic ecdysone peaks differ in timing and height among the selection lines

To investigate if the ecdysone levels vary among the selection lines, ecdysteroid titers during embryonic development were determined (Figure 4-24). The results showed that 20E equivalents of fast, non-selected and slow lines remained at low concentrations during the first 80, 88 and 96 h post-oviposition, respectively. Ecdysteroid titers reached their peaks at 96, 104, and 120 h post-oviposition, respectively. After these peaks, ecdysteroid titers gradually dropped back to the relatively lower levels among the selection lines. Thus, like the start of dorsal closure, the ecdysone peaks also differ consistently in timing among the selection lines.

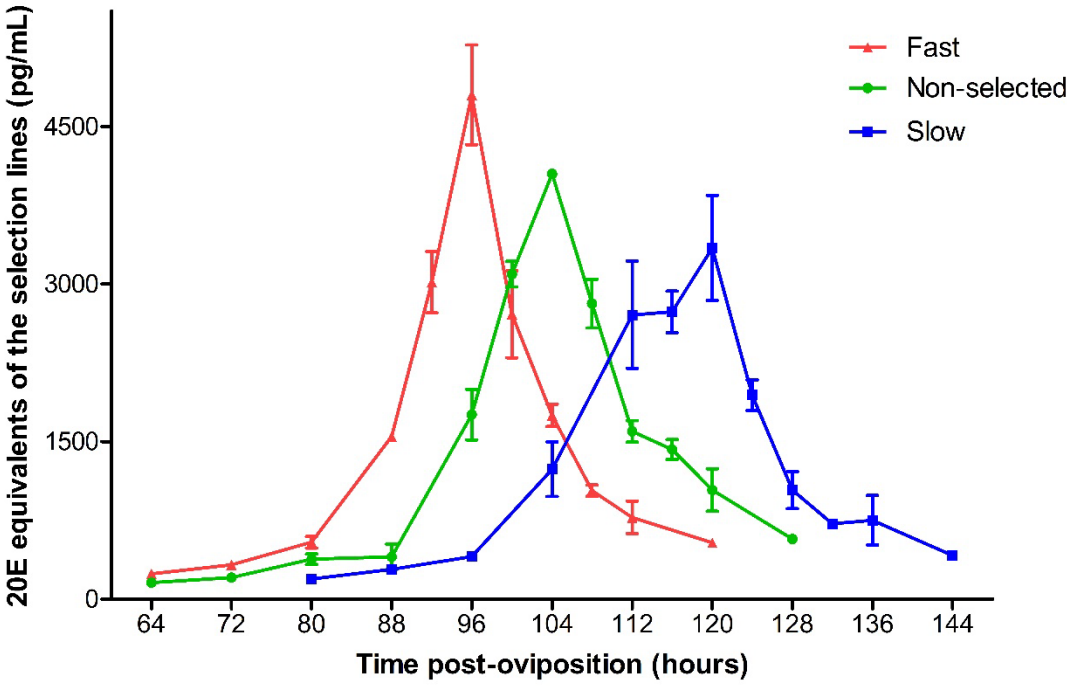

Figure 4-24. Ecdysteroid levels of the eggs of the selection lines of *Tribolium castaneum*. Each time point represents the mean ecdysteroid levels of two biological replicates (each biological replicate is based on two technical replicates according to the protocol of the kit).

High frequency of a 222 bp deletion upstream of *Cyp18a1* in the fast lines

As *Cyp18a1* was identified as the main candidate gene, we inspected the pooled resequencing data around this gene in more detail. At position 1,613,941 on chromosome 9, less than 300 bp downstream of the *Cyp18a1* lead SNP (the highest SNP on chromosome 9, Supplementary Table 4-1), and around 6kb upstream of the *Cyp18a1* transcription start site (TSS), a conspicuous 445 bp sequence starts consisting of two 222 bp repeats. We named the two 222 bp repeats repeat 1 and repeat 2 (Figure 4-25). The alignment of two 222 bp repeats is in Supplementary Figure 4-5. Surprisingly, the pooled resequencing data suggest that one of these repeats is deleted in the fast lines, and that the frequency of this 222 bp deletion is 1 in the fast lines, 0 in the slow lines, and 0.15 and 0.16 in the two non-selected lines (Table 4-3). So, we also called this 222 bp deletion the fast allele (F in Figure 4-25), and the 445 bp repeated region the slow allele (S in Figure 4-25) in this study.

Table 4-3. Number of reads discovered that carry the specific 1 or 2 repeat sequence (Fast or Slow allele, respectively).. These sequences are "AATTTTTTTAAATTCATTATTTCAATTTTTTTATCCTTCCC" for the fast allele and "AATTTTTTTAAATTTATTATTTCAAATTTTTTATCCTTCCC" for the slow allele. The forward and reverse complement added summed (totals first two columns: 'All reads'). We corrected for doubles (overlap of the paired ends), and duplicates (identical sequencing PCR duplications close in position on the flow cell) in the last two columns.

	All reads		Doubles and Duplications removed	
	F allele	S allele	F allele	S allele
FastA	41	0	35	0
FastB	30	0	24	0
SlowA	0	37	0	25
SlowB	0	27	0	17
NSA	3	23	3	17
NSB	7	36	5	26

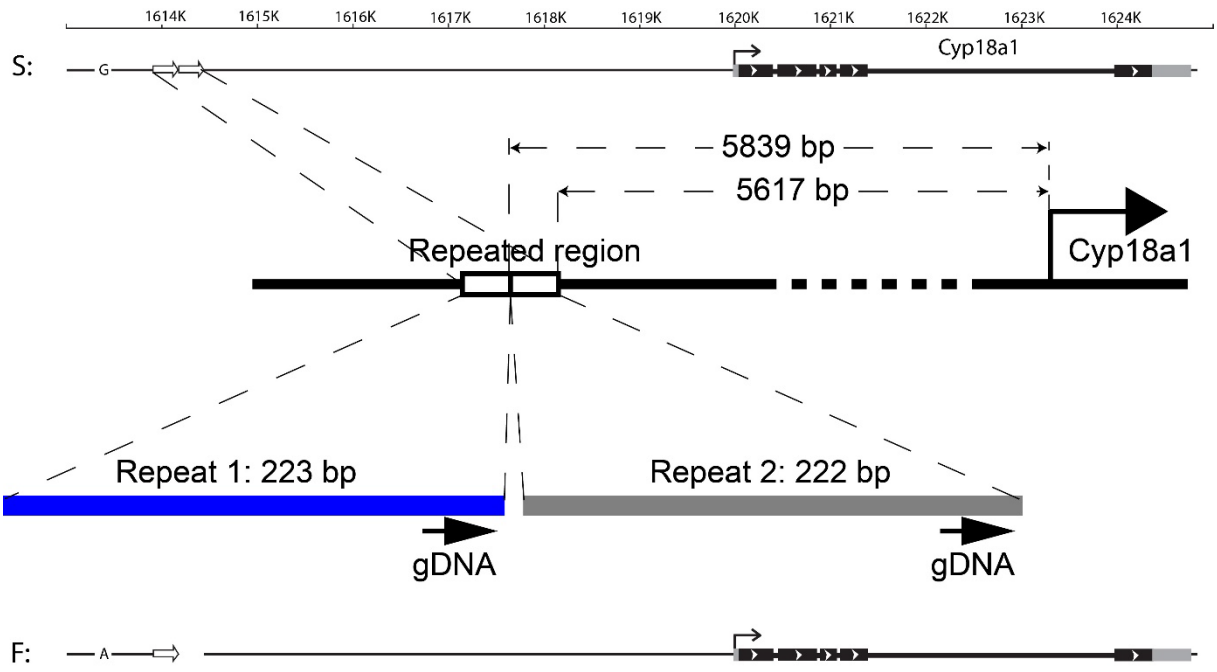

Figure 4-25. Schematic overview of the repeated region in the upstream of *Cyp18a1* comprising 223 bp repeat 1 and 222 bp repeat 2. S: It contains the repeated region with 445 bp close to the lead SNP of *Cyp18a1*. F: It has the deleted region with 223 bp. The distance from the *Cyp18a1* transcription start site to repeat 1 and repeat 2 is 5839 and 5617 bp, respectively.

The presence of such F and S alleles was supported by Sanger sequenced cloned PCR products obtained from fast, non-selected and slow beetles. In total, we sequenced one clone from 19 different individuals: from 4 from Fast A, Non-selected A and Non-selected B each, 3 from Fast B, and 2 beetles from Slow A and Slow B each. Alignments of these cloned Sanger-sequenced PCR products are shown in Supplementary File 4-1. The unique sequences used to distinguish the fast and slow allele in the pooled resequencing data (Table 4-3) is shaded in grey. The results show that all sequences from fast individuals contain the 222 bp deletion (F allele). Only one of the 8 sequences from the non-selected lines contains the deletion. All other sequences, including all sequences from the slow lines, contain the 445 bp repeat (S allele). These numbers correspond well with the pooled resequencing counts (Table 4-3).

When aligning 445 bp repeated region comprising repeat 1 and repeat 2 from the 445 bp repeated region, with the fast allele, we found some single-nucleotide variants of the fast allele are identical to repeat 1, some of them are identical to repeat 2, but still some are unique (Figure 4-26).

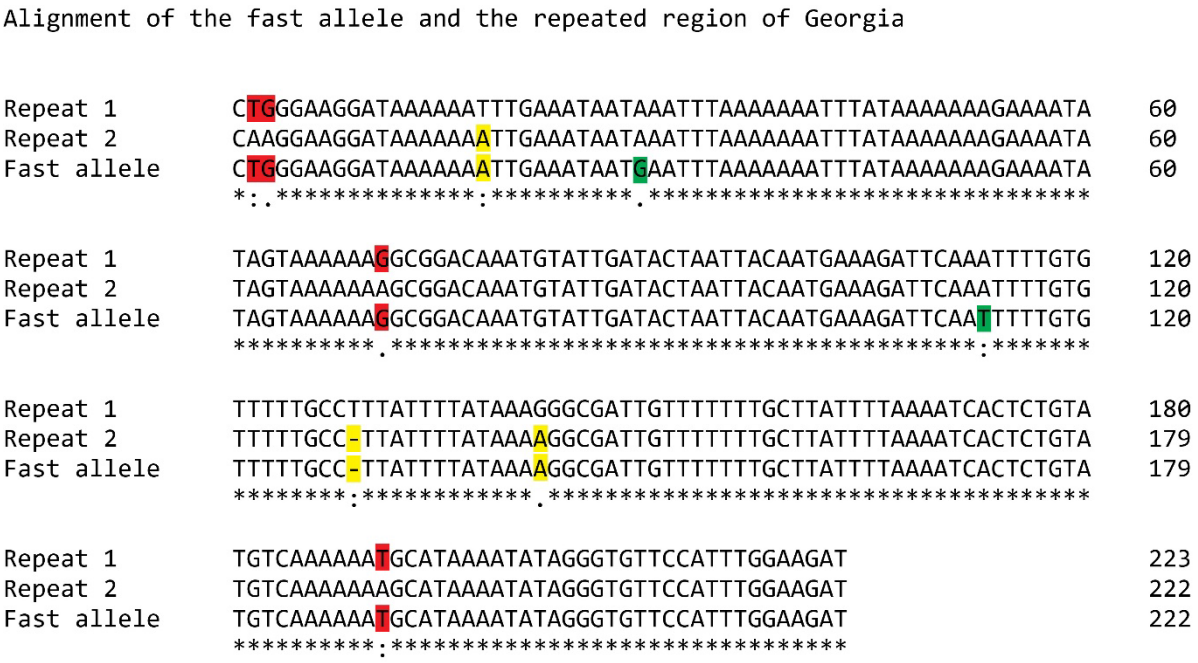

Figure 4-26. Alignment of repeat 1, repeat 2 and fast allele. The red box indicates single-nucleotide variants of fast allele are same with repeat 1, and yellow is single-nucleotide variants of fast allele are same with repeat 2. If they are not orthologous to both repeat 1 and repeat 2, single-nucleotide variants of fast allele is in the green box.

Using PCR genotyping, we can distinguish the three different genotypes (FF, FS and SS), see Supplementary Figure 4-6. We genotyped 24 stored individuals of generation 0, 3, 7, 10 and 21 from the Fa, Fb, Na and Nb selection lines for absence or presence of the deletion. The results of PCR genotyping are shown in Table 4-4. This reveals that the allele frequency of the 222 bp deletion fluctuated in the non-selected beetles, but increased in the fast lines over the course of the selection (Figure 4-27). Allele frequency of fast allele did not differ between the fast and non-selected lines in generation 0 and 3. However, we did find the significant difference of the allele frequency of fast allele between the fast and non-selected lines in generation 7, 10 and 21, as confirmed by the chi-square test (Table 4-5).

Table 4-4. PCR genotyping results show three types of genotypes in the upstream of *Cyp18a1* for in total of 480 beetles in generation 0, 3, 7, 10 and 22 of the fast and non-selected lines. Key: FF, homozygotes with the 222 bp deleted region; SS, homozygotes with the 445 bp repeated region; and FS, heterozygotes with both of the deleted region and the repeated region.

Fast A	FF	FS	SS	**Fast B**	FF	FS	SS
Gen. 0	3	17	4	Gen. 0	8	10	6
Gen. 3	16	6	2	Gen. 3	12	9	3
Gen. 7	20	3	1	Gen. 7	11	12	1
Gen. 10	18	6	0	Gen. 10	19	4	1
Gen. 21	24	0	0	Gen. 21	20	4	0
NS A	FF	FS	SS	**NS B**	FF	FS	SS
Gen. 0	6	14	4	Gen. 0	12	10	2
Gen. 3	11	9	4	Gen. 3	8	13	3
Gen. 7	11	11	2	Gen. 7	6	10	8
Gen. 10	7	14	3	Gen. 10	3	11	10
Gen. 21	6	10	8	Gen. 21	9	13	2

Table 4-5. Pearson's Chi-squared test was performed to compare fast allele and slow allele between the fast and non-selected lines in generation 0, 3, 7, 10 and 21.

	X-squared	Degree of freedom	P-value
Gen. 0	2.1223	1	0.1452
Gen. 3	2.4027	1	0.1211
Gen. 7	10.691	1	0.001077
Gen. 10	34.114	1	5.196e-09
Gen. 21	40.682	1	1.791e-10

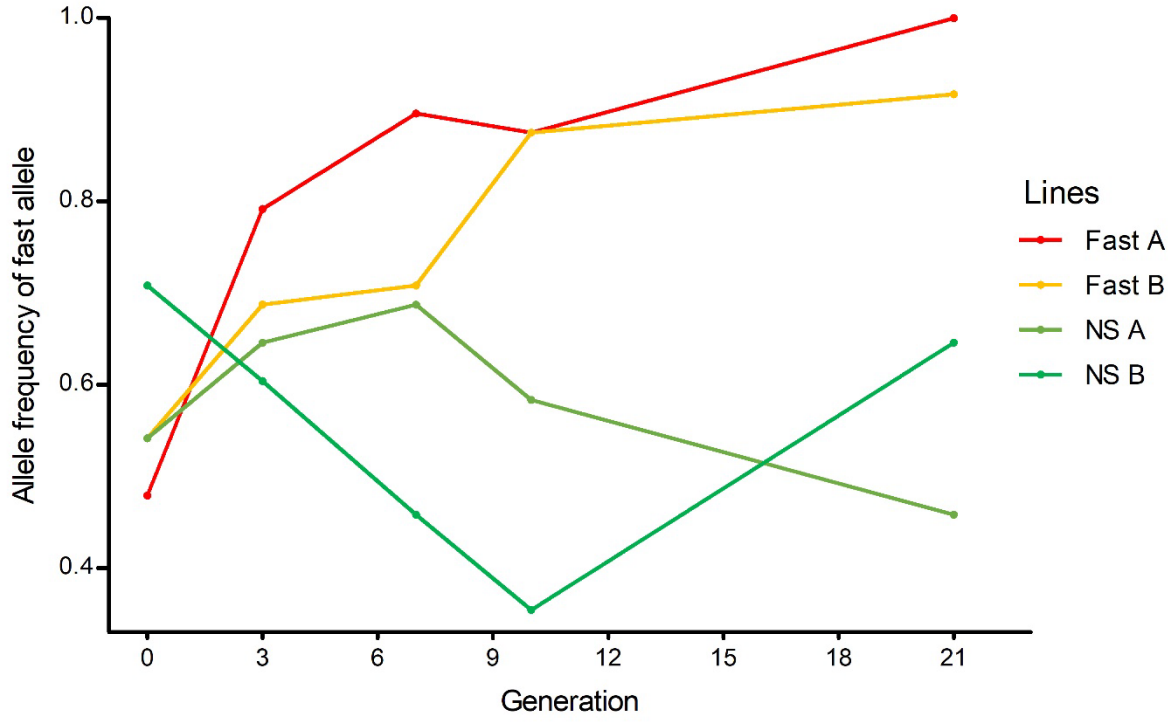

Figure 4-27. Change of allele frequency of fast allele (the 222 bp deleted region) in the upstream of *Cyp18a1* in the fast and non-selected lines over the course of the selection.

Using these data, we fitted a population genetics model with and without fitness differences for these three genotypes. For both Fast A and Fast B the model with different fitness values of the three genotypes was highly significantly different from the model without fitness differences (P <0.001), while for NSA this was not the case (P =0.148), and for NSB this was only significant at a level of P <0.05. Furthermore, while for Fast A and Fast B the fitness for FF was higher compared to FS, which had higher estimated fitness than SS, for NSB the fitness was highest for the heterozygote, so that selection is non-directional. The fit for the three difference fitness values of Fast A, Fast B and NSB can be found in Figure 4-28, while for NSA the null-hypothesis without fitness differences was accepted. Thus, the F allele has been under strong positive selection in the fast lines.

Table 4-6. Best fit estimates for the fitness values of the genotypes FF, FS and SS combined with the bets starting allele frequency at generation 0. The columns with L, indicate the likelihoods of the models. Chi indicates the test statistic as calculated by equation (1). Key: *, P<0.05; ****, P<0.0001.

	Model with fitness differences					Model without fitness differences		
Line	WFF	WFS	WSS	pP(FF)	L	p(FF)	L	Chi
FastA	**1**	**0,888**	**0,291**	**0,489**	-15.99	0,808	-39,47	**46,96****
FastB	**1**	**0,950**	**0,650**	**0,545**	-16,23	0,746	-27,48	**22,5****
NSA	0,787	0,437	1	0,617	-18,90	**0,583**	-20,81	3,82
NSB	**0,474**	**1**	**0,488**	**0,717**	-21,38	0,554	-24,98	**7,20***

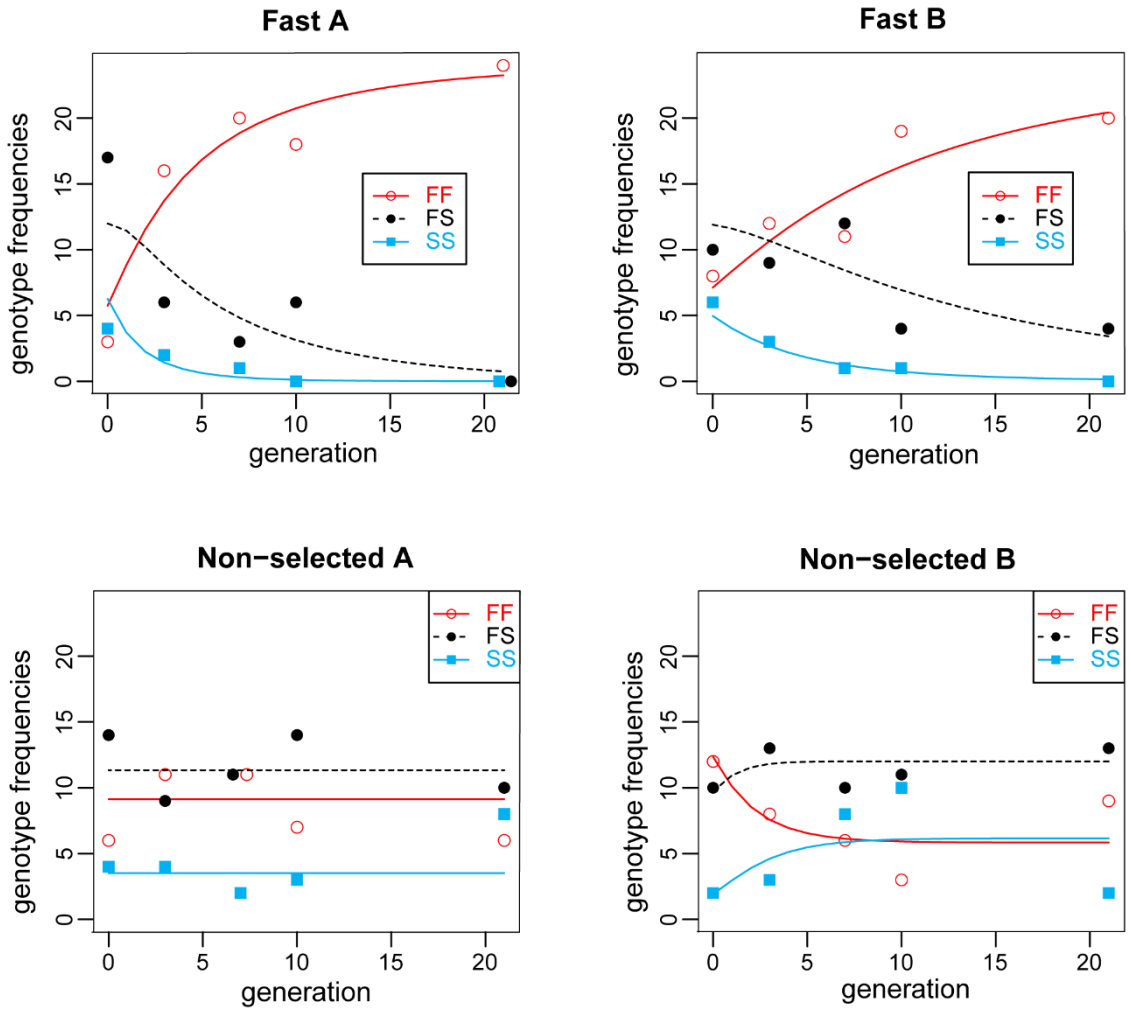

Figure 4-28. Counts of the three genotypes for generation 0, 3, 7, 10 and 21. For each subpanel counts for each genotype is indicates by the different symbols and the estimates change from the models are indicated by the different lines (see legend). Key: FF, homozygotes with the 222 bp deleted region; SS, homozygotes with the 445 bp repeated region; and FS, heterozygotes with both of the deleted region and the repeated region.

In the end, we genotyped 48 beetles from the original wild population that was used to set up our outbred starting population. We found both alleles (F and S alleles) are present in this original wild population (Figure 4-29). Of which, 31 show only a 720 bp band (homozygous F allele), 2 show only a 942 bp band (homozygous S allele), and 14 are heterozygote (both bands + a hybrid band present). Thus, the allele frequency of F is 0.81, and S is 0.19 in this natural population.

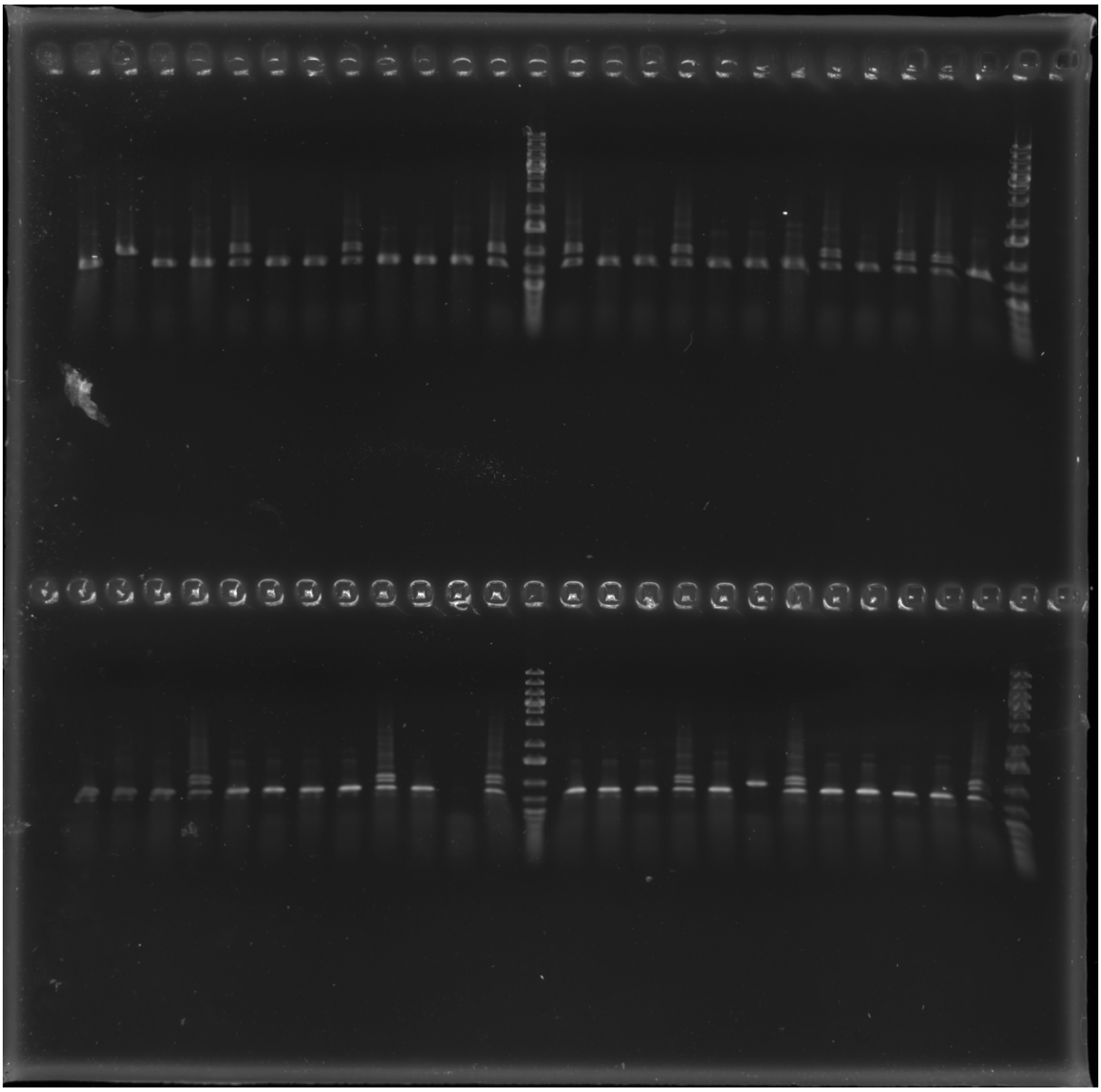

Figure 4-29. Allele frequency of F in a natural population is 0.81. Genotyping PCR (Ethidium bromide staining shown on a 1.0% agarose gel) of 48 beetles from the wild population collected by Rentokil from a bakery in The Netherlands (see Materials and methods). Ladder is GeneRuler 1kb plus DNA ladder (Invitrogen).

Together, these data show that the F allele is a natural allele that was present in the outbred population, but dramatically increased in frequency during selection for fast development.

The F allele is associated with fast development in a non-selected line

To see if there is a relation between the F allele and fast development, we genotyped the 64 larvae that had the fastest embryonic development, and the 64 larvae that had the slowest embryonic development out of more than 2000 larvae for both the non-selected A and non-selected B line. This extreme genotyping within the non-selected lines shows that the frequency of the 222 bp (F allele) is significantly associated with fast development in the NS B line. However, this was not the case in the NSA line (Table 4-7). This suggests that the F allele has a role in fast development, but that genetic background and other alleles are also important.

Table 4-7. Extreme genotyping. Beetles from the non-selected A (NS A) and from the non-selected B (NS B) lines were allowed to lay eggs for 2h, and hatching was recorded in 2h intervals on the selection machine (see methods). In total, more than 2000 eggs were analyzed for each non-selected line. The fastest and slowest 64 beetles were genotyped. $\chi 2$ -tests show that FF beetles are only significantly overrepresented (and SS beetles significantly underrepresented) among the fastest beetles of the NSB line, but not significantly in the NSA lines.

Selection line		Genotype			Chi-squared test		
		FF	FS	SS	X-squared	Degree of freedom	P-value
NS A	fastest	11	35	18	1.4652	2	0.4807
	slowest	8	32	24			
NS B	fastest	12	33	19	6.1722	2	0.04568
	slowest	5	28	31			

The CRISPR deletion strain of *T. castaneum* develops faster, but has reduced fecundity

In order to study the role of the F allele in isolation, we recreated this deletion in the homogenous genetic background of the GA-1 (Georgia) lab strain (that is homozygous for the repeat) by applying CRISPR-Cas9 technology using a single guide (Figure 4-1). We set up a stock homozygous for the deletion. Sanger sequencing data shows that the recovered 4 alleles present in the stock are more or less an exact reproduction of the Fast allele, with a maximum indel of 9 bp around the PAM site (Figure 4-30). We called them Allele1, Allele2, Allele3 and Allele4. The length of the deletion is 230, 217, 218 and 214 bp, respectively. The alleles present in this stock are aligned in Figure 4-30. Interestingly, the remaining first repeat in Allele1 and Allele2 also contains some SNPs characteristic for the second repeat (Figure 4-30), possibly caused by DNA repair from this sequence.

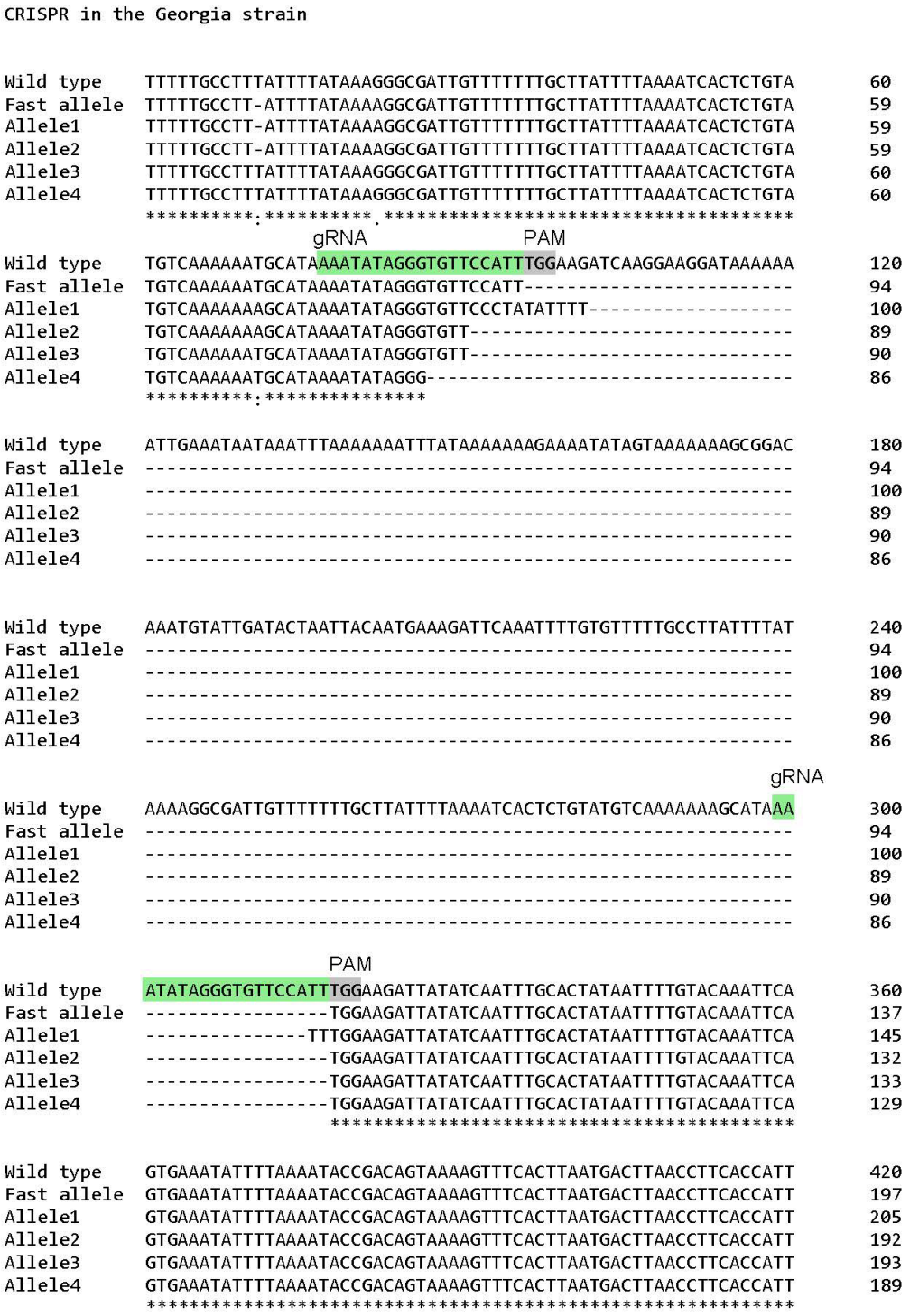

Figure 4-30. Alignment of the PAM region of wild type, fast allele, and Crispr alleles. Of which, wild type is from genome-sequenced Georgia strain, fast allele is from the pooled resequencing data of fast lines in our selection lines, and allele 1-4 is from the Crispr experiment. The guide RNA (gRNA) is shadowed in green. The protospacer adjacent motif (PAM) is shadowed in grey.

First, we compared embryonic developmental time of the CRISPR-induced deletion strain and the wild type GA-1 strain of *T. castaneum*. The average time of embryonic development of Crispr line is significantly smaller than that of GA-1. The difference between GA-1 and Crispr lines is 5 h (Figure 4-31). Thus, this allele has a large effect on developmental time.

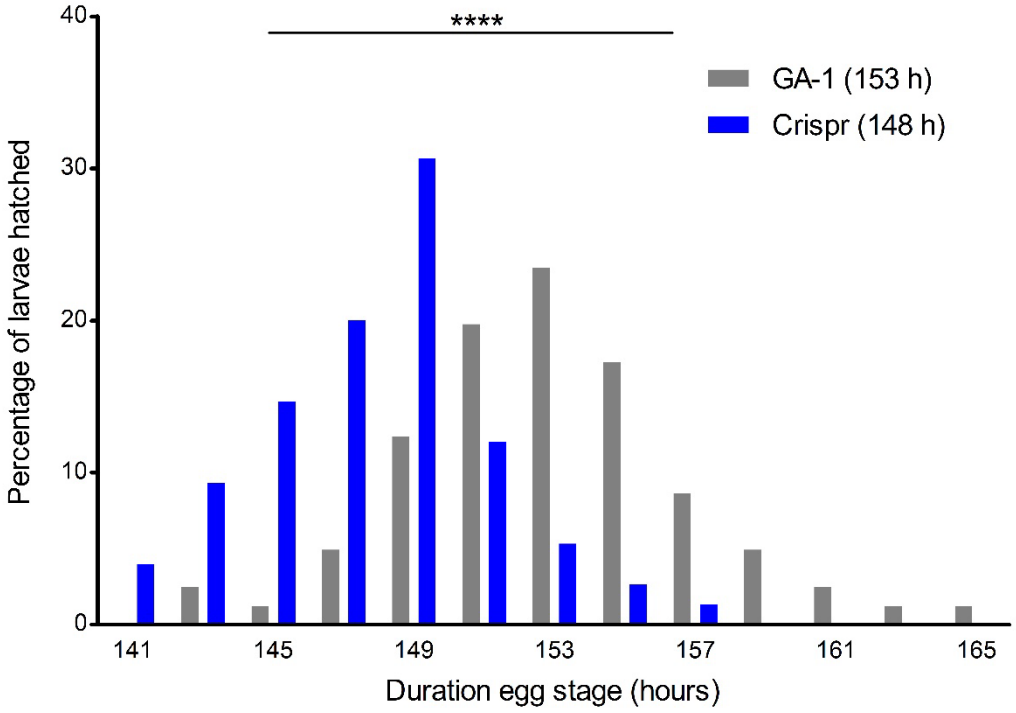

Figure 4-31. Hatching time of eggs of the Georgia 1 (GA-1) line and its Crispr line. Hatching time of eggs of the Georgia 1line (GA-1, grey) and its Crispr line (blue). The average hatching time of GA-1 and Crispr lines is 153 h and 148 h post-oviposition, respectively. The student t-test was performed to compare GA-1 and its Crispr. Asterisks, significant difference in hatching time (****, $P < 0.0001$).

Second, we measured pupal weight and early fecundity of GA-1 strain and the Crispr line. The methods are described in Chapter 3 under 'Pupal weight' and 'Fecundity assays'. We did not find significant difference of pupal weight between GA-1 strain and the Crispr line (Figure 4-32A), but there was also no significant difference in pupal weight between the fast selection lines and the non-selected lines (Chapter 3, Figure 3-7). However, the number of eggs laid by 50 Crispr female adults was significant smaller than GA-1 strain (Figure 4-32B), just like the fecundity of the fast lines is reduced compared to the non-selected lines (Chapter 3, Figure 3-8). Thus, this single deletion speeds up development, and causes a trade-off with fecundity.

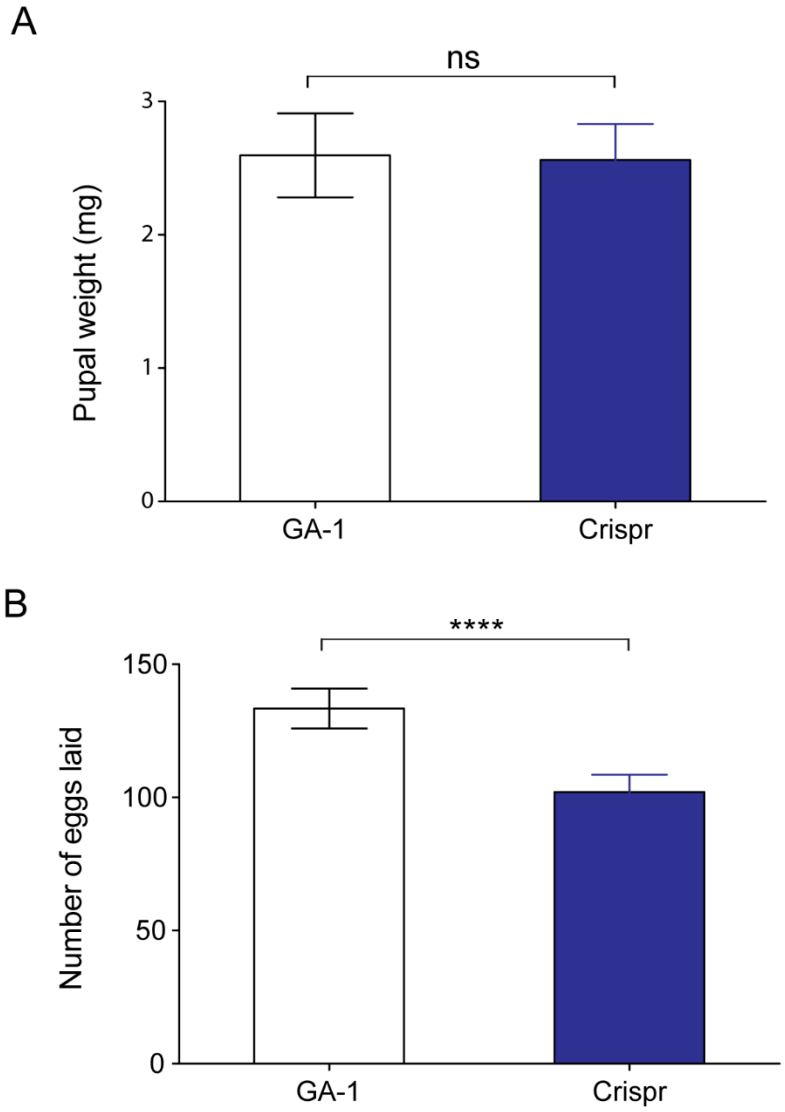

Figure 4-32. Life-history trade-offs of Crispr experiments. A, weight of the newly-hatched pupae of GA-1 strain and its Crispr line. Each vertical bar indicates Mean ± SD (n=60). Key: ns, no significant difference observed in hatching time. B, Fecundity of 50 *Tribolium castaneum* females laid within 4 h of GA-1 strain and its Crispr line. Each vertical bar indicates Mean ± SD (n=9). Asterisks, significant difference in fecundity (****, $P < 0.0001$).

The deletion advances the embryonic ecdysone peak

Further, we analyzed *Cyp18a1* expression and ecdysone dynamics in the CRISPR strain. Transcript levels of *Cyp18a1* were normalized to the reference gene ribosomal protein 13a (RPL13a) (TC013477). The results showed that *Cyp18a1* mRNA reached the peaks at 120 h and then kept in the relative higher level in both Crispr and GA-1 strain. However, the increase of *Cyp18a1* expression in GA-1 strain started much earlier than Crispr strain. Namely, GA-1 strain started to induce *Cyp18a1* mRNA at 104 h, while Crispr strain was at 112 h post-oviposition (Figure 4-33).

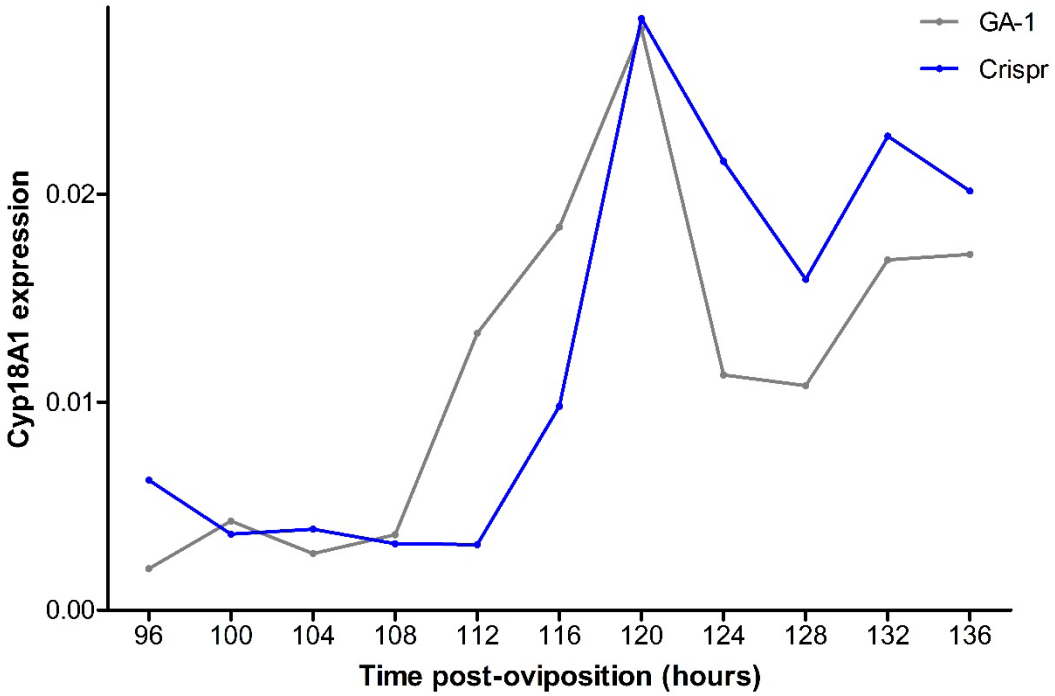

Figure 4-33. Relative expression of *Cyp18a1* in the Georgia 1 (GA-1) line and its Crispr line during later embryonic development. Each point represents the mean *Cyp18a1* expression based on two biological replicates (each replicate is the mean of two technical replicates).

At the same time, we measured 20E titers during dorsal closure. The Crispr and GA-1 lines reached their peaks at 114 and 120 h post-oviposition, respectively. Meanwhile, 20E peak of Crispr line is earlier and stronger than that of GA-1 line (Figure 4-34).

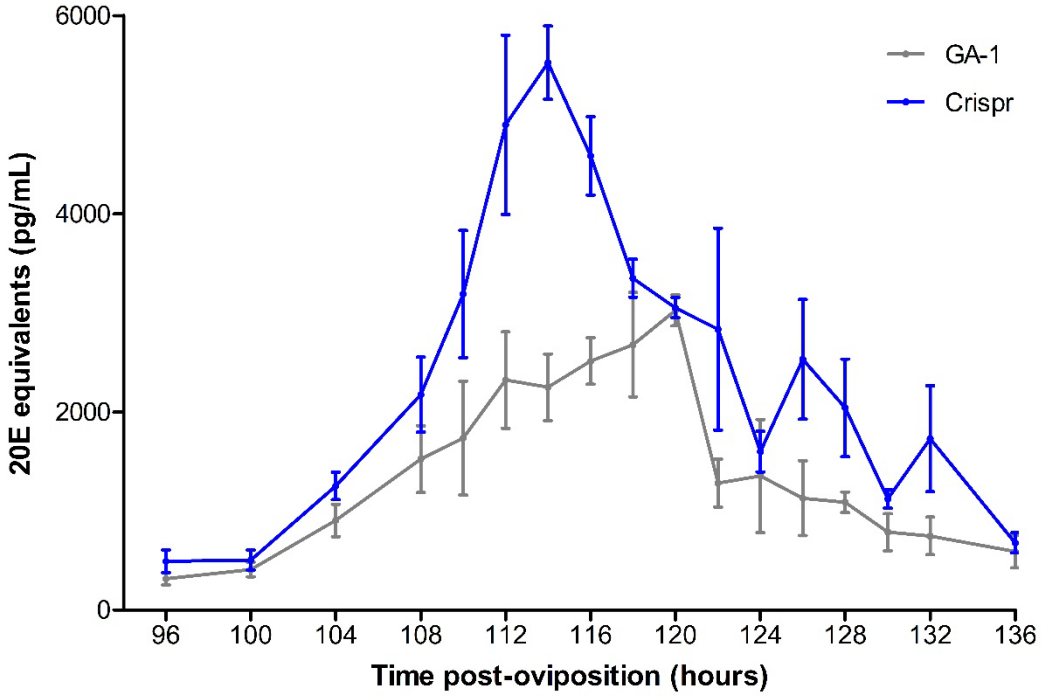

Figure 4-34. Ecdysteroid titer in the Georgia 1 (GA-1) line and its Crispr line during later embryonic development. Each point represents the mean ecdysteroid titer plus standard error based on three biological replicates (each replicate is the mean of two technical replicates according to the protocol of the kit).

Thus, the F allele delays *Cyp18a1* expression, but advances the embryonic ecdysone peak.

Live imaging shows that the deletion advances dorsal closure

In order to establish whether the F allele drives earlier dorsal closure, we crossed our CRISPR line to the nGFP line (Sarrazin et al., 2012) for confocal live imaging of their heterozygous offspring. The nGFP line is homozygous for the 445 bp S allele (confirmed by PCR in Supplementary Figure 4-8). As control, we crossed GA-1 to the nGFP line. Imaging analysis shows that the completely retracted germband stage in the heterozygous CRISPR/nGFP embryos occurs at the same time as in the heterozygous GA-1/nGFP embryos. However, the start of dorsal closure stage of nGFP-CRISPR embryos occurs earlier than in heterozygous nGFP-GA-1 offspring ($P < 0.05$, Figure 4-35). As a consequence, completion of dorsal closure is also earlier in CRISPR-nGFP offspring (Figure 4-35). However, this acceleration is not caused by the duration dorsal closure, as no significant difference found between nGFP-GA-1 and nGFP-Crispr offspring (Figure 4-36B); it is only the consequence of dorsal closure starting earlier. Thus, the 222 bp deletion shortens the interval between completely retracted germband and the start of dorsal closure during embryonic development of *Tribolium* (Figure 4-36A, see stills of representative movies in Supplementary Figure 4-9 and Supplementary Figure 4-10).

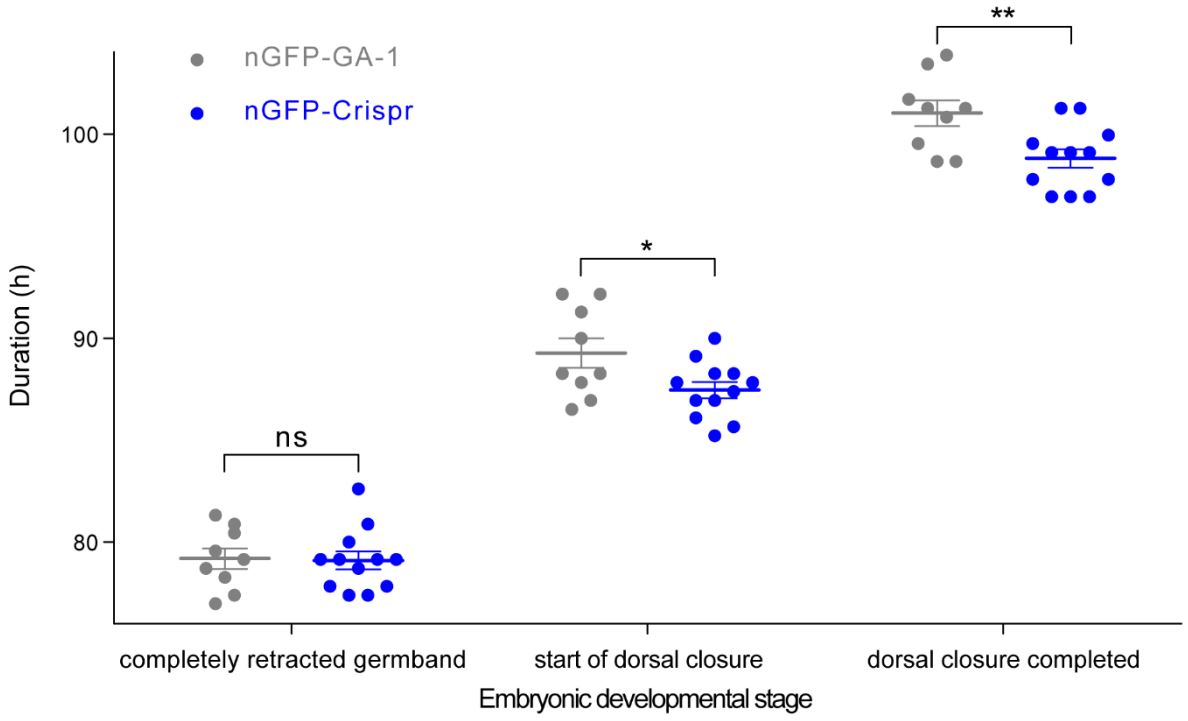

Figure 4-35. Duration embryonic developmental stages, including completely retracted germband, start of dorsal closure and dorsal closure completed. To the stage of completely retracted germband, there is no significant difference of duration between nGFP-GA-1 and nGFP-Crispr offspring. To the stage of start of dorsal closure or dorsal closure completed, nGFP-Crispr develops significantly faster than nGFP-GA-1 offspring. P-values are shown in the figure and indicated with ns, no significance; *, $P < 0.05$; **, $P < 0.01$.

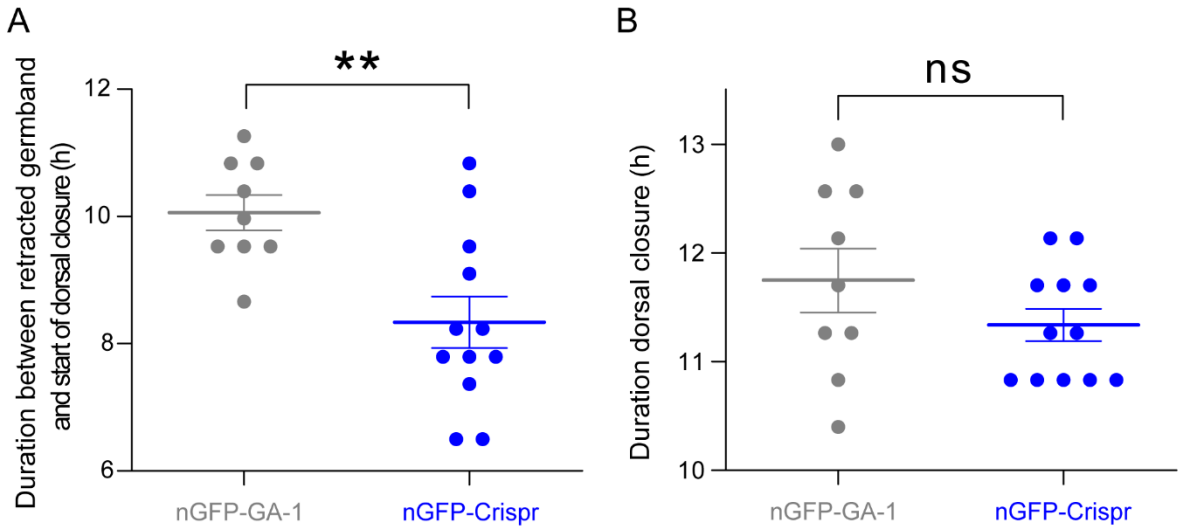

Figure 4-36. Duration between two embryonic developmental stages. A, Duration between completely retracted germband and start of dorsal closure. B, Duration between start of dorsal closure and dorsal closure completed. P-values are shown in the figure and indicated with **, $P < 0.01$; ns, no significance.

In conclusion, this recreated deletion advances the embryonic ecdysone peak inducing dorsal closure, shortens development, and causes a trade-off with fecundity. This single deletion may thus be considered a major life-history allele.

Discussion

Identification of candidate genes on chromosome 3 and 9

Whole-genome sequencing of pools of individual DNAs (Pool-seq) represents an attractive and cost-effective approach. In *Drosophila melanogaster*, for instance, Pool-seq identified two cis-regulatory regions near *tan* and *bric-à-brac 1*, associating with light and dark abdominal pigmentation of females (Kofler et al., 2012). Pool-seq has been proven to be accurate and reliable to estimate the allele frequency differences in evolve and resequence (E&R) studies (Schlötterer et al., 2014; Vlachos and Kofler, 2019). In our study, sequencing pools of eggs of four selection lines with fast and non-selected embryonic development revealed two genomic regions on chromosome 3 and 9 with alleles under strong selection (Figure 4-3).

In these two regions, we identified 57 lead SNPs. However, it is likely that not all of them play a role in fast development, due to linkage disequilibrium (LD). LD is the non-random association of alleles at two or more loci, and can be caused by many factors including genetic drift and reduced recombination because of small physical distance on the chromosome. The effect of genetic drift is probably low in our study, as we used large population (>500 beetles). However, reduced recombination could well play a role. This effect is known as the hitchhiking. As a result, hundreds of surrogate SNPs can be yielded for each linked group of the actual SNPs. These hitchhiking mutations can achieve a high frequency due to close physical linkage with the driver allele on the same chromosome (Lang et al., 2013; Papadopoulos et al., 1999; Tenaillon et al., 2012). For example, 92 of 116 mutations have no obvious benefit on fitness (adaptation in asexual populations) in 11 yeast evolved populations adapted to high glucose medium (Buskirk et al., 2017). In the end, additional assays are always needed to distinguish a driver allele from neutral hitchhiking mutations.

As none of our lead SNPs leads to alternative proteins, our first additional assay was a gene expression analysis. In genome-wide association experiments, most SNPs are found in non-coding regions of the DNA (Tak and Farnham, 2015). For example, in *D. melanogaster*, the majority of SNPs (84.4%) affecting sleep are located in non-coding regions (Harbison et al., 2013). In 25 human colon cancer risk SNPs, only one is located in the third exon of the *MYNN* gene, while the others are located in non-coding regions (Yao et al., 2014). These non-coding regions are introns and intergenic regions that contain cis-regulatory elements (CREs), such as silencers, promoters, and enhancers (Barrett et al., 2012). These CREs contain multiple 4–30 bp DNA motifs that function as binding sites for sequence-specific transcription factors (TFs) (Marand and Schmitz, 2022; Wittkopp and Kalay, 2012). Sequence variation in these binding sites can thus alter gene expression. Mutations in *cis*-regulatory elements and resulting variation in gene regulation is considered to be crucial for evolution (Carroll, 2008), which has been confirmed over and over again (Mazo-Vargas et al., 2022; Siepel and Arbiza, 2014; Verta and Jones, 2019).

In general, our transcriptional analysis did not reduce the number of candidate genes drastically. In our RNAseq analysis, 997 genes were differentially expressed between the fast and non-selected lines, of which 9 were also genes with our lead SNPs. In our qPCR analysis, 27 of the 45 genes with these 57 lead SNPs showed differential expression on at least one timepoint. Thus, many genes are differentially expressed between the fast- and non-selected lines. In Supplementary File 4-2, information about each of the 27 genes detected by qPCR is given. The RNAseq at 76 hrs is more reliable than the qPCR data, as it is based on three biological replicates, instead of two. However, the qPCR data involve two extra later timepoints during (92 hrs) and after dorsal closure (108 hrs), providing a better temporal resolution. Thus, our transcriptional analysis was not very effective in distinguishing driver alleles from hitchhikers, as quite a number of candidate genes remained. Likely, many of them display differential expression as a consequence of fast development, and are not causative. A functional RNAi screen was needed to distinguish the driving genes from neutral ones.

RNA interference (RNAi) has been well established in *Tribolium* for functional analysis (Horn et al., 2022; Tomoyasu et al., 2008). RNAi was first found in *Caenorhabditis elegans* in 1998. By introducing a double-stranded RNA (dsRNA) of a specific gene into cells, the endonuclease protein Dicer which is conserved in fungi, plants, worms, flies, and mammals, cuts the dsRNA into 21-23 nucleotide guide sequences. These small interfering RNA (siRNA), are incorporated into a protein complex, forming the RNA-induced silencing complex (RISC). Subsequently, the sense (non-guide) strand (or passenger strand) of the siRNA is removed, and leaves the guide RNA single stranded. This guide RNA directs the RISC complex to the specific target messenger RNA (mRNA), and cleaves this mRNA, achieving mRNA degradation and gene silencing (Bernstein et al., 2001; Bumcrot et al., 2006; Fire et al., 1998). Robust, systemic RNAi is observed across every life-history stage of many insects, including *T. castaneum* (Miller et al., 2012; Tomoyasu et al., 2008). A genome-wide RNAi project has been undertaken in *T.castaneum*, and a growing database for RNAi phenotypes is available. A database for RNAi phenotypes from a large-scale RNAi screen, iBeetle-Base, is available for *Tribolium* (Dönitz et al., 2015). Parental RNAi in *Tribolium* has the advantage of knockdown responses achieved in offspring embryos upon RNAi in mothers. Parental RNAi efficacy in offspring can persist for weeks (Bucher et al., 2002; Horn et al., 2022).

Our pRNAi screen did drastically reduce the number of candidate genes to four. Two genes, *melted* and *SLC25-35-2* are located adjacently to each other on chromosome 3. *Melted* is a likely candidate. By interacting with tuberous sclerosis 1 (Tsc1) and FOXO, Melted enhances insulin/TOR (target of rapamycin) activity (Teleman et al., 2005), a pivotal pathway enhancing growth rate (Baker and Thummel, 2007; Nijhout et al., 2014). It is unclear, however, how solute carrier family 25 member 35-2 (SLC25-35-2) can affect developmental time. It may be possible that RNAi against *SLC25-35-2* reduces transcription of the adjacent *melted* gene, similar to the observed spreading of RNAi-induced transcriptional silencing in pericentromeric repeats of yeast (Noma et al., 2004). Thus, *melted* seems

the driving gene here. The causative allele is likely located in the intergenic region between *melted* and *SLC25-35-2*. However, mapping of the Illumina reads to this area of chromosome 3 suggests major rearrangements such as large insertions or inversions that are impossible to reconstruct using these short reads. Future long-read nanopore sequencing may resolve this issue.

The two high peaks on chromosome 3 (Figure 4-3A, B, D), are located on either side of the centromere. The centromere is a the eukaryotic chromosomal site where the two chromatids are joined at mitosis and meiosis. Recombination rates are reduced around the centromere (Blair et al., 2018; Nachman, 2002; Sardell et al., 2018). Thus, it is even possible that the only allele under selection on chromosome 3 was the chromosomal rearrangement affecting *melted*, and that the peak at the other side of the centromere was dragged along during selection.

The two other genes, *CAT1* and *Cyp18a1* are located on chromosome 9. *CAT1* is a likely candidate, as it is orthologous to slimfast, an amino acid sensor in the fat body that can overrule peripheral insulin/TOR activity by PI3K modulation affecting developmental time (Baker and Thummel, 2007; Colombani et al., 2003). However, the effect of its knockdown on embryonic developmental time is small (2.75h) and minimally significant (Figure 4-6). This does not mean that he allele affecting slimfast has no effect. On the contrary, small-effect alleles help reach genotypes closer to a fitness optimum. If the populations are near their optimum, large-effect alleles are often deleterious. However, large-effect alleles are more likely to be favored when populations are far from the adaptive peak (Dittmar et al., 2016), and possibly during strong artificial selection such as in our experiment. The knockdown with the largest effect on embryonic developmental time is that of Cytochrome P450 18A1 (*Cyp18a1*, gene 32, Figure 4-6).

In conclusion, our pooled resequencing, expression analysis, and RNAi screen identify two main alleles under selection. One chromosomal rearrangement affecting melted on chromosome 3. And an allele affecting *Cyp18a1* on chromosome 9. The broad high peak on chromosome 9, and the two narrow peaks on each side of the centromere on chromosome 3 may all be the consequence of selection on these two alleles only.

The function of the Halloween orthologs in larvae, pupae and adults of *Tribolium*

Cyp18a1 is a cytochrome P450 enzyme that catabolizes active ecdysone (20-hydroxyecdysone, 20E) by 26-hydroxylation (Guittard et al., 2011; Rewitz et al., 2010). The steroid hormone 20E is crucial in controlling developmental timing such as molting and metamorphosis, and is synthesized by other Cytochrome P450 enzymes collectively called the Halloween genes (Gilbert, 2004; Niwa and Niwa, 2016; Yamanaka et al., 2013). The initial step of ecdysone biosynthesis is the dehydrogenation of cholesterol to 7-dehydrocholesterol in the prothoracic gland by the Rieske oxygenase neverland (Nvd) (Figure 4-37). It is worth noting that Nvd is not present in the genome of *T. castaneum*. Surprisingly, Nvd seems to be absent in all holometabolous insects, except the Diptera. All hemimetabolous insect genomes do contain a Nvd ortholog. Using the Halloween genes *spook* (*Spo*, *Cyp307A1*), *spookier* (*Spok*, *Cyp307A2*), *phantom* (*Phm*, *Cyp306A1*), *disembodied* (*Dib*, *Cyp302A1*) and *shadow* (*Sad*, *Cyp315A1*), insects can convert cholesterol and/or plant sterols to ecdysone. The uncharacterized conversion steps, "BLACK BOX", have not been identified so far as the precise intermediates between 7dC and 5β-ketodiol are chemically unstable (Figure 4-37).The small and fat-soluble steroidal prohormone ecdysone can easily pass through the cell membrane. When it enters the cytoplasm, it is converted to the active form 20E by the Halloween gene *shade* (*Shd*, *Cyp314A1*) (Gilbert, 2004).

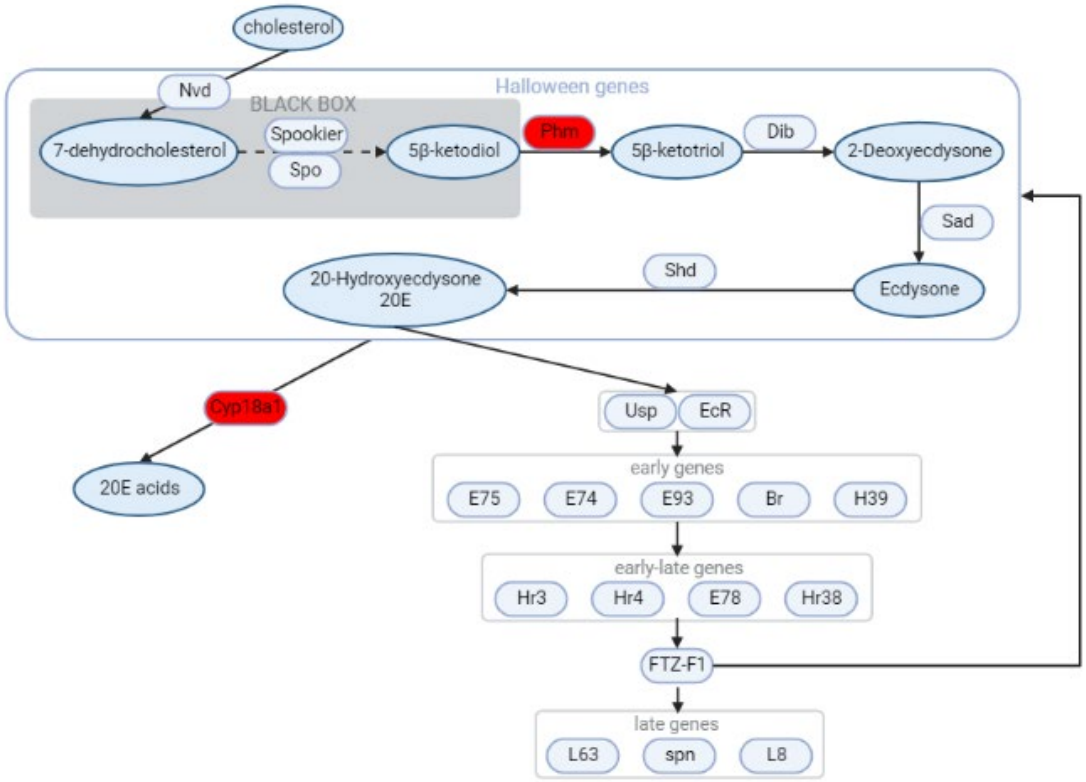

Figure 4-37. Ecdysone biosynthesis and 20E signaling pathway in insects. Modified from (Luan et al., 2013; Niwa and Niwa, 2014). Candidate genes identified in this study are shown in red boxes. The Halloween genes including *neverland* (*Nvd*), *spook* (*Spo*), *phantom* (*Phm*), *disembodied* (*Dib*), *shadow* (*Sad*) and *shade* (*Shd*) are responsible for biosynthesis of ecdysone and 20E, and *Cyp18a1* is used for 20E inactivation. The 20E/EcR/USP complex initiates 20E signaling with the expression of the early genes, early–late genes and late genes. USP, Ultraspiracle; EcR, ecdysone receptor; E75, ecdysone-inducible gene 75; E74, ecdysone-inducible gene 74; E93, ecdysone-induced protein 93F; Br, broad; HR39, hormone receptor-like in 39; HR3, hormone receptor 3; HR4, hormone receptor 4; E78, ecdysone-inducible gene 78; HR38, hormone receptor-like in 38; FTZ-F1, Fushi-tarazu transcription factor 1; L63, Ecdysone-induced protein 63E; Spn, D-spinophilin; L82, mustard.

The active 20E goes on to bind a heterodimeric complex of nuclear receptors comprising ecdysone receptor (EcR) and ultraspiracle (USP). The 20E/EcR/USP complex initiates various gene expression cascades by attaching to the DNA of the early target genes (Niwa and Niwa, 2014; Schumann et al., 2018). These early genes, such as ecdysone-inducible gene 74 (*E74*), ecdysone-inducible gene 75 (*E75*) and *Br*, further induce the “early-late” and ”late” genes which directly control biological responses (Luan et al., 2013; Thummel, 2002). Ecdysone also induces expression of *Cyp18a1* encoding an ecdysteroid 26-hydroxylase that catabolizesd active ecdysone.

RNAi silencing of the Halloween genes has been performed in many insects. However, the knockdown phenotypes are distinct in different insects with dose-dependent effects. For example, *Phm* RNAi resulted in lethality in *D. melanogaster* (Chung et al., 2009). In the small brown planthopper *Laodelphax striatellus*, *Phm* silencing decreased *EcR* expression levels, caused a higher nymphal mortality rate, and delayed development (Jia et al., 2015). From other arthropods, *Phm* RNAi has been reported to affect the molting of *Macrobrachium nipponense* and inhibit its growth (Pan et al., 2022). However, larval and pupal RNAi against *Phm* in our study did not affect mortality rate or post-embryonic development of *Tribolium* (Figure 4-8). As we did not confirm knockdown of the transcript by qPCR, it is possible that our RNAi against Phm was not efficient.

RNAi depletion of the Halloween genes and *Cyp18a1* delayed the molting process of *Bemisia tabaci* by 1–3 days (in total of 9 days in the control treatment) at the 4th nymphal stage (Liu et al., 2020). In

our study, pRNAi silencing of *Spo*, *Sad* and *Shd* rendered beetles permanently sterile and therefore no eggs were produced by the injected mothers. However, mothers injected with *Dib* and *Phm* dsRNA can normally lay eggs and the embryonic development of their offspring was not disrupted. This is very similar to knockdown experiments in the desert locust *Schistocerca gregaria*. Depleting the expression of *Spo*, *Sad* and *Shd* in *S. gregaria* significantly affected oogenesis and oviposition, and drastically altered the shapes of the growing oocytes, while silencing *Phm* and *Dib* did not have any effect (Schellens et al., 2022). In the cabbage beetle *Colaphellus bowringi*, knocking down *Spo*, *Sad*, *Shd* and *EcR* in the females inhibited yolk deposition and ovarian growth and development (Guo et al., 2021), confirming a general role for ecdysone in oogenesis.

In *Drosophila*, silencing of *Cyp18a1* caused a high lethality in the larval or pupal stage (Guittard et al., 2011). We found a dramatic increase of *Cyp18a1* expression in prepupae and pupae, already indicating that *Cyp18a1* is required for metamorphosis and eclosion of *Tribolium*, as reported in *Drosophila* (Rewitz et al., 2010). Indeed, *Cyp18a1* inactivation in these post embryonic stages caused a high lethality, and prevented pupation and eclosion (Figure 4-12). Taken together, our data suggest that the requirement of ecdysone degradation for pupation and eclosion is conserved between *Drosophila* and *Tribolium*. Surprisingly, *Cyp18a1* pRNAi did not lead to sterility, providing us with the chance to study its function during embryonic development.

Ecdysone during embryonic development of *Tribolium*

Here, we systemically studied gene expression profiles of the Halloween genes, *Cyp18a1* and *Br* during embryogenesis of *T. castaneum*. We found two expression peaks of them at early and later embryonic development, but not in the middle stage. The same is true for ecdysone itself with two peaks at 40 h and 120 h post-oviposition (Figure 4-14). In *Drosophila*, only a late peak was found and was recently shown to regulate dorsal closure during embryogenesis (Yoo et al., 2021). In our study, we focused on the late peak.

We showed that these late peaks in the selection lines and Georgia strain all occurred at the complete dorsal closure stage. We also demonstrated that the high ecdysteroid titer was closely followed by high *Cyp18a1* expression after dorsal closure (Figure 4-14). In our selection lines, the fast lines started and finished dorsal closure earlier than the non-selected lines (Figure 4-2). As a result, relative expression of *Cyp18a1* in the fast lines compared to the non-selected lines was higher before dorsal closure but lower after dorsal closure (Figure 4-5).

Interestingly, the expression peak of *Shd*, the last Halloween gene expression seemed to largely precede the ecdysone peak (Figure 4-15). This pattern of ecdysone levels and *Shd* expression suggests that Shd is a long-lived protein that can continue to modify ecdysone in an efficient and effective way, and that more precise rise of the ecdysone peak is regulated by earlier Halloween genes, such as *Spook* whose expression exactly overlaps with the ecdysone peak (Figure 4-14).

Strikingly, silencing of *Cyp18a1* by pRNAi resulted in continuously rising ecdysteroid levels (Figure 4-21), and failure to start dorsal closure (Figure 4-19). This demonstrates that a pulse of ecdysone is required to start dorsal closure. Continuous high levels of ecdysone are not sufficient, as also shown for the juvenile-adult transition (Rewitz et al., 2010).

In early-stage eggs, we also observed the conspicuous earlier phenotype of incomplete germband extension and shortened germbands (Figure 4-18). This may be caused by disrupted segmentation, as Cruz *et al*. recently found that 20E signaling is essential for germband formation and segmentation in hemimetabolous insect *Blattella germanica* (Cruz et al., 2022). When using embryonic RNAi (eRNAi) against *Spo*, we also found that the injected eggs cannot survive to germband retraction and were arrested during segmentation and germband elongation. Together, these results suggest that the first

lower peak of ecdysone around 40h is required for segmentation, while the second high peak of ecdysone at 120h is required for dorsal closure. However, duration of segmentation and germband extension did not differ among our selection lines, only dorsal closure (Figure 4-2).

Further work needed to fully understand the role of Cyp18a1 or even ecdysone in early embryonic development. Although a third of *Cyp18a1* RNAi embryos hatched (Figure 4-20), most of them did not survive to larvae (Figure 4-7), mainly as a consequence of disrupted segmentation and dorsal closure.

The role of the deletion

We have identified a 222 bp deletion that increased in frequency during selection in the fast lines, and has a frequency of 0 in the slow lines (Table 4-3). We tested the function of this deletion by applying a CRISPR/Cas9 strategy in which we used a single guide targeting the repeated sequence to exactly recreate this deletion in the homogenous genetic background of the Georgia lab astrain. The effectivity of CRISPR-Cas9 has been demonstrated in *Tribolium* before (Gilles et al., 2015), and we could also efficiently generate the desired excision. Sequencing of the alleles present in our stock show that a maximum indel of 9 bp was present around the PAM (Figure 4-30). In two alleles, the remaining first repeat contained some SNPs typical for the second repeat (Figure 4-30). Possibly, these SNPs were introduced into the first repeat by DNA repair using the excised second repeat as template.

We assume that the deletion is located in a cis-regulatory element (CRE/enhancer) that regulates *Cyp18a1* expression. Using the JASPAR database and FIMO, we indeed find a binding site for Tramtrack (Ttk), and a high-affinity binding site for Broad (Br) in the deletion, immediately followed by a binding site for the Ecdysone Receptor (Figure 4-39). The Ttk and Br binding sites are thus duplicated when the repeat is present (the slow allele, Supplementary Figure 4-7), but only single Ttk and Br binding sites exist in the fast allele.

Both Ttk and Br encode Cys_2/His_2 zinc-finger proteins (DiBello et al., 1991; Fairall et al., 1993), and belong to the Broad-complex/Tramtrack/Bric-à-brac or poxvirus and zinc finger (BTB/POZ) family. BTB/POZ proteins not only play a critical role in transcriptional regulation but also in chromatin remodeling or modification (Chaharbakhshi and Jemc, 2016). Br has four protein isoforms (Br-Z1 to Br-Z4) and is an early ecdysone target gene (Bayer et al., 1996; Mugat et al., 2000). Crucially, Broad has been shown to regulate Ecdysone target genes, for instance during metamorphosis (Huang et al., 2013; Karim et al., 1993; Mugat et al., 2000; Truman, 2019; Uhlirova et al., 2003). Ttk usually acts as a transcriptional repressor during development (Badenhorst et al., 2002; Li et al., 1997; Pagans et al., 2002; Xiong and Montell, 1993) . The transcriptional repression of *fushi tarazu* (*FTZ*) by Ttk, for instance, is probably caused by alterations of chromatin structure (Harrison and Travers, 1990; Li et al., 1997). However, Ttk has also been shown to be a strong activator of gene expression (Yu et al., 1999), and required for the ecdysone-induced upregulation of *Cut* in *Drosophila* (Sun et al., 2008).

In the 20E signaling pathway, the formation of chromatin loops establishing contacts between enhancers and basal promoters is required to start transcriptional regulation of early ecdysone-induced genes, such as *Br*, *E74* and *E75* (Bernardo et al., 2014). Recent studies established that the steroid hormone ecdysone can stimulate the activation of chromatin architectural alterations in *Drosophila*, activating genes (Cheng et al., 2022; Gutierrez-Perez et al., 2019; Hitrik et al., 2016; Kreher et al., 2017). For example, Gutierrez-Perez et al. revealed that ecdysone induces dramatic changes in three-dimensional chromatin architecture by connecting enhancers bound by Polycomb and Pipsqueak to their promoters, thus froming a chromatin loop to start target gene transcription (Gutierrez-Perez et al., 2019).

In conclusion, it is highly likely that our deletion is located in an ecdysone-inducible enhancer that regulates *Cyp18a1* expression. We wondered if the shifted ecdysone peak could be caused by altered *Cyp18a1* expression. To test this hypothesis, we developed a mathematical model.

We model Cyp18a1 as a sigmoidal function of ecdysone levels, in which we can vary the sensitivity to ecdysone by changing s (Figure 4-38A equation (I); Figure 4-38B). Total levels of Cyp18a1 are then its production rate in response to ecdysone, minus a degradation lambda (Figure 4-38A equation (II)). We model that ecdysone levels (E) are dependent on a self-regulated positive feedback loop (b) minus its degradation by Cyp18a1 (C) (Figure 4-38A equation (III)). This model shows that lower sensitivity to ecdysone (larger s) induces Cyp18a1 expression later (Figure 4-38C), resulting in a higher and earlier ecdysone peak (Figure 4-38D). Thus, an earlier ecdysone peak is caused by later induction of Cyp18a1 by ecdysone. This is exactly what we measured in the CRISPR line: delayed induction of *Cyp18a1* (Figure 4-33), but an earlier ecdysone peak (Figure 4-34). Thus, the deletion makes the *Cyp18a1* enhancer less sensitive to ecdysone.

A

(I) $$f(E) = \frac{V_{max}}{1+exp(\frac{\theta - E}{s})}$$

(II) $$\frac{dC}{dt} = f(E) - \lambda C$$

(III) $$\frac{dE}{dt} = bE - kCE$$

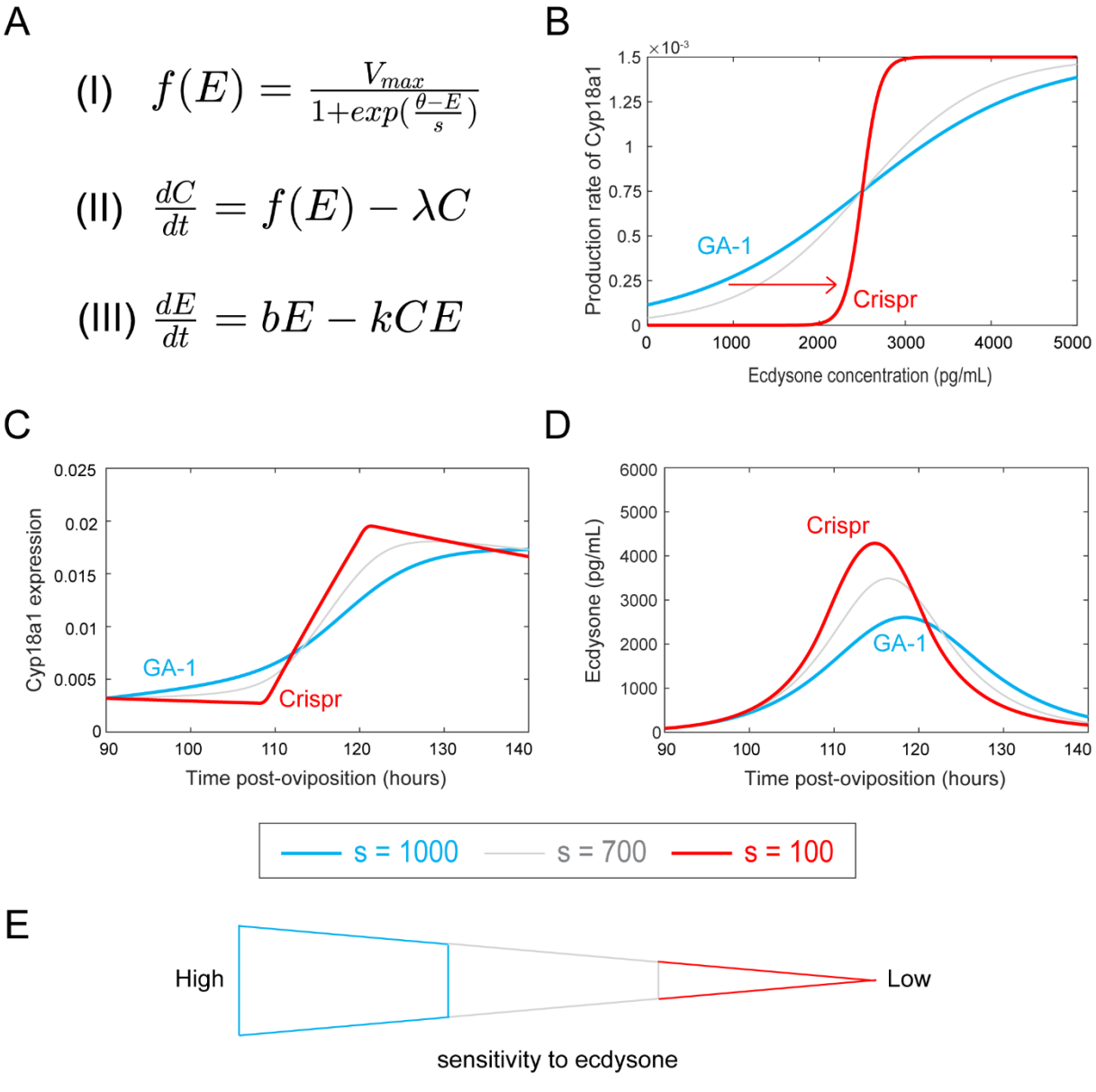

Figure 4-38. The mathematical model used for the dynamics of *Cyp18a1* expression and ecdysone levels. A, We model Cyp18a1 levels (C) as a sigmoidal function of Ecdysone (f(E)) in which we can vary sensitivity to ecdysone (s) (formula i) minus a degradation rate (lambda) (formula ii). We assume Ecdysone levels (E) are dependent on a self-regulated positive feedback loop (b) minus its degradation by Cyp18a1 (C) (formula iii). See details in Supplementary File 4-3. B, Proposed production of Cyp18a1 as function of Ecdysone concentration (f(E)) at different sensitivities for ecdysone (s=1000 for GA-1, blue; s= 100 for Crispr, red). C, Resulting Cyp18a1 expression over time, taking the assumptions from B. C, In Crispr (F allele, red), Cyp18a1 expression starts to rise later and steeper than in GA-1 (S allele, blue). D, Resulting Ecdysone levels over time, taking the assumptions from B. In the CRISPR line, the Ecdysone peak is higher and earlier (F allele, red), as observed in the fast lines. E, Schematic overview of sensitivity to ecdysone by changing s.

In other words, the 445 bp repeated region or 222 bp deleted region act as an enhancer. To start *Cyp18a1* transcription, the formation of a chromatin loop is required to connect the enhancer with the basal promotor. This looping requires a certain amount of ecdysone. As the BTB/POZ architectural binding sites are doubled in the GA strain, low levels of ecdysone are already sufficient to form the chromatin loop, turning on *Cyp18a1* transcription. But with only half of the BTB/POZ architectural binding sites, higher levels of ecdysone are required to form this chromatin loop in the Crispr line with the deletion (Figure 4-39B).

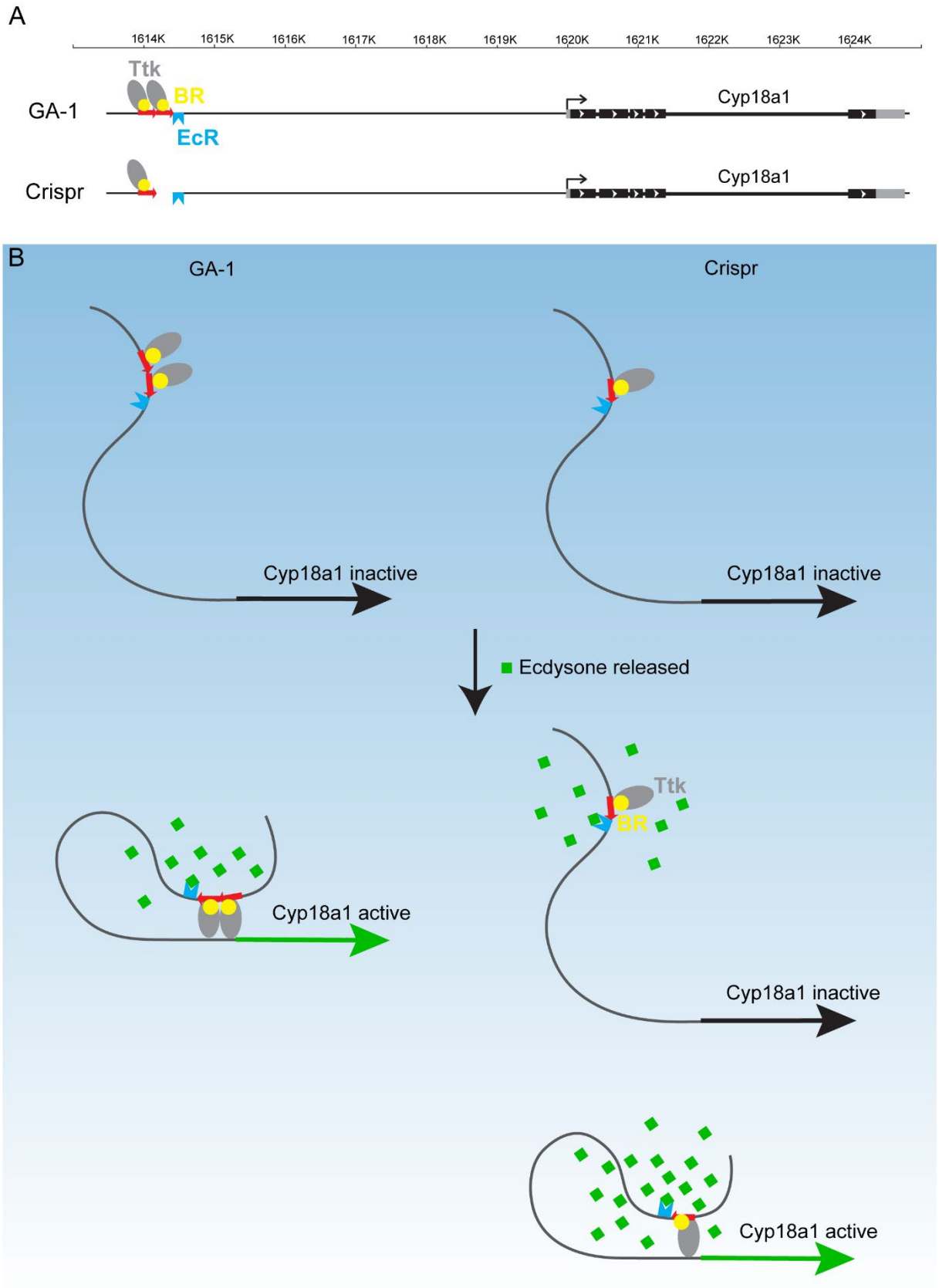

Figure 4-39. Control of *Cyp18a1* transcription through an enhancer–promoter loop. A, motifs of transcription factor binding sites (Supplementary Table 4-6) including Tramtrack (grey oval), Broad (yellow circle), and ecdysone receptor (cyan polygon) in the upstream of *Cyp18a1*. The repeated region in the Georgia strain (GA-1) and its Crispr result in the genome are indicated with red arrows. In addition, GA-1 has doubled binding sites in

this repeated region, compared to its Crispr line. B, when ecdysone (green square) released into the cytoplasm, it will bind to ecdysone receptor, driving the formation of the loop. Further, high levels of ecdysone are required to form the enhancer–promoter loop in the Crispr line, as it has deleted region with half ecdysone-related transcription factor binding sites. Once forming the enhancer–promoter loop, *Cyp18a1* transcription can be activated.

The inconsistent aspect of this model, is that multiple binding sites for transcription factor in an enhancer, usually lead to a steeper response in transcription of the cis-regulated gene (Giorgetti et al., 2010; Jens and Rajewsky, 2015). This phenomenon is caused by cooperative binding (Stefan and Le Novere, 2013). In our case, however, we would have to assume that deleting binding sites (as in the CRISPR) causes a steeper response of Cyp18a1. It could be that the supposed enhancer is affecting *Cyp18a1* expression in another way. The supposed enhancer may be the enhancer of another gene, for instance of *Cyp306a1*, *Phantom*, that is oriented tail to tail with *Cyp18a1* in *Tribolium*. This is not only the case in *Tribolium* but in all insects (Figure 4-40), including *Drosophila*, *Apis*, *Bombyx*, *Aedes aegypti*, *Aphis gossypii*, *Bactrocera latifrons*, *Cryptotermes secundus*, *Helicoverpa armigera*, *Leptinotarsa decemlineata*, *Melanaphis sacchari*, *Nasonia vitripennis*, *Nilaparvata lugens*, *Plutella xylostella*, *Sipha flava* and *Zeugodacus cucurbitae*, and crustaceans *Daphnia magna* in the NCBI database. This pattern in genomic order might suggest a regulatory switch either enabling transcription of *phantom* making ecdysone or enabling transcription of *Cyp18a1* degrading ecdysone. Future chromosome conformation capture technologies would be required to experimentally prove this hypothesis (McCord et al., 2020).

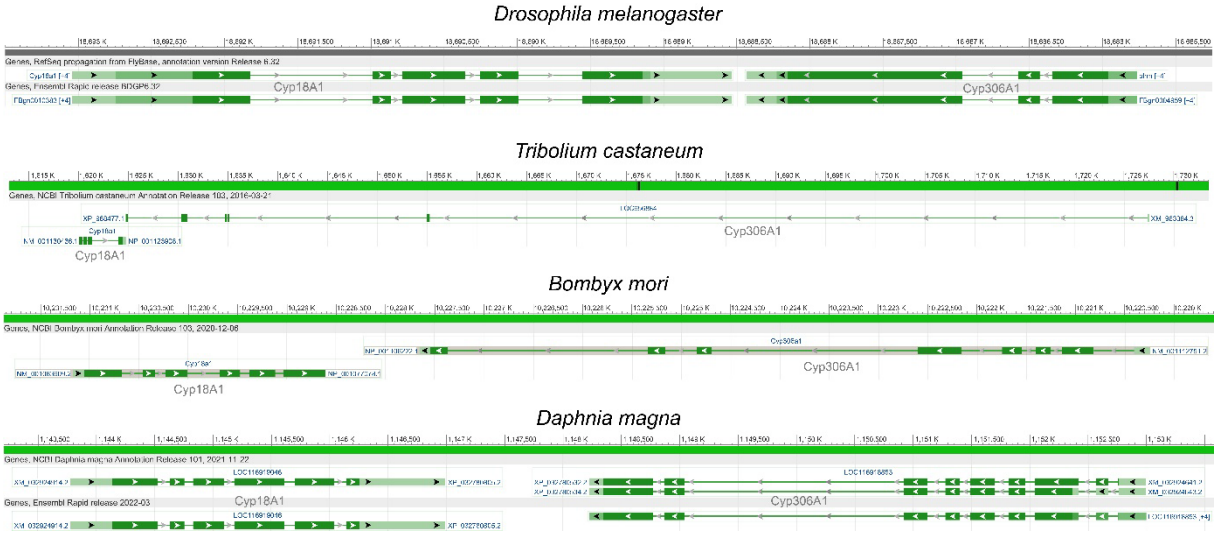

Figure 4-40. A schematic representation of *Cyp18a1* and *Cyp306a1* in genomic order of insects, including *D. melanogaster*, *T. castaneum*, *B.mori* and *D. magna*. Cyp18a1 and Cyp306a1 are shown in grey.

The role of the fast and slow allele in nature

We have identified two alternative, pleiotropic life-history alleles affecting ecdysone dynamics. Both alleles, the fast and slow allele, are present in the original wild population that was used to set up our outbred starting population (Figure 4-29). The maintenance of this polymorphism may be explained by balancing selection (Charlesworth, 2015). For instance, when food sources are temporary, rapid adult dispersal may be required, resulting in selection for fast development. Thus, in such environments, the

fast allele may be favored. In more stable conditions, however, the slow allele having a higher fecundity may be favored.

Classically, quantitative traits are thought to be determined by many alleles of small effect (Charlesworth and Edwards, 2018). Our study, however, demonstrates the existence of large effect life history alleles in natural populations. Such alleles must be crucial when climate change requires rapid adaptation of insect developmental time.

Insects respond to higher temperatures by faster development (Gilbert and Raworth, 1996; Ratte, 1985). Overall temperature of our planet has been ongoingly increasing since the pre-industrial period, namely global warming (Masson-Delmotte et al., 2018). Classically, fast development of insects trades off with small size or low weight, whereas slow development trades off with big size or high weight (Flatt and Heyland, 2011; Stearns, 1992). These trade-offs were also found in our selection lines in *T. castaneum* in Chapter 3, where we also showed that fast development trades off with high fecundity. In this chapter, we provide molecular underpinnings for such corrected responses to selection for fast or slow embryonic development of *Tribolium*. This also means that climate change is not only expected to causes responses in developmental time of insects, but also in other life history traits including fecundity.

References

Anders, S., Pyl, P. T. and Huber, W. (2015). HTSeq—a Python framework to work with high-throughput sequencing data. *bioinformatics* **31**, 166-169.

Badenhorst, P., Finch, J. T. and Travers, A. A. (2002). Tramtrack co-operates to prevent inappropriate neural development in Drosophila. *Mechanisms of development* **117**, 87-101.

Baker, K. D. and Thummel, C. S. (2007). Diabetic larvae and obese flies—emerging studies of metabolism in Drosophila. *Cell metabolism* **6**, 257-266.

Barrett, L. W., Fletcher, S. and Wilton, S. D. (2012). Regulation of eukaryotic gene expression by the untranslated gene regions and other non-coding elements. *Cellular and molecular life sciences* **69**, 3613-3634.

Bayer, C. A., Holley, B. and Fristrom, J. W. (1996). A Switch inBroad-ComplexZinc-Finger Isoform Expression Is Regulated Posttranscriptionally during the Metamorphosis ofDrosophilaImaginal Discs. *Developmental biology* **177**, 1-14.

Berghammer, A. J., Weber, M., Trauner, J. and Klingler, M. (2009). Red flour beetle (Tribolium) germline transformation and insertional mutagenesis. *Cold Spring Harb Protoc* **2009**, pdb prot5259.

Bernardo, T. J., Dubrovskaya, V. A., Xie, X. and Dubrovsky, E. B. (2014). A view through a chromatin loop: insights into the ecdysone activation of early genes in Drosophila. *Nucleic acids research* **42**, 10409-10424.

Bernstein, E., Caudy, A. A., Hammond, S. M. and Hannon, G. J. (2001). Role for a bidentate ribonuclease in the initiation step of RNA interference. *Nature* **409**, 363-366.

Blair, M. W., Cortés, A. J., Farmer, A. D., Huang, W., Ambachew, D., Penmetsa, R. V., Carrasquilla-Garcia, N., Assefa, T. and Cannon, S. B. (2018). Uneven recombination rate and linkage disequilibrium across a reference SNP map for common bean (Phaseolus vulgaris L.). *PloS one* **13**, e0189597.

Bolger, A. M., Lohse, M. and Usadel, B. (2014). Trimmomatic: a flexible trimmer for Illumina sequence data. *Bioinformatics* **30**, 2114-2120.

Brakefield, P. M. (2003). Artificial selection and the development of ecologically relevant phenotypes. *Ecology* **84**, 1661-1671.

Brinkman, R. (2017). Synchrony of Winter Moth (Operophtera Brumata) Larval Eclosion With Bud-Break of Different Tree Species in New England and Its Effect on Defoliation.

Bucher, G., Scholten, J. and Klingler, M. (2002). Parental rnai in tribolium (coleoptera). *Current Biology* **12**, R85-R86.

Bumcrot, D., Manoharan, M., Koteliansky, V. and Sah, D. W. (2006). RNAi therapeutics: a potential new class of pharmaceutical drugs. *Nature chemical biology* **2**, 711-719.
Burke, M. K., Dunham, J. P., Shahrestani, P., Thornton, K. R., Rose, M. R. and Long, A. D. (2010). Genome-wide analysis of a long-term evolution experiment with Drosophila. *Nature* **467**, 587-U111.
Buskirk, S. W., Peace, R. E. and Lang, G. I. (2017). Hitchhiking and epistasis give rise to cohort dynamics in adapting populations. *Proceedings of the National Academy of Sciences* **114**, 8330-8335.
Campbell, J. F., Athanassiou, C. G., Hagstrum, D. W. and Zhu, K. Y. (2022). Tribolium castaneum: A model insect for fundamental and applied research. *Annual Review of Entomology* **67**, 347-365.
Carroll, S. B. (2008). Evo-devo and an expanding evolutionary synthesis: a genetic theory of morphological evolution. *Cell* **134**, 25-36.
Castro-Mondragon, J. A., Riudavets-Puig, R., Rauluseviciute, I., Lemma, R. B., Turchi, L., Blanc-Mathieu, R., Lucas, J., Boddie, P., Khan, A., Manosalva Perez, N., et al. (2022). JASPAR 2022: the 9th release of the open-access database of transcription factor binding profiles. *Nucleic Acids Res* **50**, D165-D173.
Chaharbakhshi, E. and Jemc, J. C. (2016). Broad-complex, tramtrack, and bric-à-brac (BTB) proteins: Critical regulators of development. *Genesis* **54**, 505-518.
Charlesworth, B. (2015). Causes of natural variation in fitness: evidence from studies of Drosophila populations. *Proceedings of the National Academy of Sciences* **112**, 1662-1669.
Charlesworth, B. and Edwards, A. W. (2018). A century of variance. *Significance* **15**, 20-25.
Cheng, D., Dong, Z., Lin, P., Shen, G. and Xia, Q. (2022). Transcriptional Activation of Ecdysone-Responsive Genes Requires H3K27 Acetylation at Enhancers. *International Journal of Molecular Sciences* **23**, 10791.
Chippindale, A. K., Alipaz, J. A., Chen, H. W. and Rose, M. R. (1997). Experimental evolution of accelerated development in Drosophila .1. Developmental speed and larval survival. *Evolution* **51**, 1536-1551.
Chung, H., Sztal, T., Pasricha, S., Sridhar, M., Batterham, P. and Daborn, P. J. (2009). Characterization of Drosophila melanogaster cytochrome P450 genes. *Proceedings of the National Academy of Sciences* **106**, 5731-5736.
Cingolani, P., Platts, A., Wang, L. L., Coon, M., Nguyen, T., Wang, L., Land, S. J., Lu, X. Y. and Ruden, D. M. (2012). A program for annotating and predicting the effects of single nucleotide polymorphisms, SnpEff: SNPs in the genome of Drosophila melanogaster strain w(1118); iso-2; iso-3. *Fly* **6**, 80-92.
Colombani, J., Raisin, S., Pantalacci, S., Radimerski, T., Montagne, J. and Léopold, P. (2003). A nutrient sensor mechanism controls Drosophila growth. *Cell* **114**, 739-749.
Consortium, T. G. S. (2008). The genome of the model beetle and pest Tribolium castaneum. *Nature* **452**, 949.
Cruz, J., Maestro, O., Franch-Marro, X. and Martín, D. (2022). Ecdysone signaling controls early embryogenesis in the short-germ hemimetabolous insect Blattella germanica. *bioRxiv*.
DiBello, P., Withers, D., Bayer, C., Fristrom, J. and Guild, G. (1991). The Drosophila Broad-Complex encodes a family of related proteins containing zinc fingers. *Genetics* **129**, 385-397.
Dittmar, E. L., Oakley, C. G., Conner, J. K., Gould, B. A. and Schemske, D. W. (2016). Factors influencing the effect size distribution of adaptive substitutions. *Proceedings of the Royal Society B: Biological Sciences* **283**, 20153065.
Dönitz, J., Schmitt-Engel, C., Grossmann, D., Gerischer, L., Tech, M., Schoppmeier, M., Klingler, M. and Bucher, G. (2015). iBeetle-Base: a database for RNAi phenotypes in the red flour beetle Tribolium castaneum. *Nucleic acids research* **43**, D720-D725.
Fairall, L., Schwabe, J. W., Chapman, L., Finch, J. T. and Rhodes, D. (1993). The crystal structure of a two zinc-finger peptide reveals an extension to the rules for zinc-finger/DNA recognition. *Nature* **366**, 483-487.
Fire, A., Xu, S., Montgomery, M. K., Kostas, S. A., Driver, S. E. and Mello, C. C. (1998). Potent and specific genetic interference by double-stranded RNA in Caenorhabditis elegans. *nature* **391**, 806-811.

Fischer, K., Zwaan, B. J. and Brakefield, P. M. (2007). Realized correlated responses to artificial selection on pre-adult life-history traits in a butterfly. *Heredity* **98**, 157-164.
Flatt, T. and Heyland, A. (2011). *Mechanisms of life history evolution: the genetics and physiology of life history traits and trade-offs*: Oxford university press.
Franks, S. J., Genovese, N., Stockdale, M., Weber, J. J., Ansaldi, B. H. and van Wilgenburg, E. (2018). The Effects of Artificial Selection for Rapid Cycling in Brassica rapa on Herbivore Preference and Performance. *International Journal of Plant Sciences* **179**, 175-181.
Franks, S. J. and Hoffmann, A. A. (2012). Genetics of climate change adaptation. *Annual review of genetics* **46**, 185-208.
Gilbert, L. I. (2004). Halloween genes encode P450 enzymes that mediate steroid hormone biosynthesis in Drosophila melanogaster. *Molecular and cellular endocrinology* **215**, 1-10.
Gilbert, N. and Raworth, D. (1996). Insects and temperature—a general theory. *The Canadian Entomologist* **128**, 1-13.
Gilles, A. F., Schinko, J. B. and Averof, M. (2015). Efficient CRISPR-mediated gene targeting and transgene replacement in the beetle Tribolium castaneum. *Development* **142**, 2832-2839.
Giorgetti, L., Siggers, T., Tiana, G., Caprara, G., Notarbartolo, S., Corona, T., Pasparakis, M., Milani, P., Bulyk, M. L. and Natoli, G. (2010). Noncooperative interactions between transcription factors and clustered DNA binding sites enable graded transcriptional responses to environmental inputs. *Molecular cell* **37**, 418-428.
Gissis, S. B., Gissis, S., Jablonka, E. and Zeligowski, A. (2011). *Transformations of Lamarckism: from subtle fluids to molecular biology*: MIT press.
Grant, C. E., Bailey, T. L. and Noble, W. S. (2011). FIMO: scanning for occurrences of a given motif. *Bioinformatics* **27**, 1017-1018.
Graves, J. L., Hertweck, K. L., Phillips, M. A., Han, M. V., Cabral, L. G., Barter, T. T., Greer, L. F., Burke, M. K., Mueller, L. D. and Rose, M. R. (2017). Genomics of Parallel Experimental Evolution in Drosophila. *Molecular Biology and Evolution* **34**, 831-842.
Grimaldi, D. and Engel, M. S. (2005). *Evolution of the Insects*: Cambridge University Press.
Guittard, E., Blais, C., Maria, A., Parvy, J.-P., Pasricha, S., Lumb, C., Lafont, R., Daborn, P. J. and Dauphin-Villemant, C. (2011). CYP18A1, a key enzyme of Drosophila steroid hormone inactivation, is essential for metamorphosis. *Developmental biology* **349**, 35-45.
Guo, S., Tian, Z., Wu, Q.-W., King-Jones, K., Liu, W., Zhu, F. and Wang, X.-P. (2021). Steroid hormone ecdysone deficiency stimulates preparation for photoperiodic reproductive diapause. *PLoS genetics* **17**, e1009352.
Gutierrez-Perez, I., Rowley, M. J., Lyu, X., Valadez-Graham, V., Vallejo, D. M., Ballesta-Illan, E., Lopez-Atalaya, J. P., Kremsky, I., Caparros, E. and Corces, V. G. (2019). Ecdysone-Induced 3D chromatin reorganization involves active enhancers bound by pipsqueak and polycomb. *Cell reports* **28**, 2715-2727. e2715.
Harbison, S. T., McCoy, L. J. and Mackay, T. F. (2013). Genome-wide association study of sleep in Drosophila melanogaster. *BMC genomics* **14**, 1-18.
Harrison, S. D. and Travers, A. A. (1990). The tramtrack gene encodes a Drosophila finger protein that interacts with the ftz transcriptional regulatory region and shows a novel embryonic expression pattern. *The EMBO journal* **9**, 207-216.
Herndon, N., Shelton, J., Gerischer, L., Ioannidis, P., Ninova, M., Donitz, J., Waterhouse, R. M., Liang, C., Damm, C., Siemanowski, J., et al. (2020). Enhanced genome assembly and a new official gene set for Tribolium castaneum. *BMC Genomics* **21**, 47.
Hitrik, A., Popliker, M., Gancz, D., Mukamel, Z., Lifshitz, A., Schwartzman, O., Tanay, A. and Gilboa, L. (2016). Combgap promotes ovarian niche development and chromatin association of EcR-binding regions in BR-C. *PLoS Genetics* **12**, e1006330.
Hoedjes, K. M., van den Heuvel, J., Kapun, M., Keller, L., Flatt, T. and Zwaan, B. J. (2019). Distinct genomic signals of lifespan and life history evolution in response to postponed reproduction and larval diet in Drosophila. *Evolution Letters* **3**, 598-609.
Horn, T., Narov, K. D. and Panfilio, K. A. (2022). Persistent parental RNAi in the beetle Tribolium castaneum involves maternal transmission of long double-stranded RNA. *Advanced Genetics* **3**, 2100064.

Huang, J.-H., Lozano, J. and Belles, X. (2013). Broad-complex functions in postembryonic development of the cockroach Blattella germanica shed new light on the evolution of insect metamorphosis. *Biochimica et Biophysica Acta (BBA)-General Subjects* **1830**, 2178-2187.
Jacobs, C. G., Rezende, G. L., Lamers, G. E. and van der Zee, M. (2013). The extraembryonic serosa protects the insect egg against desiccation. *Proceedings of the Royal Society B: Biological Sciences* **280**, 20131082.
Jacobs, C. G., Spaink, H. P. and van der Zee, M. (2014). The extraembryonic serosa is a frontier epithelium providing the insect egg with a full-range innate immune response. *elife* **3**, e04111.
Jacobs, C. G. and van der Zee, M. (2013). Immune competence in insect eggs depends on the extraembryonic serosa. *Developmental & Comparative Immunology* **41**, 263-269.
Jens, M. and Rajewsky, N. (2015). Competition between target sites of regulators shapes post-transcriptional gene regulation. *Nature Reviews Genetics* **16**, 113-126.
Jia, S., Wan, P. J. and Li, G. Q. (2015). Molecular cloning and characterization of the putative Halloween gene Phantom from the small brown planthopper Laodelphax striatellus. *Insect Science* **22**, 707-718.
Karim, F. D., Guild, G. M. and Thummel, C. S. (1993). The Drosophila Broad-Complex plays a key role in controlling ecdysone-regulated gene expression at the onset of metamorphosis. *Development* **118**, 977-988.
Kharouba, H. M., Ehrlen, J., Gelman, A., Bolmgren, K., Allen, J. M., Travers, S. E. and Wolkovich, E. M. (2018). Global shifts in the phenological synchrony of species interactions over recent decades. *Proceedings of the National Academy of Sciences of the United States of America* **115**, 5211-5216.
Klingler, M. (2004). Tribolium. *Current Biology* **14**, R639-R640.
Klingler, M. and Bucher, G. (2022). The red flour beetle T. castaneum: elaborate genetic toolkit and unbiased large scale RNAi screening to study insect biology and evolution. *EvoDevo* **13**, 1-11.
Knaus, B. J. and Grunwald, N. J. (2017). VCFR: a package to manipulate and visualize variant call format data in R. *Mol Ecol Resour* **17**, 44-53.
Koboldt, D. C., Chen, K., Wylie, T., Larson, D. E., McLellan, M. D., Mardis, E. R., Weinstock, G. M., Wilson, R. K. and Ding, L. (2009). VarScan: variant detection in massively parallel sequencing of individual and pooled samples. *Bioinformatics* **25**, 2283-2285.
Kofler, R., Betancourt, A. J. and Schlötterer, C. (2012). Sequencing of pooled DNA samples (Pool-Seq) uncovers complex dynamics of transposable element insertions in Drosophila melanogaster. *PLoS genetics* **8**, e1002487.
Kozlova, T. and Thummel, C. S. (2003). Essential roles for ecdysone signaling during Drosophila mid-embryonic development. *Science* **301**, 1911-1914.
Kreher, J., Kovač, K., Bouazoune, K., Mačinković, I., Ernst, A. L., Engelen, E., Pahl, R., Finkernagel, F., Murawska, M. and Ullah, I. (2017). EcR recruits dMi-2 and increases efficiency of dMi-2-mediated remodelling to constrain transcription of hormone-regulated genes. *Nature communications* **8**, 1-13.
Lang, G. I., Rice, D. P., Hickman, M. J., Sodergren, E., Weinstock, G. M., Botstein, D. and Desai, M. M. (2013). Pervasive genetic hitchhiking and clonal interference in forty evolving yeast populations. *Nature* **500**, 571-574.
Larson, G. and Fuller, D. Q. (2014). The evolution of animal domestication. *Annual Review of Ecology, Evolution, and Systematics* **45**, 115-136.
Li, H., Handsaker, B., Wysoker, A., Fennell, T., Ruan, J., Homer, N., Marth, G., Abecasis, G., Durbin, R. and Proc, G. P. D. (2009). The Sequence Alignment/Map format and SAMtools. *Bioinformatics* **25**, 2078-2079.
Li, S., Li, Y., Carthew, R. W. and Lai, Z.-C. (1997). Photoreceptor cell differentiation requires regulated proteolysis of the transcriptional repressor Tramtrack. *Cell* **90**, 469-478.
Linz, D. M., Clark-Hachtel, C. M., Borràs-Castells, F. and Tomoyasu, Y. (2014). Larval RNA interference in the red flour beetle, Tribolium castaneum. *JoVE (Journal of Visualized Experiments)*, e52059.
Liu, S., He, C., Liang, J., Su, Q., Hua, D., Wang, S., Wu, Q., Xie, W. and Zhang, Y. (2020). Molecular characterization and functional analysis of the Halloween genes and CYP18A1 in Bemisia tabaci MED. *Pesticide Biochemistry and Physiology* **167**, 104602.

Livak, K. J. and Schmittgen, T. D. (2001). Analysis of relative gene expression data using real-time quantitative PCR and the 2(-Delta Delta C(T)) Method. *Methods* **25**, 402-408.
Long, A., Liti, G., Luptak, A. and Tenaillon, O. (2015). Elucidating the molecular architecture of adaptation via evolve and resequence experiments. *Nature Reviews Genetics* **16**, 567-582.
Lord, J. C., Hartzer, K., Toutges, M. and Oppert, B. (2010). Evaluation of quantitative PCR reference genes for gene expression studies in Tribolium castaneum after fungal challenge. *Journal of microbiological methods* **80**, 219-221.
Love, M. I., Huber, W. and Anders, S. (2014). Moderated estimation of fold change and dispersion for RNA-seq data with DESeq2. *Genome biology* **15**, 1-21.
Luan, J.-B., Ghanim, M., Liu, S.-S. and Czosnek, H. (2013). Silencing the ecdysone synthesis and signaling pathway genes disrupts nymphal development in the whitefly. *Insect Biochemistry and Molecular Biology* **43**, 740-746.
Manning, A. (1961). The effects of artificial selection for mating speed in Drosophila melanogaster. *Animal Behaviour* **9**, 82-92.
Marand, A. P. and Schmitz, R. J. (2022). Single-cell analysis of cis-regulatory elements. *Current Opinion in Plant Biology* **65**, 102094.
Marinkovic, D. A., F.J. (1986). Selection for different rates of embryonic development in Drosophila melanogaster and Drosophila simulans. *Genetika* **18**, 205-219.
Maróy, P., Kaufmann, G. and Dübendorfer, A. (1988). Embryonic ecdysteroids of Drosophila melanogaster. *Journal of Insect Physiology* **34**, 633-637.
Masson-Delmotte, V., Zhai, P., Pörtner, H.-O., Roberts, D., Skea, J., Shukla, P. R., Pirani, A., Moufouma-Okia, W., Péan, C. and Pidcock, R. (2018). Global warming of 1.5 C. *An IPCC Special Report on the impacts of global warming of* **1**, 43-50.
Mazo-Vargas, A., Langmüller, A. M., Wilder, A., van der Burg, K. R., Lewis, J. J., Messer, P. W., Zhang, L., Martin, A. and Reed, R. D. (2022). Deep cis-regulatory homology of the butterfly wing pattern ground plan. *Science* **378**, 304-308.
McCord, R. P., Kaplan, N. and Giorgetti, L. (2020). Chromosome conformation capture and beyond: toward an integrative view of chromosome structure and function. *Molecular cell* **77**, 688-708.
McKenna, A., Hanna, M., Banks, E., Sivachenko, A., Cibulskis, K., Kernytsky, A., Garimella, K., Altshuler, D., Gabriel, S., Daly, M., et al. (2010). The Genome Analysis Toolkit: A MapReduce framework for analyzing next-generation DNA sequencing data. *Genome Research* **20**, 1297-1303.
McLaughlin, J. F., Hellmann, J. J., Boggs, C. L. and Ehrlich, P. R. (2002). Climate change hastens population extinctions. *Proceedings of the National Academy of Sciences of the United States of America* **99**, 6070-6074.
Miller, S. C., Miyata, K., Brown, S. J. and Tomoyasu, Y. (2012). Dissecting systemic RNA interference in the red flour beetle Tribolium castaneum: parameters affecting the efficiency of RNAi. *PloS one* **7**, e47431.
Mugat, B., Brodu, V., Kejzlarova-Lepesant, J., Antoniewski, C., Bayer, C. A., Fristrom, J. W. and Lepesant, J.-A. (2000). Dynamic expression of broad-complex isoforms mediates temporal control of an ecdysteroid target gene at the onset of Drosophila metamorphosis. *Developmental biology* **227**, 104-117.
Nachman, M. W. (2002). Variation in recombination rate across the genome: evidence and implications. *Current opinion in genetics & development* **12**, 657-663.
Neyfakh, A. A. and Hartl, D. L. (1993). Genetic-Control of the Rate of Embryonic-Development - Selection for Faster Development at Elevated-Temperatures. *Evolution* **47**, 1625-1631.
Nijhout, H. F., Riddiford, L. M., Mirth, C., Shingleton, A. W., Suzuki, Y. and Callier, V. (2014). The developmental control of size in insects. *Wiley Interdisciplinary Reviews: Developmental Biology* **3**, 113-134.
Niwa, R. and Niwa, Y. S. (2014). Enzymes for ecdysteroid biosynthesis: their biological functions in insects and beyond. *Bioscience, biotechnology, and biochemistry* **78**, 1283-1292.
Niwa, Y. S. and Niwa, R. (2016). Transcriptional regulation of insect steroid hormone biosynthesis and its role in controlling timing of molting and metamorphosis. *Development, growth & differentiation* **58**, 94-105.

Noma, K.-i., Sugiyama, T., Cam, H., Verdel, A., Zofall, M., Jia, S., Moazed, D. and Grewal, S. I. (2004). RITS acts in cis to promote RNA interference–mediated transcriptional and post-transcriptional silencing. *Nature genetics* **36**, 1174-1180.

Nunney, L. (1996). The response to selection for fast larval development in Drosophila melanogaster and its effect on adult weight: An example of a fitness trade-off. *Evolution* **50**, 1193-1204.

Pagans, S., Ortiz-Lombardía, M., Espinás, M. L., Bernués, J. and Azorín, F. (2002). The Drosophila transcription factor tramtrack (TTK) interacts with Trithorax-like (GAGA) and represses GAGA-mediated activation. *Nucleic acids research* **30**, 4406-4413.

Pan, F., Fu, Y., Zhang, W., Jiang, S., Xiong, Y., Yan, Y., Gong, Y., Qiao, H. and Fu, H. (2022). Characterization, expression and functional analysis of CYP306a1 in the oriental river prawn, Macrobrachium nipponense. *Aquaculture Reports* **22**, 101009.

Panfilio, K. A. (2008). Extraembryonic development in insects and the acrobatics of blastokinesis. *Developmental biology* **313**, 471-491.

Papadopoulos, D., Schneider, D., Meier-Eiss, J., Arber, W., Lenski, R. E. and Blot, M. (1999). Genomic evolution during a 10,000-generation experiment with bacteria. *Proceedings of the National Academy of Sciences* **96**, 3807-3812.

Pointer, M. D., Gage, M. J. and Spurgin, L. G. (2021). Tribolium beetles as a model system in evolution and ecology. *Heredity* **126**, 869-883.

Prasad, N. G., Shakarad, M., Gohil, V. M., Sheeba, V., Rajamani, M. and Joshi, A. (2000). Evolution of reduced pre-adult viability and larval growth rate in laboratory populations of Drosophila melanogaster selected for shorter development time. *Genet Res* **76**, 249-259.

Rafiqi, A. M., Lemke, S., Ferguson, S., Stauber, M. and Schmidt-Ott, U. (2008). Evolutionary origin of the amnioserosa in cyclorrhaphan flies correlates with spatial and temporal expression changes of zen. *Proceedings of the National Academy of Sciences* **105**, 234-239.

Ratte, H. T. (1985). Temperature and insect development. *Environmental physiology and biochemistry of insects*, 33-66.

Renner, S. S. and Zohner, C. M. (2018). Climate change and phenological mismatch in trophic interactions among plants, insects, and vertebrates. *Annual review of ecology, evolution, and systematics* **49**, 165-182.

Rewitz, K. F., Yamanaka, N. and O'Connor, M. B. (2010). Steroid hormone inactivation is required during the juvenile-adult transition in Drosophila. *Developmental cell* **19**, 895-902.

Ritchie, M. G. and Kyriacou, C. P. (1996). Artificial selection for a courtship signal inDrosophila melanogaster. *Animal Behaviour* **52**, 603-611.

Rose, M. R. (1984). Artificial selection on a fitness-component in Drosophila melanogaster. *Evolution*, 516-526.

Samplonius, J. M., Atkinson, A., Hassall, C., Keogan, K., Thackeray, S. J., Assmann, J. J., Burgess, M. D., Johansson, J., Macphie, K. H., Pearce-Higgins, J. W., et al. (2021). Strengthening the evidence base for temperature-mediated phenological asynchrony and its impacts. *Nat Ecol Evol* **5**, 155-+.

Sardell, J. M., Cheng, C., Dagilis, A. J., Ishikawa, A., Kitano, J., Peichel, C. L. and Kirkpatrick, M. (2018). Sex differences in recombination in sticklebacks. *G3: Genes, Genomes, Genetics* **8**, 1971-1983.

Sarrazin, A. F., Peel, A. D. and Averof, M. (2012). A segmentation clock with two-segment periodicity in insects. *Science* **336**, 338-341.

Schellens, S., Lenaerts, C., Pérez Baca, M. d. R., Cools, D., Peeters, P., Marchal, E. and Vanden Broeck, J. (2022). Knockdown of the Halloween Genes spook, shadow and shade Influences Oocyte Development, Egg Shape, Oviposition and Hatching in the Desert Locust. *International journal of molecular sciences* **23**, 9232.

Schlötterer, C., Tobler, R., Kofler, R. and Nolte, V. (2014). Sequencing pools of individuals—mining genome-wide polymorphism data without big funding. *Nature Reviews Genetics* **15**, 749-763.

Schröder, R., Beermann, A., Wittkopp, N. and Lutz, R. (2008). From development to biodiversity—Tribolium castaneum, an insect model organism for short germband development. *Development genes and evolution* **218**, 119-126.

Schumann, I., Kenny, N., Hui, J., Hering, L. and Mayer, G. (2018). Halloween genes in panarthropods and the evolution of the early moulting pathway in Ecdysozoa. *Royal Society Open Science* **5**, 180888.
Seslija, D. and Tucic, N. (2003). Selection for developmental time in bean weevil (Acanthoscelides obtectus): correlated responses for other life history traits and genetic architecture of line differentiation. *Entomol Exp Appl* **106**, 19-35.
Shapiro, J. A. (2011). *Evolution: a view from the 21st century*: Pearson education.
Sharma, K., Mishra, N. and Shakarad, M. N. (2020). Evolution of reduced minimum critical size as a response to selection for rapid pre-adult development in Drosophila melanogaster. *Roy Soc Open Sci* **7**.
Siepel, A. and Arbiza, L. (2014). Cis-regulatory elements and human evolution. *Current opinion in genetics & development* **29**, 81-89.
Singer, M. C. and Parmesan, C. (2010). Phenological asynchrony between herbivorous insects and their hosts: signal of climate change or pre-existing adaptive strategy? *Philos T R Soc B* **365**, 3161-3176.
Stearns, S. C. (1992). *The evolution of life histories*: Oxford university press Oxford.
Stefan, M. I. and Le Novere, N. (2013). Cooperative binding. *PLoS computational biology* **9**, e1003106.
Strobl, F. and Stelzer, E. H. (2014). Non-invasive long-term fluorescence live imaging of Tribolium castaneum embryos. *Development* **141**, 2331-2338.
Sun, J., Smith, L., Armento, A. and Deng, W.-M. (2008). Regulation of the endocycle/gene amplification switch by Notch and ecdysone signaling. *The Journal of cell biology* **182**, 885-896.
Tak, Y. G. and Farnham, P. J. (2015). Making sense of GWAS: using epigenomics and genome engineering to understand the functional relevance of SNPs in non-coding regions of the human genome. *Epigenetics & chromatin* **8**, 1-18.
Tautz, D. and Pfeifle, C. (1989). A non-radioactive in situ hybridization method for the localization of specific RNAs in Drosophila embryos reveals translational control of the segmentation gene hunchback. *Chromosoma* **98**, 81-85.
Teleman, A. A., Chen, Y.-W. and Cohen, S. M. (2005). Drosophila Melted modulates FOXO and TOR activity. *Developmental cell* **9**, 271-281.
Tenaillon, O., Rodríguez-Verdugo, A., Gaut, R. L., McDonald, P., Bennett, A. F., Long, A. D. and Gaut, B. S. (2012). The molecular diversity of adaptive convergence. *science* **335**, 457-461.
Teotonio, H., Chelo, I. M., Bradic, M., Rose, M. R. and Long, A. D. (2009). Experimental evolution reveals natural selection on standing genetic variation. *Nature Genetics* **41**, 251-257.
Thackeray, S. J., Henrys, P. A., Hemming, D., Bell, J. R., Botham, M. S., Burthe, S., Helaouet, P., Johns, D. G., Jones, I. D., Leech, D. I., et al. (2016). Phenological sensitivity to climate across taxa and trophic levels. *Nature* **535**, 241-U294.
Thummel, C. (2002). Ecdysone-regulated puff genes 2000. *Insect biochemistry and molecular biology* **32**, 113-120.
Tomoyasu, Y., Miller, S. C., Tomita, S., Schoppmeier, M., Grossmann, D. and Bucher, G. (2008). Exploring systemic RNA interference in insects: a genome-wide survey for RNAi genes in Tribolium. *Genome biology* **9**, 1-22.
Truman, J. W. (2019). The evolution of insect metamorphosis. *Current Biology* **29**, R1252-R1268.
Uhlirova, M., Foy, B. D., Beaty, B. J., Olson, K. E., Riddiford, L. M. and Jindra, M. (2003). Use of Sindbis virus-mediated RNA interference to demonstrate a conserved role of Broad-Complex in insect metamorphosis. *Proceedings of the National Academy of Sciences* **100**, 15607-15612.
Van Asch, M., Salis, L., Holleman, L. J., Van Lith, B. and Visser, M. E. (2013). Evolutionary response of the egg hatching date of a herbivorous insect under climate change. *Nature Climate Change* **3**, 244-248.
van der Zee, M., Berns, N. and Roth, S. (2005). Distinct functions of the Tribolium zerknu llt genes in serosa specification and dorsal closure. *Current Biology* **15**, 624-636.

van Drongelen, R., Vazquez-Faci, T., Huijben, T. A., van der Zee, M. and Idema, T. (2018). Mechanics of epithelial tissue formation. *Journal of Theoretical Biology* **454**, 182-189.
Verta, J.-P. and Jones, F. C. (2019). Predominance of cis-regulatory changes in parallel expression divergence of sticklebacks. *Elife* **8**, e43785.
Visser, M. E. and Gienapp, P. (2019). Evolutionary and demographic consequences of phenological mismatches. *Nat Ecol Evol* **3**, 879-885.
Vlachos, C. and Kofler, R. (2019). Optimizing the power to identify the genetic basis of complex traits with evolve and resequence studies. *Molecular biology and evolution* **36**, 2890-2905.
Wittkopp, P. J. and Kalay, G. (2012). Cis-regulatory elements: molecular mechanisms and evolutionary processes underlying divergence. *Nature Reviews Genetics* **13**, 59-69.
Xia, Q., Guo, Y., Zhang, Z., Li, D., Xuan, Z., Li, Z., Dai, F., Li, Y., Cheng, D. and Li, R. (2009). Complete resequencing of 40 genomes reveals domestication events and genes in silkworm (Bombyx). *Science* **326**, 433-436.
Xiang, H., Liu, X., Li, M., Zhu, Y. n., Wang, L., Cui, Y., Liu, L., Fang, G., Qian, H. and Xu, A. (2018). The evolutionary road from wild moth to domestic silkworm. *Nature ecology & evolution* **2**, 1268-1279.
Xiong, W. C. and Montell, C. (1993). tramtrack is a transcriptional repressor required for cell fate determination in the Drosophila eye. *Genes & development* **7**, 1085-1096.
Yadav, P. and Sharma, V. K. (2013). Correlated changes in circadian clocks in response to selection for faster pre-adult development in fruit flies Drosophila melanogaster. *Journal of Comparative Physiology B-Biochemical Systems and Environmental Physiology* **183**, 333-343.
Yamanaka, N., Rewitz, K. F. and O'Connor, M. B. (2013). Ecdysone control of developmental transitions: lessons from Drosophila research. *Annual review of entomology* **58**, 497-516.
Yao, L., Tak, Y. G., Berman, B. P. and Farnham, P. J. (2014). Functional annotation of colon cancer risk SNPs. *Nature communications* **5**, 1-13.
Yoo, B., Kim, H.-y., Chen, X., Shen, W., Jang, J. S., Stein, S. N., Cormier, O., Pereira, L., Shih, C. R. and Krieger, C. (2021). 20-hydroxyecdysone (20E) signaling regulates amnioserosa morphogenesis during Drosophila dorsal closure: EcR modulates gene expression in a complex with the AP-1 subunit, Jun. *Biology open* **10**, bio058605.
Yu, Y., Yussa, M., Song, J., Hirsch, J. and Pick, L. (1999). A double interaction screen identifies positive and negative ftz gene regulators and ftz-interacting proteins. *Mechanisms of development* **83**, 95-105.
Yukuhiro, K., Sezutsu, H., Tamura, T., Kosegawa, E., Iwata, K., Ajimura, M., Gu, S.-H., Wang, M., Xia, Q. and Mita, K. (2012). Little gene flow between domestic silkmoth Bombyx mori and its wild relative Bombyx mandarina in Japan, and possible artificial selection on the CAD gene of B. mori. *Genes & genetic systems* **87**, 331-340.
Zee, M. v. d., Stockhammer, O., Levetzow, C. v., Fonseca, R. N. d. and Roth, S. (2006). Sog/Chordin is required for ventral-to-dorsal Dpp/BMP transport and head formation in a short germ insect. *Proceedings of the National Academy of Sciences* **103**, 16307-16312.
Zhu, Y.-N., Wang, L.-Z., Li, C.-C., Cui, Y., Wang, M., Lin, Y.-J., Zhao, R.-P., Wang, W. and Xiang, H. (2019). Artificial selection on storage protein 1 possibly contributes to increase of hatchability during silkworm domestication. *PLoS genetics* **15**, e1007616.
Zwaan, B., Bijlsma, R. and Hoekstra, R. F. (1995). Artificial Selection for Developmental Time in Drosophila-Melanogaster in Relation to the Evolution of Aging - Direct and Correlated Responses. *Evolution* **49**, 635-648.

Supplementary information

Supplementary Table 4-1. List of candidate genes. Candidate genes 1-16 are in chromosome 3, and 17-45 are on chromosome 9.

Candidate genes (NCBI's annotation)	Gene symbol	Acronym	Lead SNP type	SNP position and Ref/Alt	-logP-value	AF divergence
1. uncharacterized LOC656417	LOC656417	1. LOC656417	Principal SNP	13868791, T/A	59.93	0.661
2. thioredoxin reductase 1, mitochondrial	LOC103314616	2. Trxr-1	Principal SNP	13957908, A/G	61.27	0.663
		2. Trxr-1	Principal SNP	13971318, C/T	59.7	0.786
3. C-factor	LOC656669	3. C-factor	Principal SNP	14022139, T/C	58.89	0.681
4. solute carrier family 25 member 35	LOC656748	4. SLC25-35-1	Principal SNP	14051912, T/A	61.09	0.733
5. Protein melted	LOC656839	5. Melted	Principal SNP	14086409, G/T	60.56	0.879
6. solute carrier family 25 member 35, transcript variant X3	LOC657090	6. SLC25-35-2	Principal SNP	14128581, T/C	65.84	0.781
7. calcitonin gene-related peptide type 1 receptor	LOC657479	7. CalcitoninR	Principal SNP	14218183, T/C	96.72	0.803
8. probable cytochrome P450 6A14	LOC657560	8. Cyp6a14	Principal SNP	14245723, T/A	63.43	0.662
7. calcitonin gene-related peptide type 1 receptor	LOC657479	7. CalcitoninR	Principal SNP	14262745, T/C	58.89	0.724
		7. CalcitoninR	Principal SNP	14288001, A/G	63.18	0.750
		7. CalcitoninR	Principal SNP	14298023, A/T	61.91	0.756
		7. CalcitoninR	Principal SNP	14312131, C/G	62.43	0.698
9. cytochrom P450 6K1	LOC658029	9. Cyp6k1	Principal SNP	14370963, G/A	59.51	0.731
10. Uncharacterized Loc103312175	LOC103312175	10. Or327	Principal SNP	14381004, C/T	66.91	0.674
11. glycine dehydrogenase (decarboxylating), mitochondrial	LOC658613	11. GLDC	Significant SNP	15582940, G/C	40.08	0.438
12. protein transport protein Sec61 subunit alpha isoform 2	LOC658693	12. Sec61α	Significant SNP	15609700, A/C	53.41	0.852
13. MAP kinase-interacting serine/threonine-protein kinase 1	LOC658754	13. Lk6 kinase	Principal SNP	15648008, G/T	67.59	0.700
14. superkiller viralicidic activity 2-like 2	LOC658969	14. Skiv2	Principal SNP	15666693, G/C	59.59	0.668
15. cell division cycle protein 20 homolog	LOC659043	15. Cortex	Significant SNP	15717468, T/C	51.84	0.820
16. laccase-2	Lac2	16. Lac2	Principal SNP	15754769, T/C	71.21	0.738
17. sodium- and chloride-dependent GABA transporter 1	LOC655406	17. Gat	Significant SNP	412499, A/G	57.82	0.600
18. metabotropic glutamate receptor 2-like	LOC656715	18. mGluR	Significant SNP	414797, T/A	40.98	0.830
19. suppression of tumorigenicity 18 protein	LOC656465	19. St18 C2H2C	Significant SNP	966489, C/G	50.88	0.482
20. high affinity cationic amino acid transporter 1	LOC655390	20. CAT1	Significant SNP	1176055, G/A	53.19	0.497
21. cationic amino acid transporter 2	LOC655468	21. CAT2	Significant SNP	1199876, T/A	53.01	0.554
22. polycystic kidney disease 1-related protein-like	LOC107398588	22. Pkd1	Principal SNP	1236554, G/T	60.85	0.749

23. Polycystin-2-like	LOC107398589	23. Polycystin2	Principal SNP	1253862, A/G	60.95	0.669
24. high affinity cationic amino acid transporter 1	LOC655801	24. CAT3	Principal SNP	1378218, C/A	70.07	0.686
25. dynactin subunit 2	LOC655964	25. Dynactin2	Principal SNP	1409012, A/G	62.97	0.848
26. transcription factor Adf-1	LOC103314616	26. Adf-1	Principal SNP	1416931, A/T	67.72	0.751
27. lethal(3)malignant brain tumor-like protein 4	LOC656299	27. l(3)mbt	Principal SNP	1463470, A/G	78.27	0.810
28. protein-L-isoaspartate O-methyltransferase domain-containing protein 1	LOC656461	28. Pcmt	Significant SNP	1453282, G/A	63.12	0.831
29. phospholipase A-2-activating protein	LOC656630	29. Plap	Principal SNP	1489792, A/T	66.79	0.772
		29. Plap	Principal SNP	1505606, T/G	74.39	0.705
30. uncharacterized LOC107397428	LOC107397428	30. LOC107397428	Principal SNP	1540084, A/G	70.70	0.780
		30. LOC107397428	Principal SNP	1553652, T/C	72.68	0.875
31. chymase	LOC103314618	31. Chymase	Principal SNP	1574195, G/A	75.88	0.821
32. cytochrome P450 CYP18A1	Cyp18a1	32. Cyp18a1	Principal SNP	1613665, G/A	84.85	0.797
33. cytochrome P450 306A1	LOC656884	33. Cyp306a1	Principal SNP	1631265, T/C	65.80	0.759
		33. Cyp306a1	Principal SNP	1846872, A/T	70.05	0.603
34. centromere protein S	LOC103315036	34. CENP-S	Principal SNP	2168201, G/C	62.86	0.809
35. protein deadpan	LOC656046	35. Deadpan	Principal SNP	2218287, T/A	73.39	0.723
36. 60S ribosomal protein L27	LOC657523	36. RPL27	Principal SNP	2289810, C/A	67.32	0.742
37. pancreatic triacylglycerol lipase	LOC657679	37. Lipase	Principal SNP	2322171, T/C	68.34	0.716
		37. Lipase	Principal SNP	2339313, A/G	66.40	0.756
38. hypothetical protein	LOC103314394	38. LOC103314394	Principal SNP	2417247, G/A	60.44	0.729
39. SH3 domain-binding protein 5 homolog	LOC657915	39. SH3bp	Principal SNP	2427805, T/A	60.31	0.810
40. integrin alpha-PS2	LOC657993	40. Integrin αPS2	Principal SNP	2438730, T/G	65.45	0.717
		40. Integrin αPS2	Principal SNP	2452502, C/T	78.01	0.701
		40. Integrin αPS2	Principal SNP	2483912, A/G	63.49	0.771
41. inositol hexakisphosphate kinase 1	LOC658073	41. Ip6k	Principal SNP	2581813, T/G	73.88	0.795
42. uncharacterized LOC657682	LOC657682	42. LOC657682	Principal SNP	3260859, T/C	65.26	0.788
		42. LOC657682	Principal SNP	3274854, A/G	62.77	0.683
43. TATA box-binding protein-associated factor RNA polymerase I subunit B	LOC103314719	43. TAF1B	Principal SNP	3438606, C/T	61.37	0.734
44. putative uncharacterized protein DDB_G0271606	LOC103314169	44. LOC103314169	Principal SNP	3497871, A/G	75.03	0.722

45. BMP and activin membrane-bound inhibitor homolog	LOC103314170	45. Bambi	Principal SNP	3519980, T/C	61.05	0.645

Supplementary Table 4-2. Primers of candidate genes used for qPCR.

Gene acronym	Forward primer (5'-3')	Reverse primer (5'-3')
Tribolium castaneum		
1. *LOC656417*	CAGCAGAGGTGCCGTCTTTA	CCACTTGCCACCGGGATAATA
2. *Trxr-1*	GTTCATACGGTGACCAAACAG	ACGGCACCCGGTATATTAG
3. *C-factor*	AAATGCGCCACTGGATGTTG	ACCTCCATTGTGGCTTTCGT
4. *SLC25-35-1*	TTTAACTGCATTTGCTGCCAG	GCGTCGTAACAATATCAAACG
5. *Melted*	GGTGATGTGATTTGTAGCGGTG	CACCTCCAAGGATGCAAAGG
6. *SLC25-35-2*	GCGGTGGGACATCAGCATAA	GCTGAAGCCCCAACTACTGTC
7. *CalcitoninR*	GCACCAACTGAACCTTTGTCG	GTTATTCGCGCGTTTTCGTGC
8. *Cyp6a14*	TGTAGCCCTCCTGGTCATCA	GACTGTGGGTGGGAGGAATG
9. *Cyp6k1*	GATGTGAAAATGGCAGCACAAG	CCAGTTCGTAGAGAGCGAAAG
10. *Or327*	TGGCAACAATAACATCTGGC	AGATACCAAGGGATCGAAGAC
11. *GLDC*	TAACTCTTCTCCGACCACC	CGCACCAAGGACTGATTAC
12. *Sec61α*	AACAGAGGAACCCTGATGG	AAAGCTCGGTCTTTCGGTG
13. *Lk6 kinase*	TGGCATGACCCGGTACCTTA	TGGCGAAATCTTGGGTGAGG
14. *Skiv2*	AATCAGACGGCCATTCCTGG	TGGTACGATGCAATCTGTGGT
15. *Cortex*	TGAAACGGACACAATTAGCC	TTCCTTTGACCTACTCCTACTG
16. *Lac2*	TACAACAGACATTTAGTTGCACCA	AGGTGGGGCCATGTAGGAAA
17. *Gat*	GATCCTTGGTTGTAACCCTGA	GGTCCAGGAACTATACTTGAG
18. *mGluR*	GCTTTATTTCACCCAGATCCC	GAAATCACCATCCACACTCC
19. *St18 C2H2C*	GGAACAGCACAAAGCAGCAG	AGGACAGCCGCTCAAAGAAC
20. *CAT1*	ATGGAAGGCGCAGCTCAATG	GGGAAATGACGATGGCTAGAGG
21. *CAT2*	TCGAAGCGGGAGGAGAACTA	CGCTCCTAATGCTATGGCAA
22. *Pkd1*	GAGAACGCTGCATGTTCAGT	CCGTTGCCAAAATCGTCCAT
23. *Polycystin2*	GCGGTGCCTTTGTGTTTTCT	AGCAGGAAGGCCCATTTCTT
24. *CAT3*	GCCCTCAGTTGTCTTGTCGT	CGCAGACGTAGCTGTAGATGT
25. *Dynactin2*	ACCCACAAGGGACGCAAATC	CGTGCTTGTTCCGGTCGATA
26. *Adf-1*	GTAAAGCCAGCACTAGCAACC	AACGATTCGTGATAACTCACGTC
27. *l(3)mbt*	GCAGCTTGCCTGGAAGTGATT	AGGCCGTAACAGCCACATTC
28. *Pcmt*	TGAAGAGCGAGCCGAAAAC	AGCAGCTCATCTCCTAAGCC
29. *Plap*	ACGCTTCCTTACCTGGCAAA	GACGCGACAAAGCACTCAAG
30. *LOC107397428*	TCCACACATGGCCCGAAAAC	CCAAAGTACCACGGTAGCAAC
31. *Chymase*	GCAGTAACAAGTGGACGACAAC	TCGGCAATCCAAGGAAAATAGG
32. *Cyp18a1*	TCCTCTTCATGCTGCATCACC	CGCAACACTTCCAACATCGTC
33. *Cyp306a1*	ACGGATTCACCGAGGCTTTT	AAGTGAGTCCAAACCGACCC
34. *CENP-S*	CACTTCTCGAAAAATGTCACGC	GAAAGCTTCTAAATCCGACGC
35. *Deadpan*	GGGAAATCGCCTTGCTTTTAC	GGAGGACTTACCGAAGTTGATG
36. *RPL27*	CATAAACGCATGGGCAAGGG	ACCGAATAACGTGTGGGCAT
37. *Lipase*	GATATTGATGCCAGCGATTTCC	ATCCAGTCCAGTGATCCTCC
38. *LOC103314394*	TGGTCTCTGCTCCTCTTACTC	ACAAAGCTCACCCAAGTTGTC

39. *SH3bp*	AACTCGAGAAGCTCAACACCA	TCGGAAAGTGGTGTTGGCTT
40. *Integrin αPS2*	GTTATTCACGCCCAGTTCGTC	AGTTCGTCCGCCGTTTTTC
41. *Ip6k*	GACCTCCTCAGACGTGACCA	CTTACAGATCGTGCTCGGGT
42. *LOC657682*	TCGCATCGTTTATTACCCACC	CAGTCACTTTGTACCCAGCC
43. *TAF1B*	GATAAGACAGCGAAGACTGAG	TCCACAAGAGACGAACGAC
44. *LOC103314169*	TGGTCTCTGCTCCTCTTACTC	ACAAAGCTCACCCAAGTTGTC
45. *Bambi*	ACCATCGGCAACTTACAAC	AGAATGACTGCTCCACAAAC

Supplementary Table 4-3. Primers used for pRNAi.

Gene acronym	Forward primer (5'-3')	Reverse primer (5'-3')	Product length (bp)
Tribolium castaneum			
1. *LOC656417*	TCAGTGCACGGACTTGTTGT	GCTCACACGAGAACTCCTCG	658
5. *Melted*	CAAGGGCTGGAGACCTGTTT	AGTGTTGACCACCACCTTGG	1977
6. *SLC25-35-2*	TGGAGCTGCACTTCTGATGC	CCAGCACCTTTGTACAAGCC	615
7. *CalcitoninR*	TTCAGTTGGTGCGCGTTTGT	TCCCAAGACGCTCCTCACAG	910
8. *Cyp6a14*	TCGACATTCTGGGCGTGTCT	TGTGTCCTTCCTGCTACCCG	1384
9. *Cyp6k1*	GACAACTGGCGCAATCTCCG	TATAGCCCCCGGGTCCAACT	1068
16. *Lac2*	CCAGCTCAGTTGACGATTCA	TCAACTTTGTGGGTGCACAT	650
20. *CAT1*	TGCTCGAGTCCCTAAGGCAG	GCATCGAAGGCAGCTGTGAA	1185
21. *CAT2*	ATGGGTCTGCGCACTATCAC	TGCCAGGGATCCAAGGAACT	1594
24. *CAT3*	GGTGTGGAGGGTGTTGACGA	TTCCCGTTCGGTTTGACGGA	1827
31. *Chymase*	GCTGCTTTTCTTTGCCTCTGA	CCGGGTGTCTATGATGTGGG	722
32. *Cyp18a1*	TGCACCTGCACTTCAGGGAT	TTCAGCGTTGATGAACCGGC	1124
33. *Cyp306a1*	ACACTTCAGGTTCGTCCCAA	GAATCCGAGACACCCACCAA	492
37. *Lipase*	CGCCTTCGGTGCTGTTTAGT	ACTCTCGTCCCGTGGTAAGG	1344
41. *Ip6k*	GAGATACTGAAACCCGCAAC	CGTCGTAGCAACAGGGGACT	954

Supplementary Table 4-4. Primers used for RNAi in ecdysone biosynthesis and 20E signaling pathway.

Gene acronym	Forward primer (5'-3')	Reverse primer (5'-3')	Product length (bp)
Tribolium castaneum			
Spo	GCTCAAGTCCTTCCTCCACC	GTCCTCTTTCCCGTGCTGAA	837
Phm	ACACTTCAGGTTCGTCCCAA	GAATCCGAGACACCCACCAA	492
Dib	CTACTGCTGTTGATCCGCCA	CTGTAGTTAGAGGGGCCGCA	1005
Sad	TTCATGGATGGGGCCAACTG	TGGTTCCCCAGCTCAACTTC	962
Shd	ACTCATACCGGGACCCTTGG	GCGTCCGGAAAATTGCGTTC	1083
Ecr	TCCGGTTACCACTACAACGC	TTCGAAATCCGCCCTCCAAA	1122
USP	ATCTCTCGATGGGCAGCTTG	TGCCCGACACACTAAACCCT	1217

Supplementary Table 4-5. Primers used for qPCR in ecdysone biosynthesis and 20E signaling pathway.

Gene acronym	Forward primer (5'-3')	Reverse primer (5'-3')
Tribolium castaneum		
Spo	GGGACGAGCCTGGACTGTT	CCCGTGCTGAAAGGAATGA
Phm	ACGGATTCACCGAGGCTTTT	AAGTGAGTCCAAACCGACCC
Dib	ACAGGAAGAGCCACCTCACC	ACCATTCGGGTCCATTTGTT
Sad	GCTAAGAGCCCGCAAATCC	GGTAAAGCCGCAAAGTCTCCT
Shd	GGTCAACGAACAAGGTGAGG	GAGTCGGTCTGCGATGTAGTTT
Br	CACAACACTTCTGTCTGCGGTG	CACAGGGTGTTTGCAAGGAG

Supplementary Table 4-6. Motifs of transcription factor binding sites found significantly enriched in sequences between Chymase and Cyp18a1 in Find Individual Motif Occurrences (FIMO) database.

Matrix ID	Name	*Drosophila* sequence	*Tribolium* sequence	p-value	Detailed class information
MA0460.1	Ttk	AAGGATAAT	AAGGATAAA	8.13e-05	C2H2 zinc finger factors
MA0013.1	Br	TAGTAAACAAA	TAGTAAAAAAA	6.36e-06	C2H2 zinc finger factors
MA0534.1	EcR::usp	GAGTTCATTGACCTT	AAATTCAGTGAAATA	7.95e-05	Nuclear receptors with C4 zinc fingers

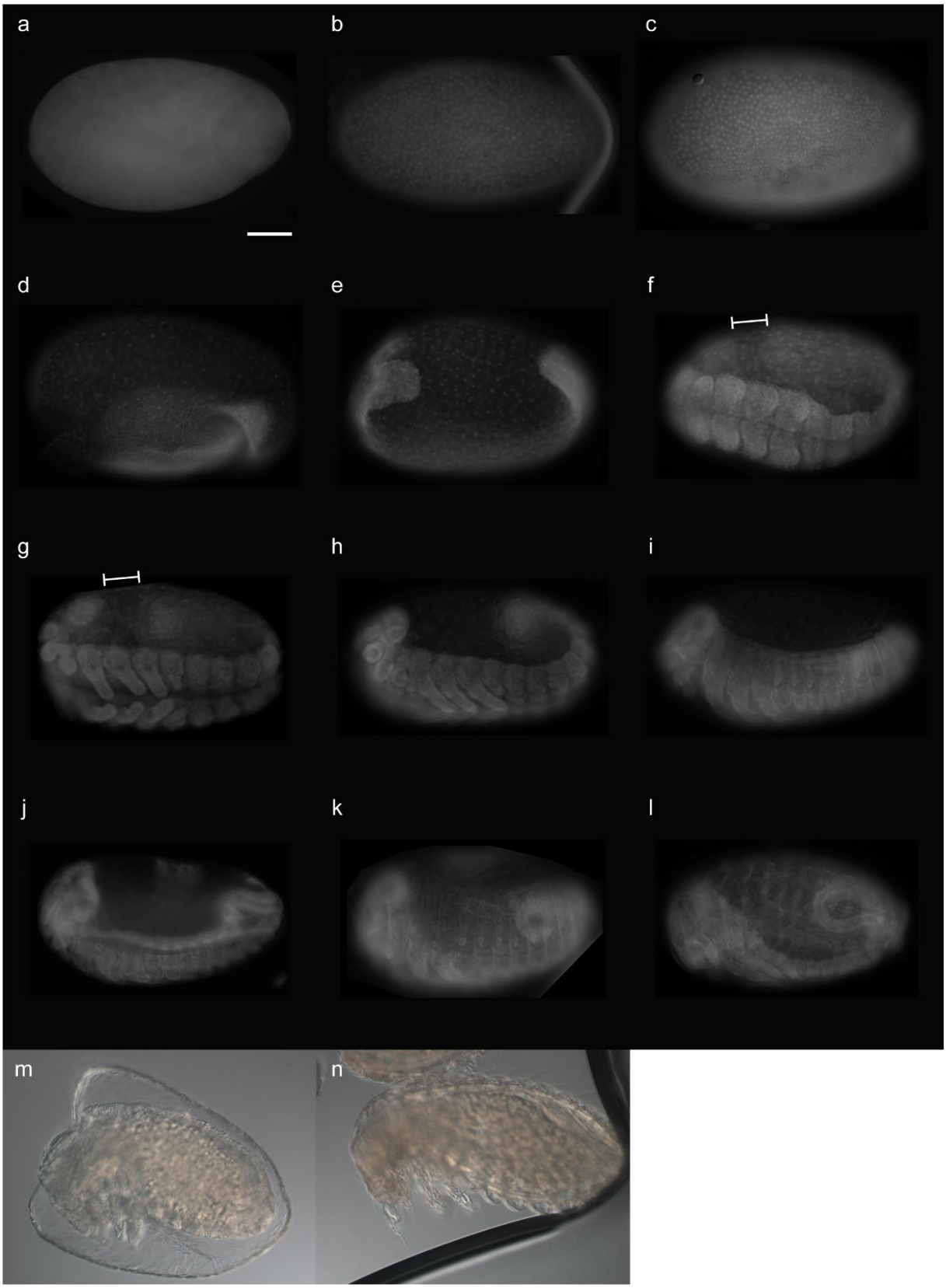

Supplementary Figure 4-1. Numerical staging table for *Tribolium castaneum*. Largely based on (Handel et al., 2000; Hilbrant et al., 2016) . **(a)** 0=no nuclei at surface; **(b)** 1=undifferentiated blastoderm (equal nuclei at the surface). **(c)** 2=differentiated blastoderm (the large polyploid nuclei of the serosa can be distinguished from the more dense, smaller nuclei of the germ rudiment). **(d)** 3=gastrulation (amnion and serosa fold over the embryo; serosal window not yet closed). **(e)** 4=extending germband (serosa closed). **(f)** 5=extended germ band (distance between posterior end and head is small, size bar; limbs are buds). **(g)** 6=limbs growing and extending (head and

posterior of the germband still close, see size bar; limbs well developing and extending). **(h)** 7=retracting germband (dorsal distance between head and posterior end of the embryo increases again). **(i)** 8=completely retracted germband. **(j)** 9=start of dorsal closure (dorsal organ formation). **(k)** 10=dorsal closure in progress (dorsal organ flatter, lateral sides of the embryo have moved towards dorsal). **(l)** 11=dorsal closure completed (lateral sides of the embryo dorsally fused). **(m)** 12=hatching (still in vitelline membrane). **(n)** 13=hatched (out of vitelline membrane). Scalebar = 200 µm.

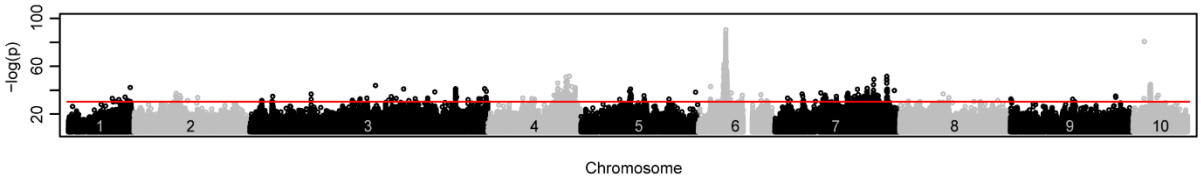

Supplementary Figure 4-2. SNP analysis on whole genome of *T. castaneum* between the slow lines and the non-selected lines. The red line indicates q = 0.01 or $-\log_{10}$P value equal to 33.0538. In total, 1258 SNPs differ in frequency significantly.

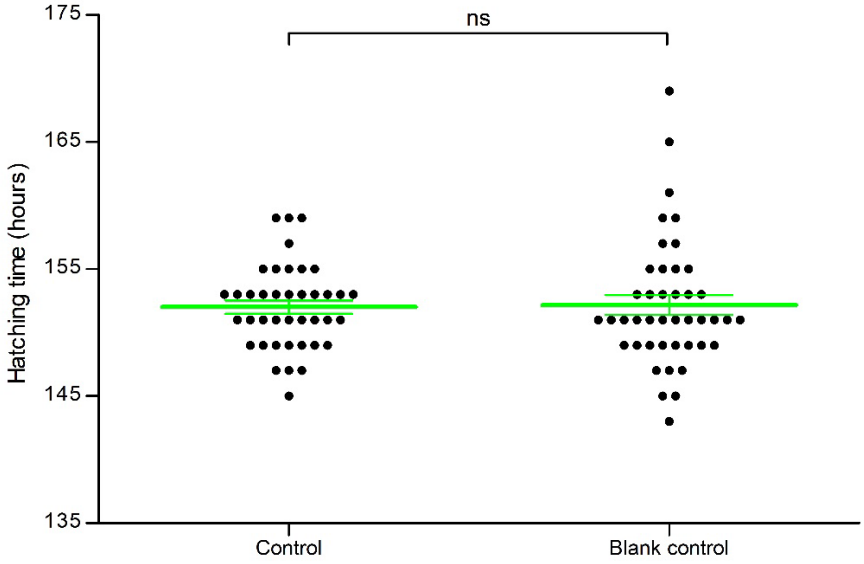

Supplementary Figure 4-3. The embryonic developmental time of offspring embryos in the blank control group, compared to injections of non-targeting control dsRNA into 50 *Tribolium* mothers. Key: Green lines, mean of embryonic developmental time plus standard error. Black dot, the time of every hatched embryo. The student t-test was performed to compare the control and blank control. Key: ns, no significant difference observed in hatching time.

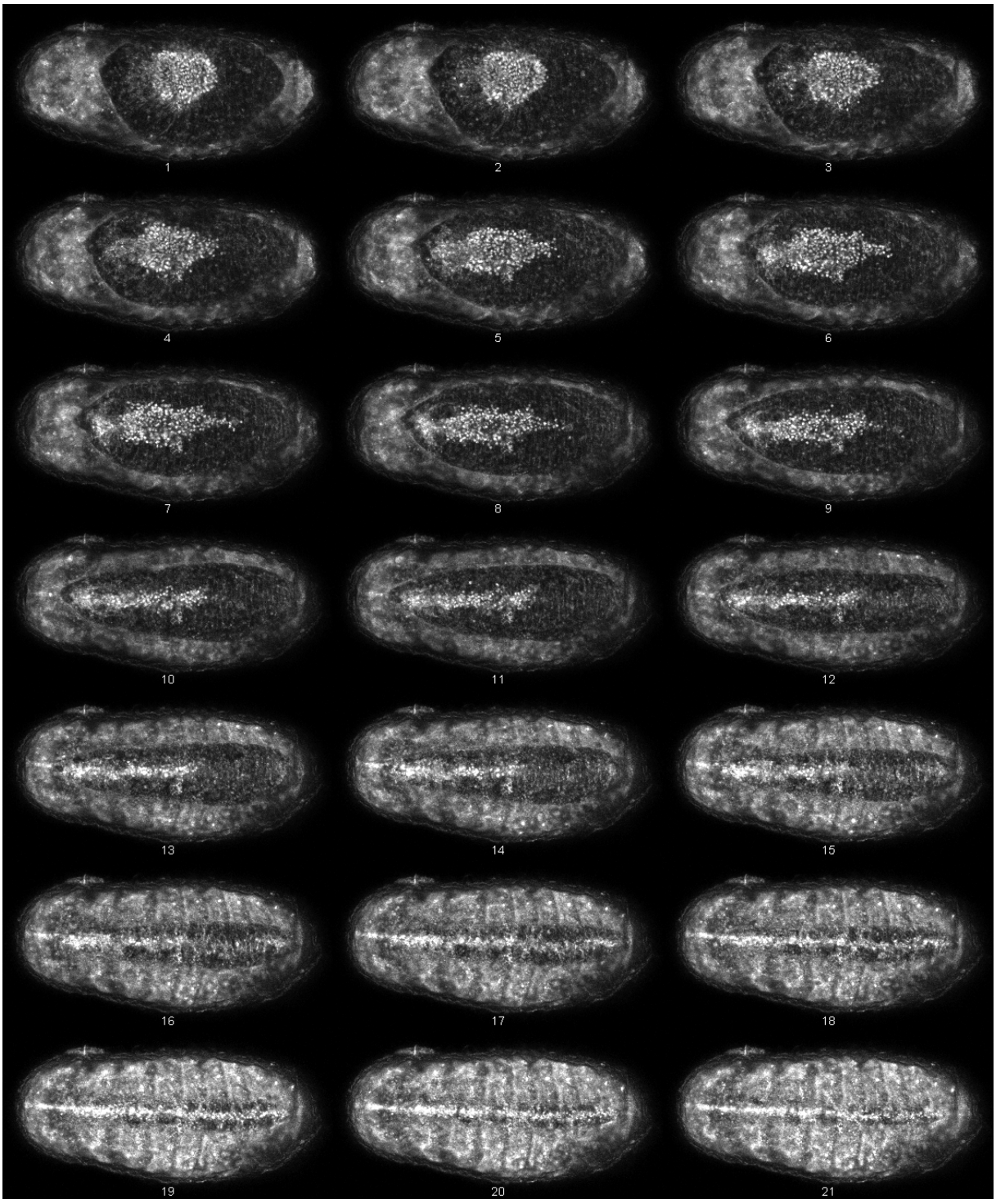

Supplementary Figure 4-4. Overview of dorsal closure process from the dorsal organ (Num. 1) to dorsal closure completely (Num. 21). The *Tribolium castaneum* LifeAct-nGFP line was used for live imaging at 27°C under a confocal microscopy. Numbers indicate 20 min intervals during development.

```
The 445 bp repeated region

Repeat 1      CTGGGAAGGATAAAAAATTTGAAATAATAAATTTAAAAAAATTTATAAAAAAAGAAAATA       60
Repeat 2      CAAGGAAGGATAAAAAAATTGAAATAATAAATTTAAAAAAATTTATAAAAAAAGAAAATA       60
              *:.**************:****************************************

Repeat 1      TAGTAAAAAAGGCGGACAAATGTATTGATACTAATTACAATGAAAGATTCAAATTTTGTG       120
Repeat 2      TAGTAAAAAAAGCGGACAAATGTATTGATACTAATTACAATGAAAGATTCAAATTTTGTG       120
              **********.************************************************

Repeat 1      TTTTTGCCTTTATTTTATAAAGGGCGATTGTTTTTTTGCTTATTTTAAAATCACTCTGTA       180
Repeat 2      TTTTTGCCTT-ATTTTATAAAAGGCGATTGTTTTTTTGCTTATTTTAAAATCACTCTGTA       179
              **********:**********.***********************************

Repeat 1      TGTCAAAAAATGCATAAAATATAGGGTGTTCCATTTGGAAGAT                        223
Repeat 2      TGTCAAAAAAAGCATAAAATATAGGGTGTTCCATTTGGAAGAT                        222
              **********:*******************************
```

Supplementary Figure 4-5. Alignment of repeat 1 and repeat 2 in the repeated region of Georgia strain.

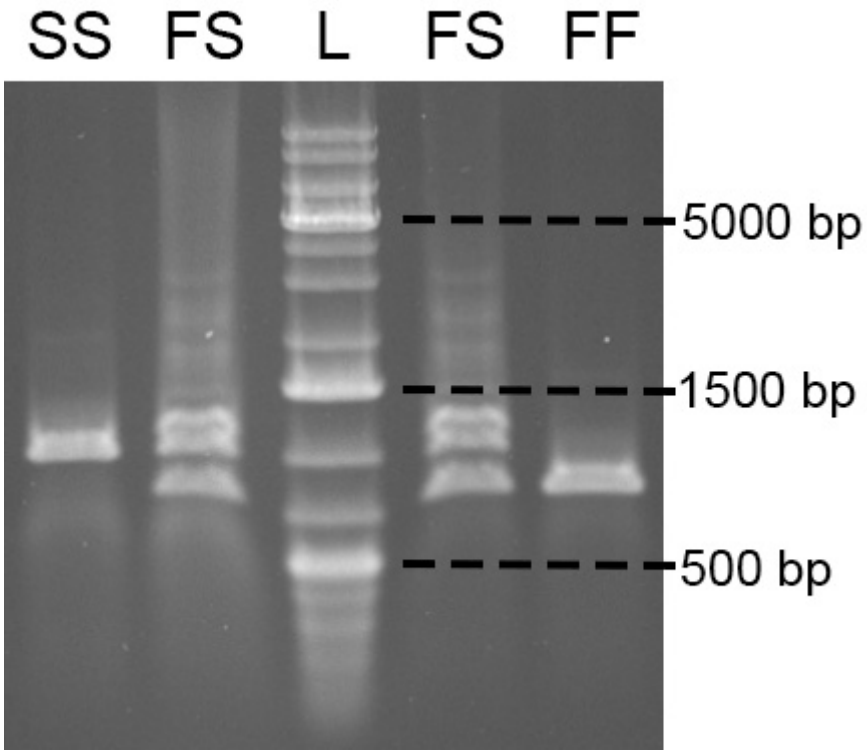

Supplementary Figure 4-6. PCR products including three types of genotypes. SS (Lane 1): homozygotes of the slow allele with the 445 bp repeated region. FS (Lane 2, 4): heterozygotes of the slow allele and the fast allele. L (Lane 3): DNA ladder, GeneRuler 1kb plus DNA ladder (Invitrogen). FF (Lane 5): homozygotes of the fast allele with the 222 bp deleted region.

Repeated region

Tramtrack

CTGGGAAGGATAAAAAATTTGAAATAATAAATTTAAAAAAATTTATAAAAAAAGAAAATA 60

Broad

TAGTAAAAAAGGCGGACAAATGTATTGATACTAATTACAATGAAAGATTCAAATTTTGTG 120

TTTTTGCCTTTATTTTATAAAGGGCGATTGTTTTTTTGCTTATTTTAAAATCACTCTGTA 180

Tramtrack

TGTCAAAAAATGCATAAAATATAGGGTGTTCCATTTGGAAGATCAAGGAAGGATAAAAAA 240

Broad

ATTGAAATAATAAATTTAAAAAAATTTATAAAAAAAGAAAATATAGTAAAAAAAAGCGGAC 300

AAATGTATTGATACTAATTACAATGAAAGATTCAAATTTTGTGTTTTTGCCTTATTTTAT 360

AAAAGGCGATTGTTTTTTTGCTTATTTTAAAATCACTCTGTATGTCAAAAAAAGCATAAA 420

ATATAGGGTGTTCCATTTGGAAGAT 445

Supplementary Figure 4-7. The transcription factor binding sites Tramtrack (red) and Broad (yellow) in the repeated region.

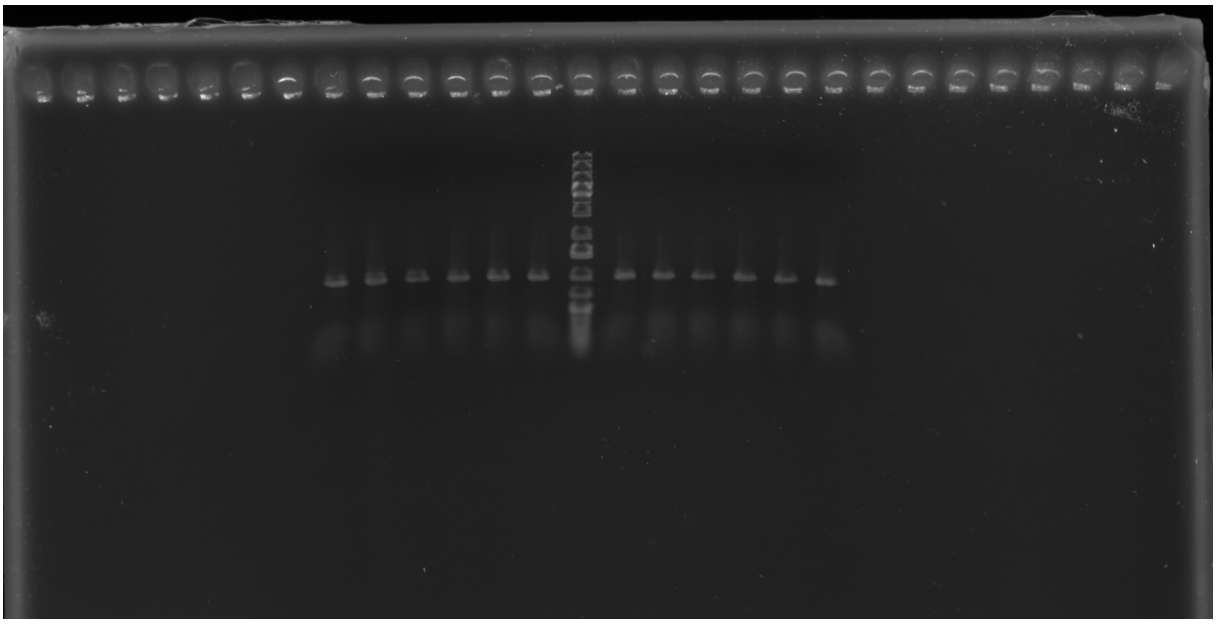

Supplementary Figure 4-8. Allele frequency of F in the nGFP line is 1. Genotyping PCR (Ethidium bromide staining shown on a 1.0% agarose gel) of 10 beetles from the nGFP line. Ladder is GeneRuler 1kb plus DNA ladder (Invitrogen).

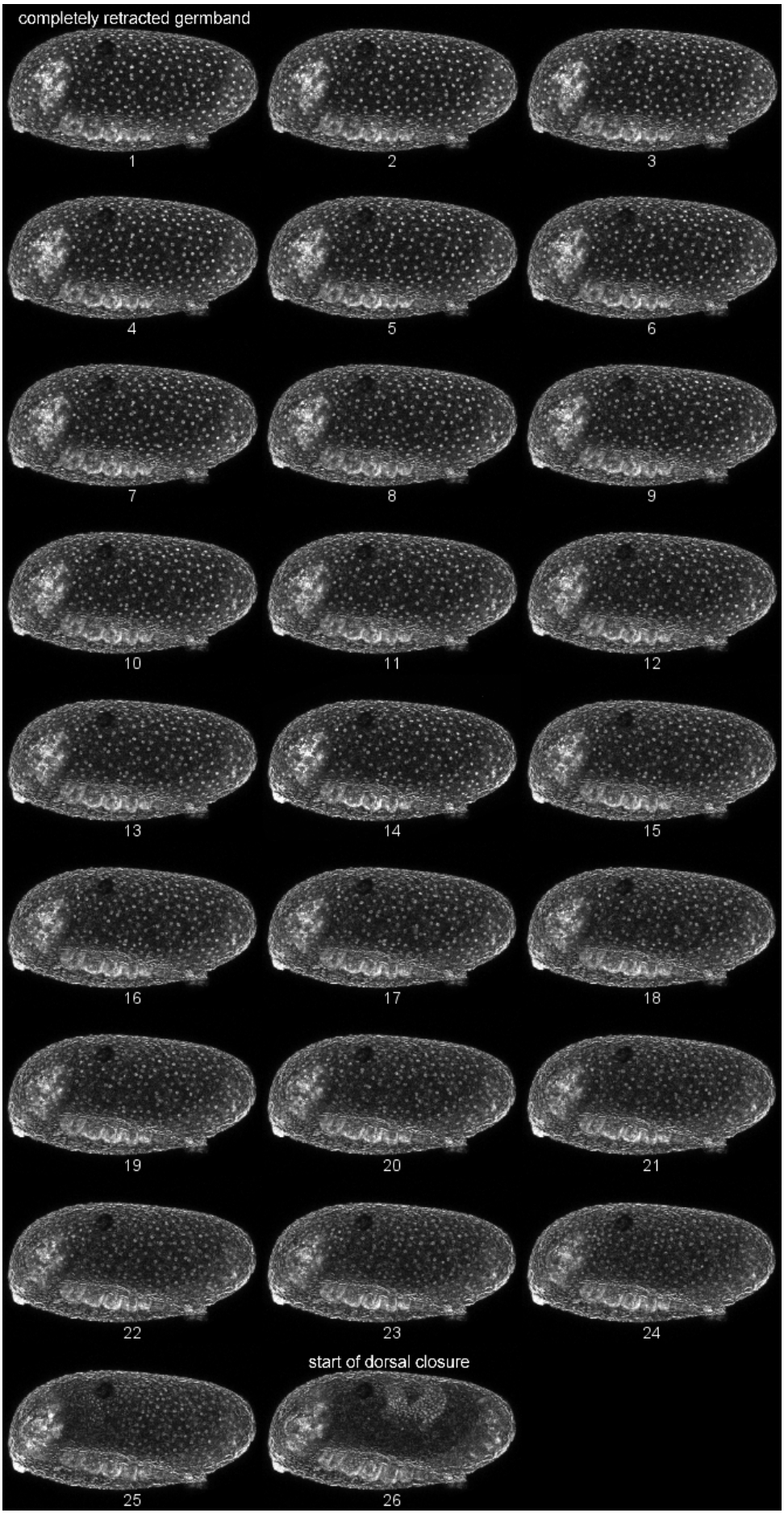
completely retracted germband
1
2
3
4
5
6
7
8
9
10
11
12
13
14
15
16
17
18
19
20
21
22
23
24
start of dorsal closure
25
26

Supplementary Figure 4-9. Duration between completely retracted germband (Num. 1) and start of dorsal closure (Num. 26) of heterozygous nGFP-GA-1 offspring. The developmental progression of the offspring was visualized for live imaging at 25°C under a confocal microscopy. Numbers stand for 26 min intervals during embryonic development.

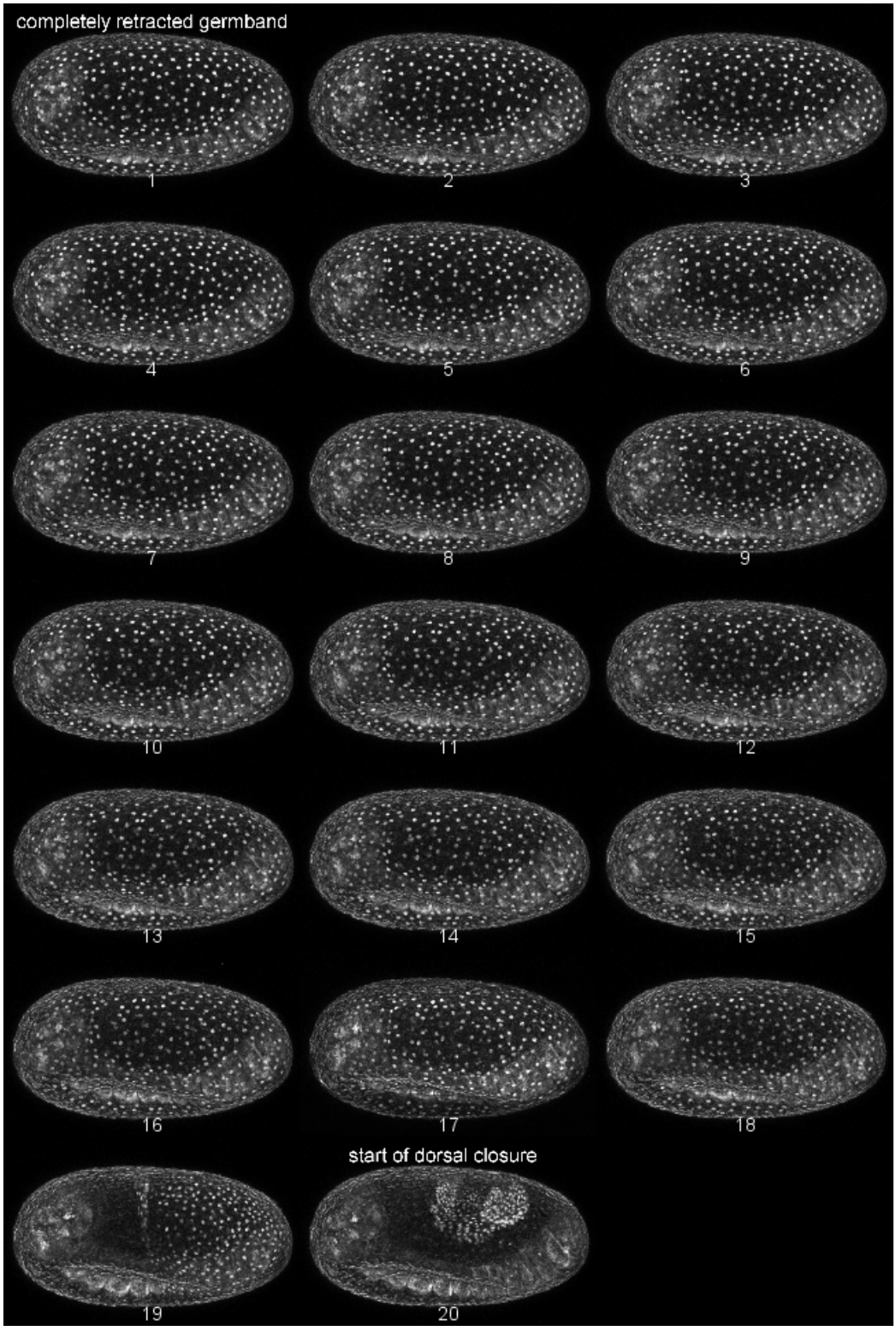

Supplementary Figure 4-10. Duration between completely retracted germband (Num. 1) and start of dorsal closure (Num. 20) of heterozygous nGFP-Crispr offspring. The developmental progression of the offspring was visualized for live imaging at 25°C under a confocal microscopy. Numbers indicate 26 min intervals during embryonic development.

Supplementary figure references

Handel, K., Grunfelder, C. G., Roth, S. and Sander, K. (2000). Tribolium embryogenesis: a SEM study of cell shapes and movements from blastoderm to serosal closure. *Dev Genes Evol* **210**, 167-179.

Hilbrant, M., Horn, T., Koelzer, S. and Panfilio, K. A. (2016). The beetle amnion and serosa functionally interact as apposed epithelia. *eLife* **5**.

Supplementary File 4-1. Alignments of cloned Sanger-sequenced PCR products from the beetles of the selection lines.

```
Fa1       AATTTTGATATTTTAATAAATAATATAAAAGCCTAATAAACAAAAGTTTTTTAAATAATA      60
Fa2       AATTTTGATATTTTAATAAATAATATAAAAGCCTAATAAACAAAAGTTTTTTAAATAATA      60
Fa3       AATTTTGATATTTTAATAAATAATATAAAAGCCTAATAAACAAAAGTTTTTTAAATAATA      60
Fa4       AATTTTGATATTTTAATAAATAATATAAAAGCCTAATAAACAAAAGTTTTTTAAATAATA      60
Fb1       AATTTTGATATTTTAATAAATAATATAAAAGCCTAATAAACAAAAGTTTTTTAAATAATA      60
Fb2       AATTTTGATATTTTAATAAATAATATAAAAGCCTAATAAACAAAAGTTTTTTAAATAATA      60
Fb3       AATTTTGATATTTTAATAAATAATATAAAAGCCTAATAAACAAAAGTTTTTTAAATAATA      60
Nb4       AATTTTGATATTTTAATAAATAATATAAAAGCCTAATAAACAAAAGTTTTTTAAATAATA      60
Na1       AATTTTGATATTTTAATAAATAATATAAAAGCCTAATGAACAAAAGTTTTTTAAATAATA      60
Na2       AATTT-GATA-TTTAATAAATAATATAAAAGC-TAATGAACAAAAGTTTTTTAAATAATA      57
Na3       AATTTTGATA-TTTAATAAATAATATAAAAGCCTAATGAACAAAAGTTTTTTAAATAATA      59
Na4       AATTTTGATATTTTAATAAATAATATAAAAGCCTAATGAACAAAAGTTTTTTAAATAATA      60
Nb1       AATTTTGATATTTTAATAAATAATATAAAAGCCTAATGAACAAAAGTTTTTTAAATAATA      60
Nb2       AATTTTGATATTTTAATAAATAATATAAAAGCCTAATGAACAAAAGTTTTTTAAATAATA      60
Nb3       AATTTTGATATTTTAATAAATAATATAAAAGCCTAATGAACAAAAGTTTTTTAAATAATA      60
Sa1       AATTT-GATA-TTTAATAAATAATATAAAAGC-TAATGAACAAAAGTTTTTTAAATAATA      57
Sa2       AATTTTGATATTTTAATAAATAATATAAAAGCCTAATGAACAAAAGTTTTTTAAATAATA      60
Sb1       AATTTTGATATTTTAATAAATAATATAAAAGCGTAATGAACAAAAGTTTTTTAAATAATA      60
Sb2       AATTT-GATATTTTAATAAATAATATAAAAGCCTAATGAACAAAAGTTTTTTAAATAATA      59
          ***** **** ********************** ****.**********************

Fa1       ATCAAAGAAATCTTTTTAATGCACATTTTTAATAAATTAATAAATTGTTATTATGTACTA      120
Fa2       ATCAAAGAAATCTTTTTAATGCACATTTTTAATAAATTAATAAATTGTTATTATGTACTA      120
Fa3       ATCAAAGAAATCTTTTTAATGCACATTTTTAATAAATTAATAAATTGTTATTATGTACTA      120
Fa4       ATCAAAGAAATCTTTTTAATGCACATTTTTAATAAATTAATAAATTGTTATTATGTACTA      120
Fb1       ATCAAAGAAATCTTTTTAATGCACATTTTTAATAAATTAATAAATTGTTATTATGTACTA      120
Fb2       ATCAAAGAAATCTTTTTAATGCACATTTTTAATAAATTAATAAATTGTTATTATGTACTA      120
Fb3       ATCAAAGAAATCTTTTTAATGCACATTTTTAATAAATTAATAAATTGTTATTATGTACTA      120
Nb4       ATCAAAGAAATCTTTTTAATGCACATTTTTAATAAATTAATAAATTGTTATTATGTACTA      120
Na1       ATCAAAGAAATCTTTTTAATGCTCATTTTTAATAAATTAATAAATTGTTATTATGTACTA      120
Na2       ATCAAAGAAATCTTTTTAATGCTCATTTTTAATAAATTAATAAATTGTTATTATGTACTA      117
Na3       ATCAAAGAAATCTTTTTAATGCTCATTTTTAATAAATTAATAAATTGTTATTATGTACTA      119
Na4       ATCAAAGAAATCTTTTTAATGCTCATTTTTAATAAATTAATAAATTGTTATTATGTACTA      120
Nb1       ATCAAAGAAATCTTTTTAATGCTCATTTTTAATAAATTAATAAATTGTTATTATGTACTA      120
Nb2       ATCAAAGAAATCTTTTTAATGCTCATTTTTAATAAATTAATAAATTGTTATTATGTACTA      120
Nb3       ATCAAAGAAATCTTTTTAATGCTCATTTTTAATAAATTAATAAATTGTTATTATGTACTA      120
Sa1       ATCAAAGAAATCTTTTTAATGCTCATTTTTAATAAATTAATAAATTGTTATTATGTACTA      117
Sa2       ATCAAAGAAATCTTTTTAATGCTCATTTTTAATAAATTAATAAATTGTTATTATGTACTA      120
Sb1       ATCAAAGAAATCTTTTTAATGCTCATTTTTAATAAATTAATAAATTGTTATTATGTACTA      120
Sb2       ATCAAAGAAATCTTTTTAATGCTCATTTTTAATAAATTAATAAATTGTTATTATGTACTA      119
          **********************:**************************************

Fa1       CGTTTAGGGTAAGTTTAAAGCAATAAAAAAGTTTATATTTCTGTTGTGGGTCATTTTTTG      180
Fa2       CGTTTAGGGTAAGTTTAAAGCAATAAAAAAGTTTATATTTCTGTTGTGGGTCATTTTTTG      180
Fa3       CGTTTAGGGTAAGTTTAAAGCAATAAAAAAGTTTATATTTCTGTTGTGGGTCATTTTTTG      180
Fa4       CGTTTAGGGTAAGTTTAAAGCAATAAAAAAGTTTATATTTCTGTTGTGGGTCATTTTTTG      180
Fb1       CGTTTAGGGTAAGTTTAAAGCAATAAAAAAGTTTATATTTCTGTTGTGGGTCATTTTTTG      180
Fb2       CGTTTAGGGTAAGTTTAAAGCAATAAAAAAGTTTATATTTCTGTTGTGGGTCATTTTTTG      180
Fb3       CGTTTAGGGTAAGTTTAAAGCAATAAAAAAGTTTATATTTCTGTTGTGGGTCATTTTTTG      180
Nb4       CGTTTAGGGTAAGTTTAAAGCAATAAAAAAGTTTATATTTCTGTTGTGGGTCATTTTTTG      180
Na1       CGTTTAGGGTAAGTTTAAAGCAATAAAAAAGTTTATATTTCTGTTGTGGGTCATTTTTTG      180
Na2       CGTTTAGGGTAAGTTTAAAGCAATAAAAAAGTTTATATTTCTGTTGTGGGTCATTTTTTG      177
Na3       CGTTTAGGGTAAGTTTAAAGCAATAAAAAAGTTTATATTTCTGTTGTGGGTCATTTTTTG      179
Na4       CGTTTAGGGTAAGTTTAAAGCAATAAAAAAGTTTATATTTCTGTTGTGGGTCATTTTTTG      180
Nb1       CGTTTAGGGTAAGTTTAAAGCAATAAAAAAGTTTATATTTCTGTTGTGGGTCATTTTTTG      180
Nb2       CGTTTAGGGTAAGTTTAAAGCAATAAAAAAGTTTATATTTCTGTTGTGGGTCATTTTTTG      180
Nb3       CGTTTAGGGTAAGTTTAAAGCAATAAAAAAGTTTATATTTCTGTTGTGGGTCATTTTTTG      180
Sa1       CGTTTAGGGTAAGTTTAAAGCAATAAAAAAGTTTATATTTCTGTTGTGGGTCATTTTTTG      177
Sa2       CGTTTAGGGTAAGTTTAAAGCAATAAAAAAGTTTATATTTCTGTTGTGGGTCATTTTTTG      180
Sb1       CGTTTAGGGTAAGTTTAAAGCAATAAAAAAGTTTATATTTCTGTTGTGGGTCATTTTTTG      180
Sb2       CGTT-AGGGTAAGTTTAAAGCAATAAAAAAGTTTATATTTCTGTTGTGGGTCATTTTTTG      178
```

```
          **** ************************************************************

Fa1       AAAAAAATCCTCGAGTAGGTCGATTTTATTTTTGTATGTATATACTACATTTTATTACTT      240
Fa2       AAAAAAATCCTCGAGTAGGTCGATTTTATTTTTGTATGTATATACTACATTTTATTACTT      240
Fa3       AAAAAAATCCTCGAGTAGGTCGATTTTATTTTTGTATGTATATACTACATTTTATTACTT      240
Fa4       AAAAAAATCCTCGAGTAGGTCGATTTTATTTTTGTATGTATATACTACATTTTATTACTT      240
Fb1       AAAAAAATCCTCGAGTAGGTCGATTTTATTTTTGTATGTATATACTACATTTTATTACTT      240
Fb2       AAAAAAATCCTCGAGTAGGTCGATTTTATTTTTGTATGTATATACTACATTTTATTACTT      240
Fb3       AAAAAAATCCTCGAGTAGGTCGATTTTATTTTTGTATGTATATACTACATTTTATTACTT      240
Nb4       AAAAAAATCCTCGAGTAGGTCGATTTTATTTTTGTATGTATATACTACATTTTATTACTT      240
Na1       AAAAAAATCCTCGAGCAGGTCGATTTTATTTTTGTATGTATATACTACATTTTATTACTT      240
Na2       AAAAAAATCCTCGAGCAGGTCGATTTTATTTTTGTATGTATATACTACATTTTATTACTT      237
Na3       AAAAAAATCCTCGAGCAGGTCGATTTTATTTTTGTATGTATATACTACATTTTATTACTT      239
Na4       AAAAAAATCCTCGAGCAGGTCGATTTTATTTTTGTATGTATATACTACATTTTATTACTT      240
Nb1       AAAAAAATCCTCGAGCAGGTCGATTTTATTTTTGTATGTATATACTACATTTTATTACTT      240
Nb2       AAAAAAATCCTCGAGCAGGTCGATTTTATTTTTGTATGTATATACTACATTTTATTACTT      240
Nb3       AAAAAAATCCTCGAGCAGGTCGATTTTATTTTTGTATGTATATACTACATTTTATTACTT      240
Sa1       AAAAAAATCCTCGAGCAGGTCGATTTTATTTTTGTATGTATATACTACATTTTATTACTT      237
Sa2       AAAAAAATCCTCGAGCAGGTCGATTTTATTTTTGTATGTATATACTACATTTTATTACTT      240
Sb1       AAAAAAATCCTCGAGCAGGTCGATTTTATTTTTGTATGTATATACTACATTTTATTACTT      240
Sb2       AAAAAAATCCTCGAGCAGGTCGATTTTATTTTTGTATGTATATACTACATTTTATTACTT      238
          *************** ****************************************

Fa1       TTAATTTTTTTTAATGACAATCGATATTTTTGGTTACTGTTTTTGATAGCAGATATTCTC      300
Fa2       TTAATTTTTTTTAATGACAATCGATATTTTTGGTTACTGTTTTTGATAGCAGATATTCTC      300
Fa3       TTAATTTTTTTTAATGACAATCGATATTTTTGGTTACTGTTTTTGATAGCAGATATTCTC      300
Fa4       TTAATTTTTTTTAATGACAATCGATATTTTTGGTTACTGTTTTTGATAGCAGATATTCTC      300
Fb1       TTAATTTTTTTTAATGACAATCGATATTTTTGGTTACTGTTTTTGATAGCAGATATTCTC      300
Fb2       TTAATTTTTTTTAATGACAATCGATATTTTTGGTTACTGTTTTTGATAGCAGATATTCTC      300
Fb3       TTAATTTTTTTTAATGACAATCGATATTTTTGGTTACTGTTTTTGATAGCAGATATTCTC      300
Nb4       TTAATTTTTTTTAATGACAATCGATATTTTTGGTTACTGTTTTTGATAGCAGATATTCTC      300
Na1       TTAATTTTTTTTAATGACAATCGATATTTTTGGTTACTGTTTTTGATAGCAGATATTCTC      300
Na2       TTAATTTTTTTTAATGACAATCGATATTTTTGGTTACTGTTTTTGATAGCAGATATTCTC      297
Na3       TTAATTTTTTTTAATGACAATCGATATTTTTGGTTACTGTTTTTGATAGCAGATATTCTC      299
Na4       TTAATTTTTTTTAATGACAATCGATATTTTTGGTTACTGTTTTTGATAGCAGATATTCTC      300
Nb1       TTAATTTTTTTTAATGACAATCGATATTTTTGGTTACTGTTTTTGATAGCAGATATTCTC      300
Nb2       TTAATTTTTTTTAATGACAATCGATATTTTTGGTTACTGTTTTTGATAGCAGATATTCTC      300
Nb3       TTAATTTTTTTTAATGACAATCGATATTTTTGGTTACTGTTTTTGATAGCAGATATTCTC      300
Sa1       TTAATTTTTTTTAATGACAATCGATATTTTTGGTTACTGTTTTTGATAGCAGATATTCTC      297
Sa2       TTAATTTTTTTTAATGACAATCGATATTTTTGGTTACTGTTTTTGATAGCAGATATTCTC      300
Sb1       TTAATTTTTTTTAATGACAATCGATATTTTTGGTTACTGTTTTTGATAGCAGATATTCTC      300
Sb2       TTAATTTTTTTTAATGACAATCGATATTTTTGGTTACTGTTTTTGATAGCAGATATTCTC      298
          ************************************************************

Fa1       TTTTATCTTTCTGGGAAGGATAAAAAAATTGAAATAATGAATTTAAAAAAATTTATAAAA      360
Fa2       TTTTATCTTTCTGGGAAGGATAAAAAAATTGAAATAATGAATTTAAAAAAATTTATAAAA      360
Fa3       TTTTATCTTTCTGGGAAGGATAAAAAAATTGAAATAATGAATTTAAAAAAATTTATAAAA      360
Fa4       TTTTATCTTTCTGGGAAGGATAAAAAAATTGAAATAATGAATTTAAAAAAATTTATAAAA      360
Fb1       TTTTATCTTTCTGGGAAGGATAAAAAAATTGAAATAATGAATTTAAAAAAATTTATAAAA      360
Fb2       TTTTATCTTTCTGGGAAGGATAAAAAAATTGAAATAATGAATTTAAAAAAATTTATAAAA      360
Fb3       TTTTATCTTTCTGGGAAGGATAAAAAAATTGAAATAATGAATTTAAAAAAATTTATAAAA      360
Nb4       TTTTATCTTTCTGGGAAGGATAAAAAAATTGAAATAATGAATTTAAAAAAATTTATAAAA      360
Na1       TTTTATCTTTCTGGGAAGGATAAAAAAATTTGAAATAATAAATTTAAAAAAATTTATAAAA      360
Na2       TTTTATCTTTCTGGGAAGGATAAAAAAATTTGAAATAATAAATTTAAAAAAATTTATAAAA      357
Na3       TTTTATCTTTCTGGGAAGGATAAAAAAATTTGAAATAATAAATTTAAAAAAATTTATAAAA      359
Na4       TTTTATCTTTCTGGGAAGGATAAAAAAATTTGAAATAATAAATTTAAAAAAATTTATAAAA      360
Nb1       TTTTATCTTTCTGGGAAGGATAAAAAAATTTGAAATAATAAATTTAAAAAAATTTATAAAA      360
Nb2       TTTTATCTTTCTGGGAAGGATAAAAAAATTTGAAATAATAAATTTAAAAAAATTTATAAAA      360
Nb3       TTTTATCTTTCTGGGAAGGATAAAAAAATTTGAAATAATAAATTTAAAAAAATTTATAAAA      360
Sa1       TTTTATCTTTCTGGGAAGGATAAAAAAATTTGAAATAATAAATTTAAAAAAATTTATAAAA      357
Sa2       TTTTATCTTTCTGGGAAGGATAAAAAAATTTGAAATAATAAATTTAAAAAAATTTATAAAA      360
Sb1       TTTTATCTTTCTGGGAAGGATAAAAAAATTTGAAATAATAAATTTAAAAAAATTTATAAAA      360
Sb2       TTTTATCTTTCTGGGAAGGATAAAAAAATTTGAAATAATAAATTTAAAAAAATTTATAAAA      358
          ***************************:**********.**********************
```

```
Fa1     ------------------------------------------------------------  360
Fa2     ------------------------------------------------------------  360
Fa3     ------------------------------------------------------------  360
Fa4     ------------------------------------------------------------  360
Fb1     ------------------------------------------------------------  360
Fb2     ------------------------------------------------------------  360
Fb3     ------------------------------------------------------------  360
Nb4     ------------------------------------------------------------  360
Na1     AAAGAAAATATAGTAAAAAAGGCGGACAAATGTATTGATACTAATTACAATGAAAGATTC  420
Na2     AAAGAAAATATAGTAAAAAAGGCGGACAAATGTATTGATACTAATTACAATGAAAGATTC  417
Na3     AAAGAAAATATAGTAAAAAAGGCGGACAAATGTATTGATACTAATTACAATGAAAGATTC  419
Na4     AAAGAAAATATAGTAAAAAAGGCGGACAAATGTATTGATACTAATTACAATGAAAGATTC  420
Nb1     AAAGAAAATATAGTAAAAAAGGCGGACAAATGTATTGATACTAATTACAATGAAAGATTC  420
Nb2     AAAGAAAATATAGTAAAAAAGGCGGACAAATGTATTGATACTAATTACAATGAAAGATTC  420
Nb3     AAAGAAAATATAGTAAAAAAGGCGGACAAATGTATTGATACTAATTACAATGAAAGATTC  420
Sa1     AAAGAAAATATAGTAAAAAAGGCGGACAAATGTATTGATACTAATTACAATGAAAGATTC  417
Sa2     AAAGAAAATATAGTAAAAAAGGCGGACAAATGTATTGATACTAATTACAATGAAAGATTC  420
Sb1     AAAGAAAATATAGTAAAAAAGGCGGACAAATGTATTGATACTAATTACAATGAAAGATTC  420
Sb2     AAAGAAAATATAGTAAAAAAGGCGGACAAATGTATTGATACTAATTACAATGAAAGATTC  418


Fa1     ------------------------------------------------------------  360
Fa2     ------------------------------------------------------------  360
Fa3     ------------------------------------------------------------  360
Fa4     ------------------------------------------------------------  360
Fb1     ------------------------------------------------------------  360
Fb2     ------------------------------------------------------------  360
Fb3     ------------------------------------------------------------  360
Nb4     ------------------------------------------------------------  360
Na1     AAATTTTGTGTTTTTGCCTTTATTTTATAAAGGGCGATTGTTTTTTTGCTTATTTTAAAA  480
Na2     AAATTTTGTGTTTTTGCCTTTATTTTATAAAGGGCGATTGTTTTTTTGCTTATTTTAAAA  477
Na3     AAATTTTGTGTTTTTGCCTTTATTTTATAAAGGGCGATTGTTTTTTTGCTTATTTTAAAA  479
Na4     AAATTTTGTGTTTTTGCCTTTATTTTATAAAGGGCGATTGTTTTTTTGCTTATTTTAAAA  480
Nb1     AAATTTTGTGTTTTTGCCTTTATTTTATAAAGGGCGATTGTTTTTTTGCTTATTTTAAAA  480
Nb2     AAATTTTGTGTTTTTGCCTTTATTTTATAAAGGGCGATTGTTTTTTTGCTTATTTTAAAA  480
Nb3     AAATTTTGTGTTTTTGCCTTTATTTTATAAAGGGCGATTGTTTTTTTGCTTATTTTAAAA  480
Sa1     AAATTTTGTGTTTTTGCCTTTATTTTATAAAGGGCGATTGTTTTTTTGCTTATTTTAAAA  477
Sa2     AAATTTTGTGTTTTTGCCTTTATTTTATAAAGGGCGATTGTTTTTTTGCTTATTTTAAAA  480
Sb1     AAATTTTGTGTTTTTGCCTTTATTTTATAAAGGGCGATTGTTTTTTTGCTTATTTTAAAA  480
Sb2     AAATTTTGTGTTTTTGCCTTTATTTTATAAAGGGCGATTGTTTTTTTGCTTATTTTAAAA  478


Fa1     ------------------------------------------------------------  360
Fa2     ------------------------------------------------------------  360
Fa3     ------------------------------------------------------------  360
Fa4     ------------------------------------------------------------  360
Fb1     ------------------------------------------------------------  360
Fb2     ------------------------------------------------------------  360
Fb3     ------------------------------------------------------------  360
Nb4     ------------------------------------------------------------  360
Na1     TCACTCTGTATGTCAAAAAATGCATAAAATATAGGGTGTTCCATTTGGAAGATCAAGGAA  540
Na2     TCACTCTGTATGTCAAAAAATGCATAAAATATAGGGTGTTCCATTTGGAAGATCAAGGAA  537
Na3     TCACTCTGTATGTCAAAAAATGCATAAAATATAGGGTGTTCCATTTGGAAGATCAAGGAA  539
Na4     TCACTCTGTATGTCAAAAAATGCATAAAATATAGGGTGTTCCATTTGGAAGATCAAGGAA  540
Nb1     TCACTCTGTATGTCAAAAAATGCATAAAATATAGGGTGTTCCATTTGGAAGATCAAGGAA  540
Nb2     TCACTCTGTATGTCAAAAAATGCATAAAATATAGGGTGTTCCATTTGGAAGATCAAGGAA  540
Nb3     TCACTCTGTATGTCAAAAAATGCATAAAATATAGGGTGTTCCATTTGGAAGATCAAGGAA  540
Sa1     TCACTCTGTATGTCAAAAAATGCATAAAATATAGGGTGTTCCATTTGGAAGATCAAGGAA  537
Sa2     TCACTCTGTATGTCAAAAAATGCATAAAATATAGGGTGTTCCATTTGGAAGATCAAGGAA  540
Sb1     TCACTCTGTATGTCAAAAAATGCATAAAATATAGGGTGTTCCATTTGGAAGATCAAGGAA  540
Sb2     TCACTCTGTATGTCAAAAAATGCATAAAATATAGGGTGTTCCATTTGGAAGATCAAGGAA  538
```

```
Fa1      ------------------------------------------AAAGAAAATATAGTAAA      377
Fa2      ------------------------------------------AAAGAAAATATAGTAAA      377
Fa3      ------------------------------------------AAAGAAAATATAGTAAA      377
Fa4      ------------------------------------------AAAGAAAATATAGTAAA      377
Fb1      ------------------------------------------AAAGAAAATATAGTAAA      377
Fb2      ------------------------------------------AAAGAAAATATAGTAAA      377
Fb3      ------------------------------------------AAAGAAAATATAGTAAA      377
Nb4      ------------------------------------------AAAGAAAATATAGTAAA      377
Na1      GGATAAAAAAATTGAAATAATAAATTTAAAAAAATTTATAAAAAAAGAAAATATAGTAAA      600
Na2      GGATAAAAAAATTGAAATAATAAATTTAAAAAAATTTATAAAAAAAGAAAATATAGTAAA      597
Na3      GGATAAAAAAATTGAAATAATAAATTTAAAAAAATTTATAAAAAAAGAAAATATAGTAAA      599
Na4      GGATAAAAAAATTGAAATAATAAATTTAAAAAAATTTATAAAAAAAGAAAATATAGTAAA      600
Nb1      GGATAAAAAAATTGAAATAATAAATTTAAAAAAATTTATAAAAAAAGAAAATATAGTAAA      600
Nb2      GGATAAAAAAATTGAAATAATAAATTTAAAAAAATTTATAAAAAAAGAAAATATAGTAAA      600
Nb3      GGATAAAAAAATTGAAATAATAAATTTAAAAAAATTTATAAAAAAAGAAAATATAGTAAA      600
Sa1      GGATAAAAAAATTGAAATAATAAATTTAAAAAAATTTATAAAAAAAGAAAATATAGTAAA      597
Sa2      GGATAAAAAAATTGAAATAATAAATTTAAAAAAATTTATAAAAAAAGAAAATATAGTAAA      600
Sb1      GGATAAAAAAATTGAAATAATAAATTTAAAAAAATTTATAAAAAAAGAAAATATAGTAAA      600
Sb2      GGATAAAAAAATTGAAATAATAAATTTAAAAAAATTTATAAAAAAAGAAAATATAGTAAA      598
                                                  *****************

Fa1      AAAGGCGGACAAATGTATTGATACTAATTACAATGAAAGATTCAATTTTTGTGTTTTTGC      437
Fa2      AAAGGCGGACAAATGTATTGATACTAATTACAATGAAAGATTCAATTTTTGTGTTTTTGC      437
Fa3      AAAGGCGGACAAATGTATTGATACTAATTACAATGAAAGATTCAATTTTTGTGTTTTTGC      437
Fa4      AAAGGCGGACAAATGTATTGATACTAATTACAATGAAAGATTCAATTTTTGTGTTTTTGC      437
Fb1      AAAGGCGGACAAATGTATTGATACTAATTACAATGAAAGATTCAATTTTTGTGTTTTTGC      437
Fb2      AAAGGCGGACAAATGTATTGATACTAATTACAATGAAAGATTCAATTTTTGTGTTTTTGC      437
Fb3      AAAGGCGGACAAATGTATTGATACTAATTACAATGAAAGATTCAATTTTTGTGTTTTTGC      437
Nb4      AAAGGCGGACAAATGTATTGATACTAATTACAATGAAAGATTCAATTTTTGTGTTTTTGC      437
Na1      AAAAGCGGACAAATGTATTGATACTAATTACAATGAAAGATTCAAATTTTGTGTTTTTGC      660
Na2      AAAAGCGGACAAATGTATTGATACTAATTACAATGAAAGATTCAAATTTTGTGTTTTTGC      657
Na3      AAAAGCGGACAAATGTATTGATACTAATTACAATGAAAGATTCAAATTTTGTGTTTTTGC      659
Na4      AAAAGCGGACAAATGTATTGATACTAATTACAATGAAAGATTCAAATTTTGTGTTTTTGC      660
Nb1      AAAAGCGGACAAATGTATTGATACTAATTACAATGAAAGATTCAAATTTTGTGTTTTTGC      660
Nb2      AAAAGCGGACAAATGTATTGATACTAATTACAATGAAAGATTCAAATTTTGTGTTTTTGC      660
Nb3      AAAAGCGGACAAATGTATTGATACTAATTACAATGAAAGATTCAAATTTTGTGTTTTTGC      660
Sa1      AAAAGCGGACAAATGTATTGATACTAATTACAATGAAAGATTCAAATTTTGTGTTTTTGC      657
Sa2      AAAAGCGGACAAATGTATTGATACTAATTACAATGAAAGATTCAAATTTTGTGTTTTTGC      660
Sb1      AAAAGCGGACAAATGTATTGATACTAATTACAATGAAAGATTCAAATTTTGTGTTTTTGC      660
Sb2      AAAAGCGGACAAATGTATTGATACTAATTACAATGAAAGATTCAAATTTTGTGTTTTTGC      658
         ***.*****************************************:**************

Fa1      CTTATTTTATAAAAGGCGATTGTTTTTTTGCTTATTTTAAAATCACTCTGTATGTCAAAA      497
Fa2      CTTATTTTATAAAAGGCGATTGTTTTTTTGCTTATTTTAAAATCACTCTGTATGTCAAAA      497
Fa3      CTTATTTTATAAAAGGCGATTGTTTTTTTGCTTATTTTAAAATCACTCTGTATGTCAAAA      497
Fa4      CTTATTTTATAAAAGGCGATTGTTTTTTTGCTTATTTTAAAATCACTCTGTATGTCAAAA      497
Fb1      CTTATTTTATAAAAGGCGATTGTTTTTTTGCTTATTTTAAAATCACTCTGTATGTCAAAA      497
Fb2      CTTATTTTATAAAAGGCGATTGTTTTTTTGCTTATTTTAAAATCACTCTGTATGTCAAAA      497
Fb3      CTTATTTTATAAAAGGCGATTGTTTTTTTGCTTATTTTAAAATCACTCTGTATGTCAAAA      497
Nb4      CTTATTTTATAAAAGGCGATTGTTTTTTTGCTTATTTTAAAATCACTCTGTATGTCAAAA      497
Na1      CTTATTTTATAAAAGGCGATTGTTTTTTTGCTTATTTTAAAATCACTCTGTATGTCAAAA      720
Na2      CTTATTTTATAAAAGGCGATTGTTTTTTTGCTTATTTTAAAATCACTCTGTATGTCAAAA      717
Na3      CTTATTTTATAAAAGGCGATTGTTTTTTTGCTTATTTTAAAATCACTCTGTATGTCAAAA      719
Na4      CTTATTTTATAAAAGGCGATTGTTTTTTTGCTTATTTTAAAATCACTCTGTATGTCAAAA      720
Nb1      CTTATTTTATAAAAGGCGATTGTTTTTTTGCTTATTTTAAAATCACTCTGTATGTCAAAA      720
Nb2      CTTATTTTATAAAAGGCGATTGTTTTTTTGCTTATTTTAAAATCACTCTGTATGTCAAAA      720
Nb3      CTTATTTTATAAAAGGCGATTGTTTTTTTGCTTATTTTAAAATCACTCTGTATGTCAAAA      720
Sa1      CTTATTTTATAAAAGGCGATTGTTTTTTTGCTTATTTTAAAATCACTCTGTATGTCAAAA      717
Sa2      CTTATTTTATAAAAGGCGATTGTTTTTTTGCTTATTTTAAAATCACTCTGTATGTCAAAA      720
Sb1      CTTATTTTATAAAAGGCGATTGTTTTTTTGCTTATTTTAAAATCACTCTGTATGTCAAAA      720
Sb2      CTTATTTTATAAAAGGCGATTGTTTTTTTGCTTATTTTAAAATCACTCTGTATGTCAAAA      718
         ************************************************************
```

```
Fa1      AATGCATAAAATATAGGGTGTTCCATTTGGAAGATTATATCAATTTGCACTATAATTTTG      557
Fa2      AATGCATAAAATATAGGGTGTTCCATTTGGAAGATTATATCAATTTGCACTATAATTTTG      557
Fa3      AATGCATAAAATATAGGGTGTTCCATTTGGAAGATTATATCAATTTGCACTATAATTTTG      557
Fa4      AATGCATAAAATATAGGGTGTTCCATTTGGAAGATTATATCAATTTGCACTATAATTTTG      557
Fb1      AATGCATAAAATATAGGGTGTTCCATTTGGAAGATTATATCAATTTGCACTATAATTTTG      557
Fb2      AATGCATAAAATATAGGGTGTTCCATTTGGAAGATTATATCAATTTGCACTATAATTTTG      557
Fb3      AATGCATAAAATATAGGGTGTTCCATTTGGAAGATTATATCAATTTGCACTATAATTTTG      557
Nb4      AATGCATAAAATATAGGGTGTTCCATTTGGAAGATTATATCAATTTGCACTATAATTTTG      557
Na1      AAAGCATAAAATATAGGGTGTTCCATTTGGAAGATTATATCAATTTGCACTATAATTTTG      780
Na2      AAAGCATAAAATATAGGGTGTTCCATTTGGAAGATTATATCAATTTGCACTATAATTTTG      777
Na3      AAAGCATAAAATATAGGGTGTTCCATTTGGAAGATTATATCAATTTGCACTATAATTTTG      779
Na4      AAAGCATAAAATATAGGGTGTTCCATTTGGAAGATTATATCAATTTGCACTATAATTTTG      780
Nb1      AAAGCATAAAATATAGGGTGTTCCATTTGGAAGATTATATCAATTTGCACTATAATTTTG      780
Nb2      AAAGCATAAAATATAGGGTGTTCCATTTGGAAGATTATATCAATTTGCACTATAATTTTG      780
Nb3      AAAGCATAAAATATAGGGTGTTCCATTTGGAAGATTATATCAATTTGCACTATAATTTTG      780
Sa1      AAAGCATAAAATATAGGGTGTTCCATTTGGAAGATTATATCAATTTGCACTATAATTTTG      777
Sa2      AAAGCATAAAATATAGGGTGTTCCATTTGGAAGATTATATCAATTTGCACTATAATTTTG      780
Sb1      AAAGCATAAAATATAGGGTGTTCCATTTGGAAGATTATATCAATTTGCACTATAATTTTG      780
Sb2      AAAGCATAAAATATAGGGTGTTCCATTTGGAAGATTATATCAATTTGCACTATAATTTTG      778
         **:************************************************************

Fa1      GACAAATTCAGTGAAATATTTTAAAATACCGACAGTAAAAGTTTCACTTAATGACTTAAC      617
Fa2      GACAAATTCAGTGAAATATTTTAAAATACCGACAGTAAAAGTTTCACTTAATGACTTAAC      617
Fa3      GACAAATTCAGTGAAATATTTTAAAATACCGACAGTAAAAGTTTCACTTAATGACTTAAC      617
Fa4      GACAAATTCAGTGAAATATTTTAAAATACCGACAGTAAAAGTTTCACTTAATGACTTAAC      617
Fb1      GACAAATTCAGTGAAATATTTTAAAATACCGACAGTAAAAGTTTCACTTAATGACTTAAC      617
Fb2      GACAAATTCAGTGAAATATTTTAAAATACCGACAGTAAAAGTTTCACTTAATGACTTAAC      617
Fb3      GACAAATTCAGTGAAATATTTTAAAATACCGACAGTAAAAGTTTCACTTAATGACTTAAC      617
Nb4      GACAAATTCAGTGAAATATTTTAAAATACCGACAGTAAAAGTTTCACTTAATGACTTAAC      617
Na1      TACAAATTCAGTGAAATATTTTAAAATACCGACAGTAAAAGTTTCACTTAATGACTTAAC      840
Na2      TACAAATTCAGTGAAATATTTTAAAATACCGACAGTAAAAGTTTCACTTAATGACTTAAC      837
Na3      TACAAATTCAGTGAAATATTTTAAAATACCGACAGTAAAAGTTTCACTTAATGACTTAAC      839
Na4      TACAAATTCAGTGAAATATTTTAAAATACCGACAGTAAAAGTTTCACTTAATGACTTAAC      840
Nb1      TACAAATTCAGTGAAATATTTTAAAATACCGACAGTAAAAGTTTCACTTAATGACTTAAC      840
Nb2      TACAAATTCAGTGAAATATTTTAAAATACCGACAGTAAAAGTTTCACTTAATGACTTAAC      840
Nb3      TACAAATTCAGTGAAATATTTTAAAATACCGACAGTAAAAGTTTCACTTAATGACTTAAC      840
Sa1      TACAAATTCAGTGAAATATTTTAAAATACCGACAGTAAAAGTTTCACTTAATGACTTAAC      837
Sa2      TACAAATTCAGTGAAATATTTTAAAATACCGACAGTAAAAGTTTCACTTAATGACTTAAC      840
Sb1      TACAAATTCAGTGAAATATTTTAAAATACCGACAGTAAAAGTTTCACTTAATGACTTAAC      840
Sb2      TACAAATTCAGTGAAATATTTTAAAATACCGACAGTAAAAGTTTCACTTAATGACTTAAC      838
          ************************************************************

Fa1      CTTCACCATTCTAAAAATTTTTGAAATCCCCTCCCCTAAAATTAATTTATTGATCCGCCC      677
Fa2      CTTCACCATTCTAAAAATTTTTGAAATCCCCTCCCCTAAAATTAATTTATTGATCCGCCC      677
Fa3      CTTCACCATTCTAAAAATTTTTGAAATCCCCTCCCCTAAAATTAATTTATTGATCCGCCC      677
Fa4      CTTCACCATTCTAAAAATTTTTGAAATCCCCTCCCCTAAAATTAATTTATTGATCCGCCC      677
Fb1      CTTCACCATTCTAAAAATTTTTGAAATCCCCTCCCCTAAAATTAATTTATTGATCCGCCC      677
Fb2      CTTCACCATTCTAAAAATTTTTGAAATCCCCTCCCCTAAAATTAATTTATTGATCCGCCC      677
Fb3      CTTCACCATTCTAAAAATTTTTGAAATCCCCTCCCCTAAAATTAATTTATTGATCCGCCC      677
Nb4      CTTCACCATTCTAAAAATTTTTGAAATCCCCTCCCCTAAAATTAATTTATTGATCCGCCC      677
Na1      CTTCACCATTCTAAAAATTTTTGAAATCCCCTCCCCCAAAATTAATTTATTGATCCGCCC      900
Na2      CTTCACCATTCTAAAAATTTTTGAAATCCCCTCCCCCAAAATTAATTTATTGATCCGCCC      897
Na3      CTTCACCATTCTAAAAATTTTTGAAATCCCCTCCCCCAAAATTAATTTATTGATCCGCCC      899
Na4      CTTCACCATTCTAAAAATTTTTGAAATCCCCTCCCCCAAAATTAATTTATTGATCCGCCC      900
Nb1      CTTCACCATTCTAAAAATTTTTGAAATCCCCTCCCCCAAAATTAATTTATTGATCCGCCC      900
Nb2      CTTCACCATTCTAAAAATTTTTGAAATCCCCTCCCCCAAAATTAATTTATTGATCCGCCC      900
Nb3      CTTCACCATTCTAAAAATTTTTGAAATCCCCTCCCCCAAA-TTAATTTATTGATCCGCCC      899
Sa1      CTTCACCATTCTAAAAATTTTTGAAATCCCCTCCCCCAAAATTAATTTATTGATCCGCCC      897
Sa2      CTTCACCATTCTAAAAATTTTTGAAATCCCCTCCCCCAAAATTAATTTATTGATCCGCCC      900
Sb1      CTTCACCATTCTAAAAATTTTTGAAATCCCCTCCCCCAAAATTAATTTATTGATCCGCCC      900
Sb2      CTTCACCATTCTAAAA-TTTTTGAAATCCCCTCCCCCAAAATTAATTTATTGATCCGCCC      897
         **************** ******************** *** ********************
```

```
Fa1      CT                                                              679
Fa2      CT                                                              679
Fa3      CT                                                              679
Fa4      CT                                                              679
Fb1      CT                                                              679
Fb2      CT                                                              679
Fb3      CT                                                              679
Nb4      CT                                                              679
Na1      CT                                                              902
Na2      CT                                                              899
Na3      CT                                                              901
Na4      CT                                                              902
Nb1      CT                                                              902
Nb2      CT                                                              902
Nb3      CT                                                              901
Sa1      CT                                                              899
Sa2      CT                                                              902
Sb1      CT                                                              902
Sb2      CT                                                              899
         **
```

Supplementary File 4-2. Information about 27 candidates differentially expressed in the fast lines.

On chromosome 3, *C-factor* encodes a short-chain dehydrogenases/reductase (SDR) and is a member of SDR superfamily (Niu et al., 2022). In insects, SDR enzymes mainly participate in the synthesis of ecdysone in a specific Black Box step of ecdysteroid biosynthesis (Niwa et al., 2010) (Figure 4-37).

SLC25-35-1, *Melted* and *SLC25-35-2* are close to each other in the genome of *T. castaneum*. We did find significant differential expression of *Melted* and *SLC25-35-2*, but not of *SLC25-35-1*. By interacting with tuberous sclerosis 1 (Tsc1) and FOXO, Melted enhances insulin/TOR (target of rapamycin) activity (Teleman et al., 2005), a pivotal pathway enhancing growth rate (Baker and Thummel, 2007; Nijhout et al., 2014). It is unclear how the mitochondrial solute carrier *SLC25-35-2* would affect developmental speeds. Hence, it could be that *Melted* acted as the driver gene and *SLC25-35-2* as the hitchhiker.

CYP6 orthologs, including *Cyp6a14* and *Cyp6k1*, have been implicated to insecticide resistance in many insects, such as *D. melanogaster* (Daborn et al., 2002), *T. castaneum* (Ercan et al., 2020; Oppert et al., 2015), *Leptinotarsa decemlineata* (Scott et al., 2020), *Anopheles gambiae* (Nikou et al., 2003), *Myzus persicae* (Chiu et al., 2008) and *Periplaneta americana* (Zhang et al., 2016). However, it has never been reported that CYP6 orthologs participate in the regulation of development.

The calcitonin receptor is homologous to a subfamily of the seven-transmembrane domain, G-protein-coupled receptor superfamily (GPCRs) in family B. In function, family B proteins of GPCRs typically recognize regulatory peptides such as parathyroid hormone, secretin, glucagon, urocortin and vasoactive intestinal polypeptide (Harmar, 2001; McLatchie et al., 1998). In *Drosophila*, family B proteins of GPCRs regulate longevity and stress responses (Lin et al., 1998). In addition, calcitonin receptor regulates the body temperature rhythm in insects as well as in mammals (Goda et al., 2018).

Odorant receptors also belong to the GPCRs family but lack homology to GPCRs in vertebrates (Buck and Axel, 1991). They contain the odorant-binding site and interact with a vast chemicals (Hallem and Carlson, 2006). In insects, odor detection is mediated by a unique class of odorant-gated ion channels (Sato et al., 2008; Wicher et al., 2008). The members of GPCRs, *CalcitoninR* and *OR327* may participate in the regulation of development by recognizing regulatory peptides.

Sec61α is participating in the transport of polypeptides into the eukaryotic endoplasmic reticulum (Park and Rapoport, 2012). Here, down-regulation of *Sec61α* in fast developing embryos might indicate that the transport of polypeptides is not much required after dorsal closure. *Lac2* controls cuticle tanning in *Tribolium* (Arakane et al., 2005). So, fast developing embryos need to catalyze cuticle tanning in advance before hatching to larvae. Although *Skiv2* was significantly down-regulated during dorsal closure (Figure 4-5A), no reports on its function in insects are available.

On chromosome 9, the *metabotropic glutamate receptors* (*mGluR*) is a member of family C GPCRs. By mediating intracellular signal transduction, the *mGluR* carries out a variety of functions, such as mobilization of calcium, modulation of a variety of ion channels (calcium or potassium currents), and activation of protein kinase C, phospholipase D, protein kinase and TOR pathways (Conn and Pin, 1997; Niswender and Conn, 2010). Thus, the up-regulation of *mGluR* found in our study may indicate that intracellular signal transduction is very active during dorsal closure.

Suppression of tumorigenicity 18 protein (ST18) encodes a zinc finger transcription factor and is involved in apoptosis and inflammation. In human, it is mainly related to occurrence of disease, such as pemphigus vulgaris (Petzl-Erler, 2020) and Alzheimer's disease (Kim et al., 2021). As no publications on the function of St18 C2H2C in insects are available, we do not discuss it here.

The main function of cationic amino acid transporters (CATs) is participating in the transport of cationic amino acids into most cells, and mediating efflux of their substrates as well (Closs et al., 2006). In this study, gene expression profiles of three CATs, including *CAT1*, *CAT2* and *CAT3*, strongly suggested that all of them are possibly involved in fast embryonic development. They are orthologous to slimfast, an amino acid sensor that can overrule peripheral insulin/TOR activity by PI3K modulation (Colombani et al., 2003). They are thus likely candidates to affect developmental speed.

The *Drosophila* transcription factor, Adh distal factor-1 (Adf-1), containing a TAF-binding motif of Myb and Myb-related proteins, binds to upstream recognition elements in a diverse group of promoters to activate their transcription, such as dopa decarboxylase and antennapedia P1 (Cutler et al., 1998; England et al., 1990). Adf-1 is only detectable in most somatic cells of later stages embryos but not in very early embryos of *Drosophila* (England et al., 1992). Here, expression data suggested that Adf-1 plays a more important role during dorsal closure than after it. In *Bemisia tabaci*, silencing Adf-1 activates autophagy and apoptosis, therefore resulting in a significant decrease in the total number of bacteriocytes (Li et al., 2022).

Protein-L-isoaspartate O-methyltransferase (Pcmt) is used to accomplish L-isoaspartate methylation, thus repairing proteins by reformation of l-aspartate (Mishra and Mahawar, 2019). The down-regulation of *Pcmt* found in our study may suggest low investment in protein repair in fast developing embryos.

LOC107397428, *Chymase*, *Cyp18a1* and *Cyp306a1* are close to each other in the genome, too. As they are all differentially expressed, all of the could be the target of selection. However, our RNAi screen suggests that a deletion affecting *Cyp18a1* expression is the driving allele. LOC107397428 is an uncharacterized gene in the NCBI gene database. As a member of neutral serine proteases, Chymase has been wildly studied in mammals and is essentially unique to mast cells (Pejler, 2020; Welle, 1997). Down-regulation of *Chymase* may suggest fewer mast cells in fast developing embryos. See Discussion for Cyp18a1 and Cyp306a1 (*phantom*).

Deadpan, a gene encoding a helix-loop-helix protein, is one direct target of Notch signaling in *Drosophila* (Bier et al., 1992; San-Juán and Baonza, 2011). The Notch signaling is participating in many aspects of communication between cells and regulating metazoan development and tissue renewal (Kopan and Ilagan, 2009). Through Notch signaling, Deadpan could be involved in many aspects of dorsal closure.

Pancreatic triacylglycerol lipase (Lipase) fulfills a key function in fat metabolism by finally breaking down dietary lipids into monoglycerides and free fatty acids (Winkler et al., 1990). In this study, *Lipase* was up-regulated before dorsal closure, and down-regulated during and after it. This pattern may indicate that fat metabolism is highly required to start dorsal closure.

Integrin aPS2 expression did not vary too much in the process of dorsal closure among the selection lines. The cell adhesion molecule integrin is likely to play an important role in morphogenetic movements such as dorsal closure (Münster et al., 2019).

Inositol hexakisphosphate kinase (Ip6k), with three isoforms in mammals but one isoform in *Drosophila*, participates in diverse cellular pathways via the synthesis of inositol pyrophosphates (Jadav et al., 2016). Inositol pyrophosphates can affect protein function by binding to protein itself or pyrophosphorylation of its β-phosphate to form pyrophosphoserine, thus participating in a diverse of metabolic, developmental, and signaling pathways (Shah et al., 2017).

Bone morphogenetic protein (BMP) and activin membrane-bound inhibitor (Bambi) is an inhibitor of the transforming growth factor-β (TGF-β) signaling but a positive modulator of Wnt signaling (Carethers, 2009; Lin et al., 2008). BMPs are multifunctional growth factors and belong to the TGF-β

superfamily. As the negative regulator, Bambi inhibits BMP and activin signaling during *Xenopus* embryogenesis (Onichtchouk et al., 1999). In this study, significant up-regulation of *Ip6k* and *Bambi* found in our study indicates that many pathways are involved in finishing dorsal closure.

Supplementary file 2 references

Arakane, Y., Muthukrishnan, S., Beeman, R. W., Kanost, M. R. and Kramer, K. J. (2005). Laccase 2 is the phenoloxidase gene required for beetle cuticle tanning. *Proceedings of the National Academy of Sciences* **102**, 11337-11342.

Baker, K. D. and Thummel, C. S. (2007). Diabetic larvae and obese flies—emerging studies of metabolism in Drosophila. *Cell metabolism* **6**, 257-266.

Bier, E., Vaessin, H., Younger-Shepherd, S., Jan, L. Y. and Jan, Y. N. (1992). deadpan, an essential pan-neural gene in Drosophila, encodes a helix-loop-helix protein similar to the hairy gene product. *Genes & Development* **6**, 2137-2151.

Buck, L. and Axel, R. (1991). A novel multigene family may encode odorant receptors: a molecular basis for odor recognition. *Cell* **65**, 175-187.

Carethers, J. M. (2009). Intersection of transforming growth factor-β and wnt signaling pathways in colorectal cancer and metastasis. *Gastroenterology* **137**, 33-36.

Chiu, T.-L., Wen, Z., Rupasinghe, S. G. and Schuler, M. A. (2008). Comparative molecular modeling of Anopheles gambiae CYP6Z1, a mosquito P450 capable of metabolizing DDT. *Proceedings of the National Academy of Sciences* **105**, 8855-8860.

Closs, E., Boissel, J.-P., Habermeier, A. and Rotmann, A. (2006). Structure and function of cationic amino acid transporters (CATs). *The Journal of membrane biology* **213**, 67-77.

Colombani, J., Raisin, S., Pantalacci, S., Radimerski, T., Montagne, J. and Léopold, P. (2003). A nutrient sensor mechanism controls Drosophila growth. *Cell* **114**, 739-749.

Conn, P. J. and Pin, J.-P. (1997). Pharmacology and functions of metabotropic glutamate receptors. *Annual review of pharmacology and toxicology* **37**, 205-237.

Cutler, G., Perry, K. M. and Tjian, R. (1998). Adf-1 is a nonmodular transcription factor that contains a TAF-binding Myb-like motif. *Molecular and cellular biology* **18**, 2252-2261.

Daborn, P., Yen, J., Bogwitz, M., Le Goff, G., Feil, E., Jeffers, S., Tijet, N., Perry, T., Heckel, D. and Batterham, P. (2002). A single P450 allele associated with insecticide resistance in Drosophila. *Science* **297**, 2253-2256.

England, B. P., Admon, A. and Tjian, R. (1992). Cloning of Drosophila transcription factor Adf-1 reveals homology to Myb oncoproteins. *Proceedings of the National Academy of Sciences* **89**, 683-687.

England, B. P., Heberlein, U. and Tjian, R. (1990). Purified Drosophila transcription factor, Adh distal factor-1 (Adf-1), binds to sites in several Drosophila promoters and activates transcription. *Journal of Biological Chemistry* **265**, 5086-5094.

Ercan, F. S., Azarkan, S. Y., Ercan, N. and Koc, M. (2020). Sequence variants of CYP345a1 and CYP6a14 gene regions in Tribolium castaneum (Coleoptera: Tenebrionidae) adults treated with the novel characterızed Bolanthus turcicus (Caryophyllaceae) extract. *Molecular Biology Research Communications* **9**, 105.

Goda, T., Doi, M., Umezaki, Y., Murai, I., Shimatani, H., Chu, M. L., Nguyen, V. H., Okamura, H. and Hamada, F. N. (2018). Calcitonin receptors are ancient modulators for rhythms of preferential temperature in insects and body temperature in mammals. *Genes & development* **32**, 140-155.

Hallem, E. A. and Carlson, J. R. (2006). Coding of odors by a receptor repertoire. *Cell* **125**, 143-160.

Harmar, A. J. (2001). Family-B G-protein-coupled receptors. *Genome biology* **2**, 1-10.

Jadav, R. S., Kumar, D., Buwa, N., Ganguli, S., Thampatty, S. R., Balasubramanian, N. and Bhandari, R. (2016). Deletion of inositol hexakisphosphate kinase 1 (IP6K1) reduces cell migration and invasion, conferring protection from aerodigestive tract carcinoma in mice. *Cellular signalling* **28**, 1124-1136.

Kim, B.-H., Nho, K., Lee, J.-M. and Initiative, A. s. D. N. (2021). Genome-wide association study identifies susceptibility loci of brain atrophy to NFIA and ST18 in Alzheimer's disease. *Neurobiology of Aging* **102**, 200. e201-200. e211.

Kopan, R. and Ilagan, M. X. G. (2009). The canonical Notch signaling pathway: unfolding the activation mechanism. *Cell* **137**, 216-233.

Li, N.-N., Jiang, S., Lu, K.-Y., Hong, J.-S., Wang, Y.-B., Yan, J.-Y. and Luan, J.-B. (2022). Bacteriocyte development is sexually differentiated in Bemesia tabaci. *Cell reports* **38**, 110455.

Lin, Y.-J., Seroude, L. and Benzer, S. (1998). Extended life-span and stress resistance in the Drosophila mutant methuselah. *Science* **282**, 943-946.

Lin, Z., Gao, C., Ning, Y., He, X., Wu, W. and Chen, Y.-G. (2008). The pseudoreceptor BMP and activin membrane-bound inhibitor positively modulates Wnt/β-catenin signaling. *Journal of Biological Chemistry* **283**, 33053-33058.

McLatchie, L. M., Fraser, N. J., Main, M. J., Wise, A., Brown, J., Thompson, N., Solari, R., Lee, M. G. and Foord, S. M. (1998). RAMPs regulate the transport and ligand specificity of the calcitonin-receptor-like receptor. *Nature* **393**, 333-339.

Mishra, P. and Mahawar, M. (2019). PIMT-mediated protein repair: Mechanism and implications. *Biochemistry (Moscow)* **84**, 453-463.

Münster, S., Jain, A., Mietke, A., Pavlopoulos, A., Grill, S. W. and Tomancak, P. (2019). Attachment of the blastoderm to the vitelline envelope affects gastrulation of insects. *Nature* **568**, 395-399.

Nijhout, H. F., Riddiford, L. M., Mirth, C., Shingleton, A. W., Suzuki, Y. and Callier, V. (2014). The developmental control of size in insects. *Wiley Interdisciplinary Reviews: Developmental Biology* **3**, 113-134.

Nikou, D., Ranson, H. and Hemingway, J. (2003). An adult-specific CYP6 P450 gene is overexpressed in a pyrethroid-resistant strain of the malaria vector, Anopheles gambiae. *Gene* **318**, 91-102.

Niswender, C. M. and Conn, P. J. (2010). Metabotropic glutamate receptors: physiology, pharmacology, and disease. *Annual review of pharmacology and toxicology* **50**, 295.

Niu, L., Yan, H., Sun, Y., Zhang, D., Ma, W. and Lin, Y. (2022). Nanoparticle facilitated stacked-dsRNA improves suppression of the Lepidoperan pest Chilo suppresallis. *Pesticide Biochemistry and Physiology* **187**, 105183.

Niwa, R., Namiki, T., Ito, K., Shimada-Niwa, Y., Kiuchi, M., Kawaoka, S., Kayukawa, T., Banno, Y., Fujimoto, Y. and Shigenobu, S. (2010). Non-molting glossy/shroud encodes a short-chain dehydrogenase/reductase that functions in the 'Black Box'of the ecdysteroid biosynthesis pathway. *Development* **137**, 1991-1999.

Onichtchouk, D., Chen, Y.-G., Dosch, R., Gawantka, V., Delius, H. and Niehrs, C. (1999). Silencing of TGF-β signalling by the pseudoreceptor BAMBI. *Nature* **401**, 480-485.

Oppert, B., Guedes, R. N., Aikins, M. J., Perkin, L., Chen, Z., Phillips, T. W., Zhu, K. Y., Opit, G. P., Hoon, K. and Sun, Y. (2015). Genes related to mitochondrial functions are differentially expressed in phosphine-resistant and-susceptible Tribolium castaneum. *BMC genomics* **16**, 1-10.

Park, E. and Rapoport, T. A. (2012). Mechanisms of Sec61/SecY-mediated protein translocation across membranes. *Annu Rev Biophys* **41**, 21-40.

Pejler, G. (2020). Novel insight into the in vivo function of mast cell chymase: Lessons from knockouts and inhibitors. *Journal of Innate Immunity* **12**, 357-372.

Petzl-Erler, M. L. (2020). Beyond the HLA polymorphism: A complex pattern of genetic susceptibility to pemphigus. *Genetics and molecular biology* **43**.

San-Juán, B. P. and Baonza, A. (2011). The bHLH factor deadpan is a direct target of Notch signaling and regulates neuroblast self-renewal in Drosophila. *Developmental biology* **352**, 70-82.

Sato, K., Pellegrino, M., Nakagawa, T., Nakagawa, T., Vosshall, L. B. and Touhara, K. (2008). Insect olfactory receptors are heteromeric ligand-gated ion channels. *Nature* **452**, 1002-1006.

Scott, I. M., Hatten, G., Tuncer, Y., Clarke, V. C., Jurcic, K. and Yeung, K. K.-C. (2020). Proteomic Analyses Detect Higher Expression of C-Type Lectins in Imidacloprid-Resistant Colorado Potato Beetle Leptinotarsa decemlineata Say. *Insects* **12**, 3.

Shah, A., Ganguli, S., Sen, J. and Bhandari, R. (2017). Inositol pyrophosphates: energetic, omnipresent and versatile signalling molecules. *Journal of the Indian Institute of Science* **97**, 23-40.

Teleman, A. A., Chen, Y.-W. and Cohen, S. M. (2005). Drosophila Melted modulates FOXO and TOR activity. *Developmental cell* **9**, 271-281.

Welle, M. (1997). Development, significance, and heterogeneity of mast cells with particular regard to the mast cell-specific proteases chymase and tryptase. *Journal of leukocyte biology* **61**, 233-245.

Wicher, D., Schäfer, R., Bauernfeind, R., Stensmyr, M. C., Heller, R., Heinemann, S. H. and Hansson, B. S. (2008). Drosophila odorant receptors are both ligand-gated and cyclic-nucleotide-activated cation channels. *Nature* **452**, 1007-1011.

Winkler, F., d'Arcy, A. and Hunziker, W. (1990). Structure of human pancreatic lipase. *Nature* **343**, 771-774.

Zhang, J., Zhang, Y., Li, J., Liu, M. and Liu, Z. (2016). Midgut transcriptome of the cockroach Periplaneta americana and its microbiota: digestion, detoxification and oxidative stress response. *PloS one* **11**, e0155254.

Supplementary File 4-3. The details on the mathematical modelling.

Here we provide a detailed derivation of the mathematical model of ecdysone dynamics. First we focus on the cross-talk between ecdysone and its own synthesis, i.e. the Halloween genes (Niwa and Niwa, 2016). A positive feedback of ecdysone into the Halloween has been well established, for instance for *phm* and *dib* (Moeller et al., 2013). In our model, we let *Spook* represent the Halloween genes. Also in *Tribolium*, there is a binding site for the ecdysone receptor just upstream of the *Spook* transcription start site, suggesting that ecdysone positively regulates transcription of *Spook*. This creates a positive feedback loop between Spook and ecdysone (*Figure S1* in this supplementary file).

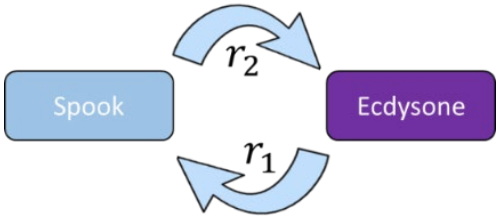

Figure S1. Diagram of the positive feedback loop between Spook and Ecdysone. The arrows indicate positive interactions.

Following the law of mass action (Lund, 1965), the reactions shown in *Figure S1* above translate to the set of ordinary differential equations,

$$\begin{cases} \frac{dS}{dt} = r_1 E - \beta_1 S, \\ \frac{dE}{dt} = r_2 S - \beta_2 E. \end{cases} \quad (1)$$

The first right-hand side terms of Eq. (1) represent the production of Spook (S) and ecdysone (E); the second right-hand side terms represent the degradation of Spook and ecdysone. To simplify the model and focus on ecdysone, we assume that ecdysone production and degradation is slow relative to Spook transcription and translation, such that the level of Spook can be expressed as an ecdysone-dependent steady state, $S = \bar{S}(E)$. The quasi-steady state assumption ($d\bar{S}/dt = 0$) then yields that:

$$\bar{S}(E) = \frac{r_1}{\beta_1} E \quad (2)$$

Substituting Eq. (2) into Eq. (1), we have following equation:

$$\frac{dE}{dt} = \beta E. \quad (3)$$

where $\beta = r_1 r_2/\beta_1 - \beta_2$. Thus Eq. (3) describes autocatalytic synthesis of ecdysone (*Figure S2* in this supplementary file, right panel).

Next we include the transcription, translation and activity of the ecdysone inactivating enzyme Cyp18a1 (denoted as C). An increase of *Cyp18a1* expression follows the onset of high ecdysone (main Figure 4-14), suggesting that ecdysone upregulates Cyp18a1 production. To model inactivation of ecdysone, we assume a simple enzymatic breakdown. The full conceptual model then becomes as shown in *Figure S2* in this supplementary file.

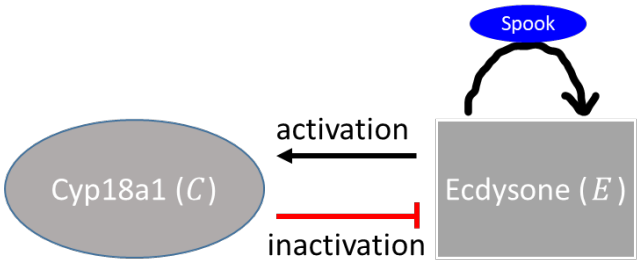

Figure S2. Diagrammatic representation of the regulation paths among the reactions of Spook, Ecdysone and Cpy18a1. The black arrows mean positive regulation and red arrow means negative regulation. The self-regulation of ecdysone is a simplified version of the feedback loops in *Figure S1* under the quasi-steady state assumption of Spook.

Mathematically, following the law of mass action (Lund, 1965) and ignoring Michaelis-Menten kinetics (Johnson and Goody, 2011), the reactions in *Figure S2* above are described by extending Eq. (3) as,

$$\begin{cases} \frac{dC}{dt} = f(E) - \lambda C, \\ \frac{dE}{dt} = bE - kCE. \end{cases} \tag{4}$$

In the first equation, we use an increasing function $f(E)$ for the ecdysone-induced transcription and translation of Cyp18a1, and a first-order degradation of Cyp18a1. Ecdysone synthesis is due to an autocatalytic production (bE; see Eq. 3), the term kCE is enzymatic degradation of ecdysone by Cyp18a1. For the form of the activation function $f(E)$, Zuin, J. et al. recently found that the gene transcription rate induced by promoter-enhancer contact satisfies a Sigmoid function (Zuin et al., 2022). Therefore, we assumed an explicit sigmoidal function

$$f(E) = \frac{V_{max}}{1+\exp((\theta-E)/s)}. \tag{5}$$

To test the validity of our model, we used the least square method to fit Eq. (3) to the ecdysone timeseries for *Tribolium* eggs in presence of *Cyp18a1* pRNAi (*Figure S3a* in this supplementary file, see also main Figure 4-21). To include the effect of Cyp18a1 and to further test our model, by selecting appropriate values for θ and s (*Table S1*), we next fitted the Eq. (4) to the timeseries of Cyp18a1 and ecdysone for normal *Tribolium* eggs (*Figure S3b* in this supplementary file, see also main Figure 4-14). The results show that our model fits very well with the data (*Figure S3a* and *Figure S3b* in this supplementary file).

In Sigmoid function (5), the regulation of ecdysone to Cyp18a1 expression, there are three parameters. V_{max} represents the maximal production rate of Cyp18a1, θ is a threshold of ecdysone at which the production rate of Cyp18a1 is half of V_{max}, and s is the slope factor which controls the response sharpness (sensitivity) of Cyp18a1 production to ecdysone. With high sensitivity (s is high), Cyp18a1 production starts at low ecdysone levels, while the start of Cyp18a1 production requires higher ecdysone levels when s is low (main Figure 4-38C). In other words, we assume that the Slow allele containing two binding sites for the anchoring protein Tramtrack is more likely to establish or maintain enhancer-promotor interactions at low ecdysone levels (main Figure 4-39B), while the F allele is more refractory to low ecdysone levels (main Figure 4-39B).

In *Figure S4*, we present the dynamics of Cyp18a1 expression and ecdysone concentration with variations in parameters V_{max}, θ and s, respectively. We observed that, with the decrease of s (i.e., reduced sensitivity of Cyp18a1 production to ecdysone), *Cyp18a1* expression becomes delayed, but ecdysone peaks earlier and more highly, in agreement with the experimental data (main Figure 4-33, Figure 4-34 and *Figure S4c*). Collectively, these simulations support the idea that changing the reaction sensitivity of Cyp18a1 to ecdysone leads to the shift of the ecdysone peak.

Table S1. Parameters and initial values used for numerical simulations.

Estimated results of equation (3)	**Par.**	**Description**	**Value**
	$\boldsymbol{\beta}$	The net growth rate of ecdysone	0.03/h
	$\boldsymbol{E_0}$	The initial value of equation (3)	592pg/ml
Parameters and initial values in equations (4) and in sigmodal function (5)	$\boldsymbol{b}$	The relative growth rate of ecdysone	0.24/h
	$\boldsymbol{k}$	Cyp18a1-mediated degradation rate of ecdysone	21.24/h
	$\boldsymbol{\lambda}$	Degradation rate of Cyp18a1	0.0087/h
	$\boldsymbol{V_{max}}$	Maximal production rate of Cyp18a1	0.0012/h
	$\boldsymbol{\theta}$	Ecdysone concentration producing half maximal production rate of Cyp18a1	2500pg/ml
	$\boldsymbol{s}$	Response sharpness (sensitivity) of Cyp18a1 to ecdysone	1000pg/ml
	$\boldsymbol{C_0}$	Initial value of Cyp18a1 in Eq (4)	0.0032pg/ml
	$\boldsymbol{E_0}$	Initial value of ecdysone in Eq (4)	89.52pg/ml

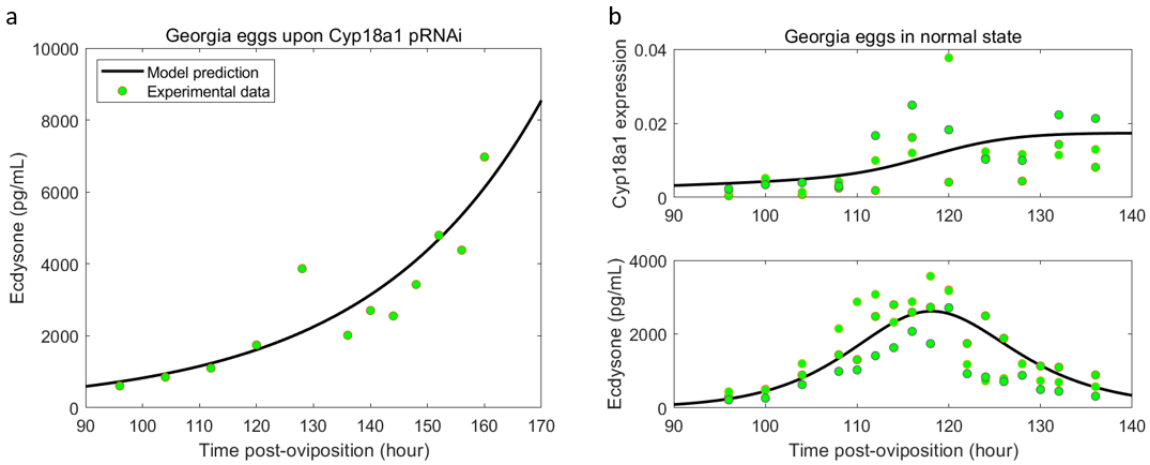

Figure S3. Data fitting and parameters estimation by matching equation (3) and equation (4) to the Cyp18a1 expression level and ecdysone concentration in Georgia eggs. (**a**) The time series of ecdysone in Georgia eggs upon Cyp18a1 pRNAi. (**b**) The dynamics of Cyp18a1 and ecdysone in wild type Georgia eggs. The growth of ecdysone in Georgia eggs exposed to Cyp18a1 pRNAi is exponential. In normal situation, ecdysone shows a peak when the level of Cyp18a1 is bigger than a certain level.

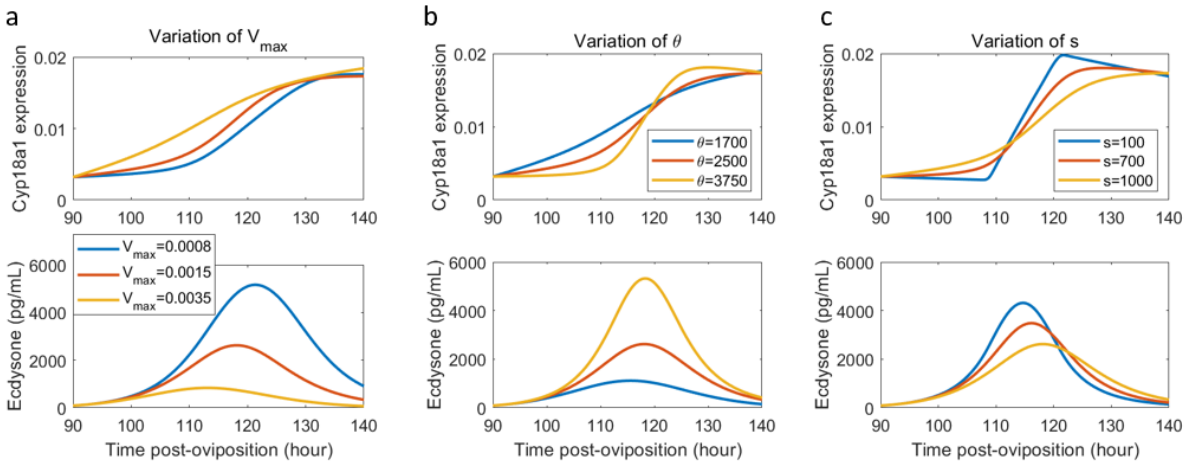

Figure S4. The dynamics of Cyp18a1 expression level and ecdysone concentration with variations in parameters V_{max} (**a**), θ (**b**) and s (**c**) of the Sigmoid function.

Supplementary file 3 references

Johnson, K. A. and Goody, R. S. (2011). The original Michaelis constant: translation of the 1913 Michaelis–Menten paper. *Biochemistry* **50**, 8264-8269.

Lund, E. W. (1965). Guldberg and Waage and the law of mass action. *Journal of Chemical Education* **42**, 548.

Moeller, M. E., Danielsen, E. T., Herder, R., O'Connor, M. B. and Rewitz, K. F. (2013). Dynamic feedback circuits function as a switch for shaping a maturation-inducing steroid pulse in Drosophila. *Development* **140**, 4730-4739.

Niwa, Y. S. and Niwa, R. (2016). Transcriptional regulation of insect steroid hormone biosynthesis and its role in controlling timing of molting and metamorphosis. *Dev Growth Differ* **58**, 94-105.

Zuin, J., Roth, G., Zhan, Y., Cramard, J., Redolfi, J., Piskadlo, E., Mach, P., Kryzhanovska, M., Tihanyi, G. and Kohler, H. (2022). Nonlinear control of transcription through enhancer–promoter interactions. *Nature* **604**, 571-577.